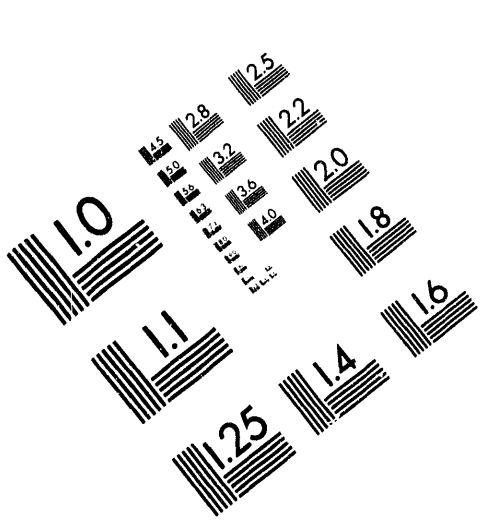

Association for Information and Image Management
1100 Wayne Avenue, Suite 1100
Silver Spring, Maryland 20910
301/587-8202

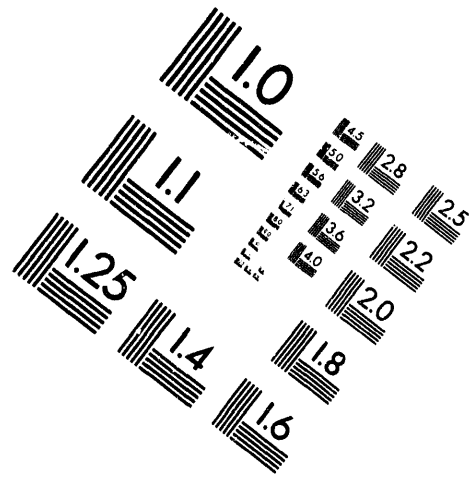

Centimeter

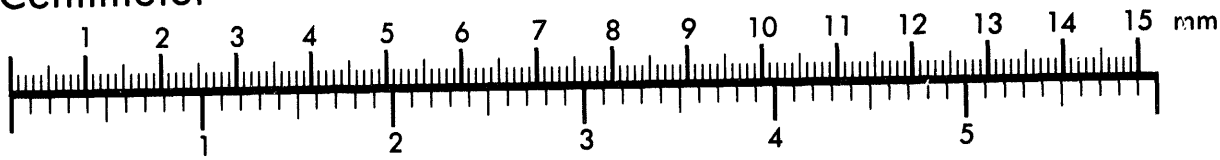

Inches

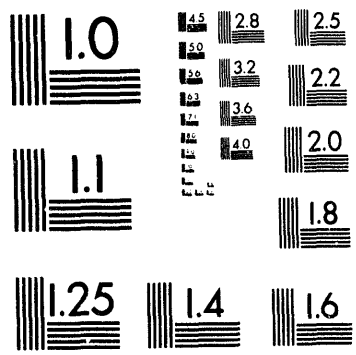

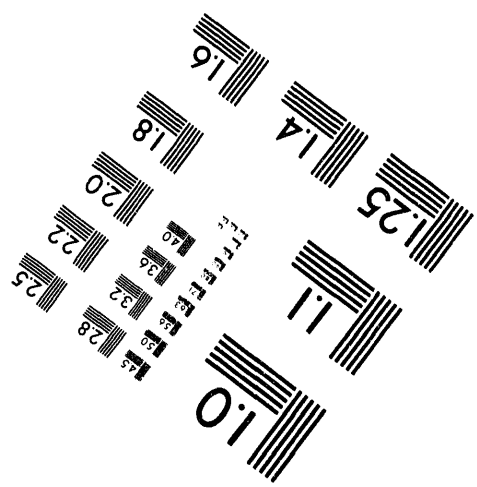

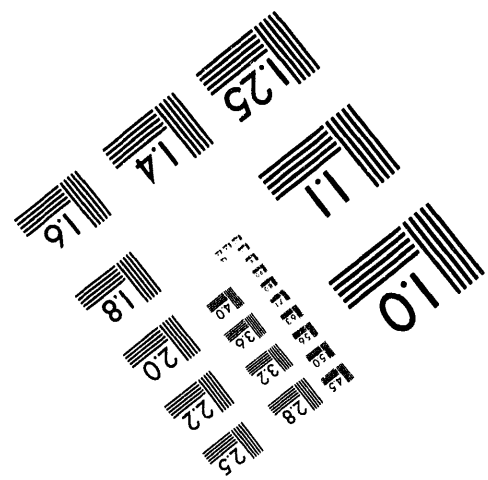

MANUFACTURED TO AIIM STANDARDS
BY APPLIED IMAGE, INC.

1 of 2

[redacted]

HW-78157
C-44a, Nuclear Technology
Materials
(M-3679, 31th Ed.)

QUARTERLY PROGRESS REPORT
METALLURGY DEVELOPMENT OPERATION
APRIL, MAY, JUNE, 1963

By

The Staff of Metallurgy Development Operation

O. J. Wick	Manager
G. A. Last	Manager, Fuels Design
J. E. Minor	Manager, Metal Fabrication Development
T. C. Nelson	Manager, Plutonium Product Development
R. W. Stewart	Manager, Plutonium Metallurgy Development

September 18, 1963

HANFORD ATOMIC PRODUCTS OPERATION
RICHLAND, WASHINGTON

Work performed under Contract No. AT(45-1)-1350 between the Atomic Energy Commission and General Electric Company

[redacted]

[redacted]

Portions of this work was formerly reported in "Fuels Development Operation Quarterly Reports" and "Plutonium Metallurgy Operation Quarterly Reports". Previous reports for 1961 and 1962 in the Fuels Development Operation series were:

HW-70556	January, February, March, 1961
HW-70557	April, May, June, 1961
HW-71422	July, August, September, 1961
HW-72346	October, November, December, 1961
HW-72347	January, February, March, 1962
HW-74377	April, May, June, 1962
HW-74378	July, August, September, 1962
HW-76228	October, November, December, 1962

Previous reports for 1961 and 1962 in the Plutonium Metallurgy Operation series were:

HW-68486	January, February, March, 1961
HW-70312	April, May, June, 1961
HW-70722	July, August, September, 1961
HW-72161	October, November, December, 1961
HW-73318	January, February, March, 1962
HW-74162	April, May, June, 1962
HW-74718	July, August, September, 1962

Previous reports for Metallurgy Development Operation were:

HW-76883	October, November, December, 1962
HW-77181	January, February, March, 1963

TABLE OF CONTENTS

[redacted] [redacted]

[redacted]

QUARTERLY PROGRESS REPORT
METALLURGY DEVELOPMENT OPERATION
APRIL, MAY, JUNE, 1963

I. SUMMARY

METALLIC FUELS TECHNOLOGY

NEW FUELS DESIGN

Experimental lithium-aluminum target elements Zircaloy-2 clad are being irradiated in high-temperature, high-pressure water cooled loops in order to evaluate the performance of these alloys under N-reactor conditions.

The recrystallization of warm and cold extruded aluminum-lithium alloy was studied and a treatment of 1 hour at 450 C was established for billet recrystallization.

Alternate fuel materials being studied include iron, silicon, and aluminum additions to uranium and iron, aluminum, and phosphorus additions to uranium-zirconium alloys for the introduction of dispersed intermetallic compounds in the structure.

A method of stress analysis has been developed for shaped end closures for tubular fuel elements. Figures showing the effect of end cap shape on stress distribution in N-fuels are presented.

FABRICATION DEVELOPMENT

N-inner tubes with the self-brazed closure, faced off to expose the braze annulus, completed 108 days in the TF7 high temperature loop (530 F, pH 10 water) without apparent corrosion of the braze annulus. A production test lot of fuel elements with this closure are prepared for irradiation testing.

[redacted] [redacted]

Development work on the Hot-Headed Projection Welded and Bonded Closure studied the effects of projection weld size, post heat conditions, and copper thickness on closure quality. Study of the shape of the ceramic restraining ring used during welding led to improvement in control of the fuel OD dimension.

A cracking problem encountered in the sizing of N fuel support was established to be associated with large hydride platelets formed during autoclaving. A simple annealing process to dissolve the hydride platelets followed by quenching restored the original ductility of the support.

Fabrication development on N-fuel support hardware continued with the processing of 58,000 inner supports, 75,000 outer supports and 27,000 outer support steel shoes during the quarter.

N-fuel containing up to 300 ppm phosphorus has been studied through fabrication to completed fuel. No detrimental effects on fabrication or fuel quality were noted for these contamination levels.

Sulfur additions to uranium result in the formation of the compound, US, and apparent eutectoid decomposition of the gamma phase.

Welding processes and assembly techniques were developed for the assembly of aluminum clad, aluminum lithium target elements, subsequently sealed in Zircaloy-2, and a production test quantity of elements were fabricated.

FUEL EVALUATION

Postirradiation examination of prototype N-reactor fuels continues to show good irradiation performance for these fuel elements. Density data continue to indicate that the fuel swelling rate in N-fuels will be nominal. A maximum volume increase of 2.5% was observed on an N-outer fuel component irradiated to 3100 Mwd/ton.

Tubular Zircaloy-2 clad uranium fuel elements have been irradiated at mean temperatures up to 535 C. At these higher temperatures the observed swelling is approaching the swelling predicted from the perfect gas laws.

N-inner fuel elements with tapered end caps (four bonded and four unbonded) completed irradiation to 1900 Mwd/ton in high temperature water. No evidence of the clad shearing mechanism was observed on either of the tapered end cap designs.

Irradiation of a fluted N-single tube fuel element continued in the ETR - M3 loop. Density measurements indicate 0.3% volume increase after 800 Mwd/ton exposure at a maximum fuel temperature of 520 C.

Examination of irradiated Zircaloy-2 clad fuel rods having striated cladding has shown that cladding defects of the order of 15% of the cladding thickness significantly reduced the uniform strain capabilities of the cladding.

A fuel element data handling system (FEDSY) has been established to assist in the analysis of experimental irradiation test information. The system will be used to correlate irradiation performance with irradiation history and preirradiation fuel element data and dimensions.

METALLIC FUELS DEVELOPMENT

High temperature irradiation testing of three Zircaloy-2 clad thorium-uranium fuel elements was initiated. The operating conditions include a maximum specific power of 70 watts/gram and a maximum fuel temperature of 600 C. Two cycles of irradiation in the ETR have been successfully completed.

Rods, 0.525 inch diameter, with 0.025 inch Zircaloy-2 cladding and Th-2.5 wt% Zr alloy core were fabricated by coextrusion to furnish stock for defect corrosion studies.

Melting and coextrusion was completed for the fabrication of Zircaloy-2 clad Th-1.5 wt% U-1 wt% Zr alloys for heat transfer studies of film build-up during irradiation. The coextrusions were 1.030 inch OD with 0.028 inch zirconium cladding and a 0.470 inch diameter Zircaloy-2 core.

Thorium additions of 0 01 to 3 wt% were made to Zr - 5 braze alloy for corrosion testing to determine the effect of thorium contamination on corrosion resistance.

[redacted]

PLUTONIUM PHYSICAL METALLURGY

T-T-T curves of the $\gamma \rightleftharpoons \beta \rightleftharpoons \alpha$ transformations of plutonium containing less than 250 ppm impurities by weight were obtained. The curves are similar to corresponding ones derived earlier from poorer quality metal but are shifted to lower times. The veining which is frequently observed on the surface of plutonium has been identified as bands of columnar grains, which form in the early stages of the $\beta \rightarrow \alpha$ transformation. Sharp discontinuities were observed on the $\delta \rightarrow \gamma$ isothermal reaction curves of metal known to contain certain impurities. The volume increases associated with each of these discontinuities were very rapid, and their number and magnitude increased with decreasing temperature. The incubation time of the $\gamma \rightarrow \beta$ transformation was two to three orders of magnitude greater in this metal than in high purity plutonium.

Preliminary studies on the weakening of plutonium under stress during transformation have shown that transformation strain is a significant portion of the total strain. Transformation strain increases with the applied stress and is greater for the $\alpha \rightarrow \beta$ transformation than for the $\beta \rightarrow \alpha$ transformation. Transformation strain also increases as the initial grain size decreases and is transformation rate dependent.

Fractography, the study of fracture interface by metallographic examination has been initiated.

Tensile testing of aluminum stabilized delta plutonium is in progress to determine the existence of the Portevin-Le Chatelier effect.

Despite the apparent lack of ductility exhibited by plutonium under tensile loading, it has been established that this material can be deformed severely (90% reduction) by flat rolling in the temperature range of 25 to 70 C (76 to 158 F). Roll pass schedules involving reductions up to 50% per pass have been successfully applied with a minimum of edge cracking. It appears that the rolling characteristics improve as the reduction per pass is increased. Preliminary X-ray diffraction data from the rolled material indicate major changes in the crystallographic orientation as compared with the as-cast structure. There is, however, no indication of line broadening

which would suggest the presence of residual stresses and/or extensive grain fragmentation. This observation is supported by the absence of significant changes in hardness after deformation at the lowest temperatures investigated (about 25 C (76 F)). This suggests that both the recovery and recrystallization temperatures are usually low.

PLUTONIUM MECHANICAL PROPERTIES

Special SR-4 strain gages are being applied to creep equipment to obtain high accuracy of very small strains.

PLUTONIUM MECHANICAL METALLURGY

Machineability of unalloyed plutonium has been studied in terms of the resolved forces at the tool post. The study has been expanded to include surface finish as an appraisal criteria In general, low tool forces are associated with good surface finish; this relationship, however, is only reliable for unworn and unchipped tools. Reducing depth of cut taken by a chipped tool to reduce tool force will not improve the surface finish.

II. METALLIC FUELS TECHNOLOGY

NEW FUELS DESIGN

Lithium-Aluminum Target Elements - V. L. Gelezunas

The fabrication of target elements for irradiation testing was completed and irradiation under simulated N-reactor conditions in the KER Test Loops 1 and 2 was initiated this quarter. The target assembly consists of a cylindrical aluminum-lithium alloy target core doubly canned (unbonded) in 2-S aluminum and Zircaloy-4 with the final closures of each can made in a helium atmosphere.

Considerable difficulty was encountered in developing techniques for the welding of the aluminum end plugs to the aluminum cans. The process which was developed consisted of electron-beam welding both end plugs, evacuating and back filling with helium through a 0.040 in. hole in one of the end caps, and sealing this hole by resistance welding a 0.040 in. thick 2-S aluminum disk to the end plug. The pressure exerted during resistance welding extruded part of the disk into the hole which provided a mechanical seal in addition to the resistance weld. Weld integrity was judged by means of X-ray examination and a helium leak check. Approximately 50% of the target elements which were processed were found to be unacceptable as a result of the aluminum welds. The Zircaloy-4 cans were sealed without difficulty.

Since further development in sealing the aluminum cans was indicated, a "Magneformer" was ordered and has been received and installed. The machine is currently being evaluated in terms of its applicability to specialized sizing and closure development associated with the fabrication of target elements.

In preparation for the irradiation test, two target elements were intentionally defected by drilling a 0.025 inch hole through the Zircaloy-4 cans. The elements were individually tested for approximately 200 hr

in an out-of-reactor water loop with the loop coolant at 280 C and 1250 psi. The loop water was sampled periodically and analyzed for aluminum. The concentration of aluminum above the background was detectable within 10 hr of start-up, peaked after 20 hr and decayed to the background level after 40 hr of the test. At the end of the test a visual macroscopic examination of the target elements showed no evidence of gross corrosion in the vicinity of the defect. The Zircaloy-4 can was removed and no evidence of gross corrosion of the aluminum was noted. These elements are being sectioned for further examination. This test indicates that a target element rupture occurring during irradiation can be detected by monitoring the irradiation test loop water for aluminum activity.

The transport of lithium in the alpha phase region of the aluminum-lithium system is being investigated. Diffusion couples have been prepared by cold-pressure welding 1.3 wt% Li-Al alloy to aluminum. The interface which has resulted is uniform to ± 0.002 in. in cylindrical samples 0.300 in. in diameter. Tests at 600 C indicate that sufficient lithium is vaporized in evacuated capsules to invalidate the results. At 300 C some evidence of lithium vaporization is indicated by a slight discoloration of the quartz sample holder. In order to eliminate this problem, diffusion samples in which the lithium alloy is not exposed at the surfaces are being prepared by co-extrusion of the aluminum-lithium alloy with aluminum.

Recrystallization Temperatures for an Extruded Al + $1\frac{1}{2}$% Li Alloy - J. C. Tverberg and P. A. Ard

Extrusion of an aluminum cladding over a lithium-aluminum core has resulted in several problems. The major problem has been that of forming a smooth, bonded interface between the core and cladding. First extrusion attempts used cast cores and 1100 aluminum cans, coextruded at 350 C at a reduction ratio of 15.4 : 1. The resulting interface was very rough and irregular. The second attempt used pre-extruded core that was considerably harder than the as-cast core. Extrusion at the same conditions resulted in an irregular but smoother interface, as shown in Figure 2.1.

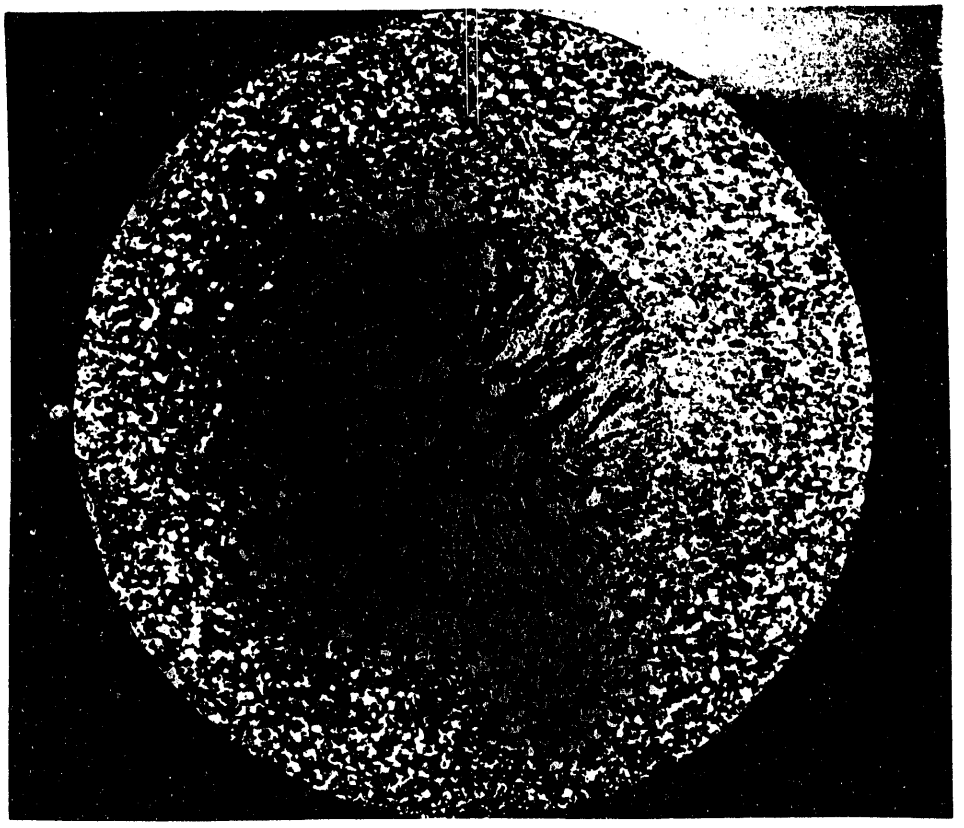

FIGURE 2.1

Cross Sectional View of a Coextruded Aluminum Clad, Al + 1.5% Li Core

(The core was pre-extruded prior to coextrusion; note the large, cast structure of the Al-Li core. NaOH etch, 4X)

Here, the cast structure is very evident, with the interfacial roughness corresponding to the cast grains. A third attempt was made using a recrystallized core and coextruded at 15.4 : 1 ratio at 400 C. The result was a very smooth, well bonded interface. A well bonded interface was dependent mainly upon the cleanliness of the components prior to assembly. Chemical cleaning would not produce a clean, well bonded interface. The best results were obtained by mechanically cleaning both the can inner surface and the core outer surface prior to assembly and welding.

Recrystallization times and temperatures were determined by heat treating a series of pre-extruded cores in argon for 30 min and 1 hr at

300, 350, 400, 450, and 500 C. The billets had two degrees of cold work. One was cold extruded at 20 C at a ratio of 3.62 : 1, the other was warm extruded at 200 C at a ratio of 3.24 : 1. The results are seen in Figures 2.2 and 2.3. Here we can clearly see the progress of recrystallization. Figure 2.2, which illustrates the rate of recrystallization of the 20 C extruded core, shows a much faster rate of approach to the equilibrium condition than Figure 2.3 which gives the recrystallization rate of the 200 C extruded core. This difference in recrystallization rate is due to the amount of cold work in the material, hence to the number of nuclei available as recrystallization sites. A comparison of the structures after identical heat treatments, namely 450 C for 1 hr, is seen in Figures 2.4 and 2.5. Here we see that the 20 C extrusion has a considerably finer grain than the material extruded at 200 C. The warm extruded material required grain growth to remove the worked structure while the cold extruded material achieved the same result solely through recrystallization. Very little of the wrought structure is seen in the recrystallized cold extruded material while the wrought texture is clearly seen in the warm extruded material. After 1 hr at 500 C both specimens showed some grain growth, but the warm extruded material showed a higher growth rate than the cold worked material.

One more point of interest is observed from the hardness curves of Figures 2.2 and 2.3. The 30 min anneal at 300 C in both materials shows a slight hardness increase. This indicates an age-hardening effect which would be expected in a system such as the aluminum-lithium system that shows an increasing solid solubility with increasing temperature. In both cases the material was quench cast into a water cooled mold. Although the material was theoretically within solid solubility limits at room temperature, there probably existed domains of higher lithium content. Upon heating to 300 C, which is just within the two phase region, precipitation began to occur. Quenching the specimen after 30 min preserved this minute amount of second phase, resulting in a hardness increase. The longer heating time, 1 hr, resulted in partial resolution of the second phase by diffusion, thus resulting in a lower hardness. This is further confirmed in the warm extruded

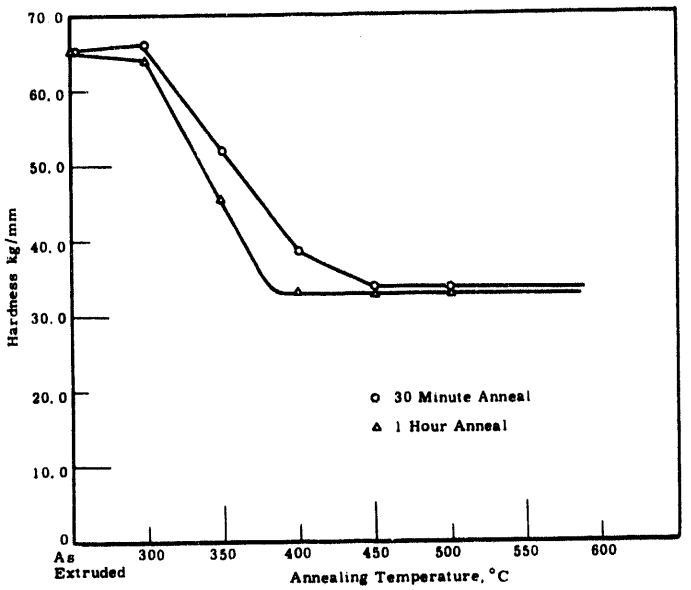

FIGURE 2.2

Hardness of Cold Extruded (Room Temperature) Al + 1.3% Li As a Function of Annealing Time and Temperature (Recrystallization is complete after 1 hr at 400 C or 30 min at 450 C. After these times grain growth begins.)

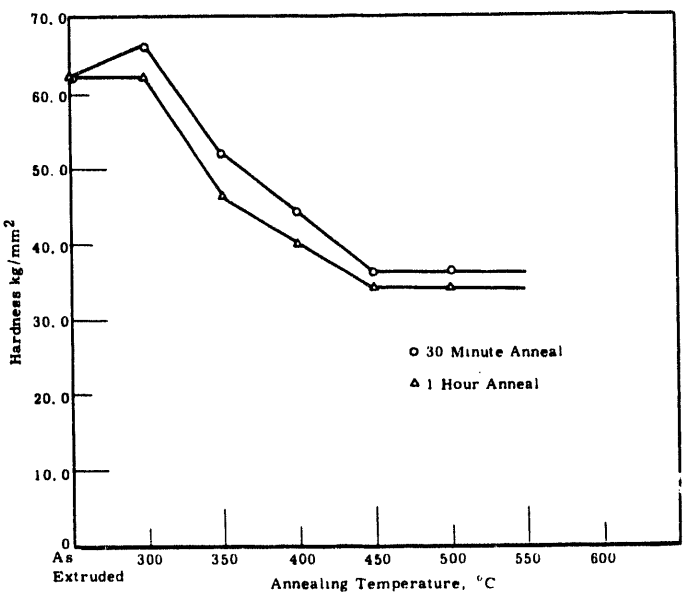

FIGURE 2.3

Hardness of Warm Extruded (300 C) Al + 1.5% Li as a Function of Annealing Time and Temperature

AEC-GE RICHLAND, WASH

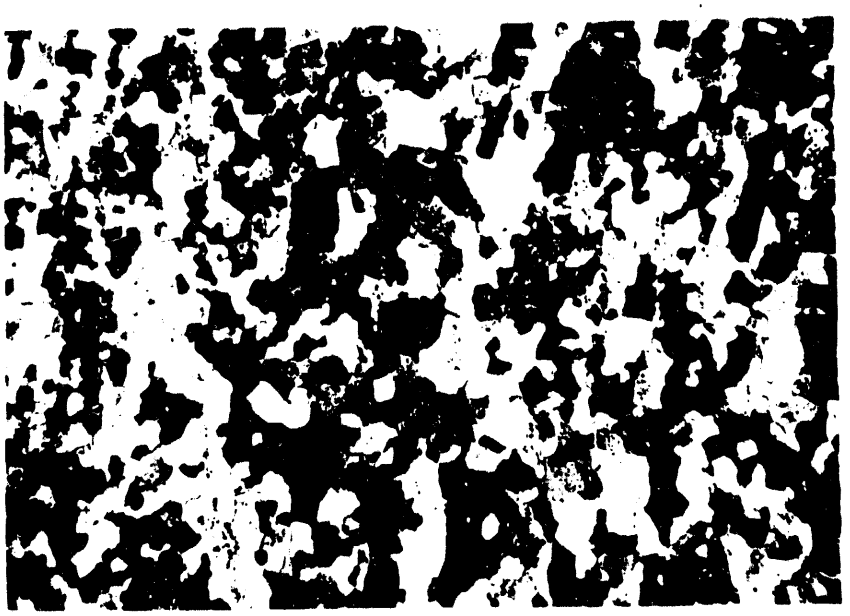

FIGURE 2.4

Recrystallized Structure of an Al + 1.3% Li Core

(Extruded at 20 C, heat treated 1 hr at 450 C. Note the fine recrystallized structure and the lack of extruded texture. Polarized Light (100X))

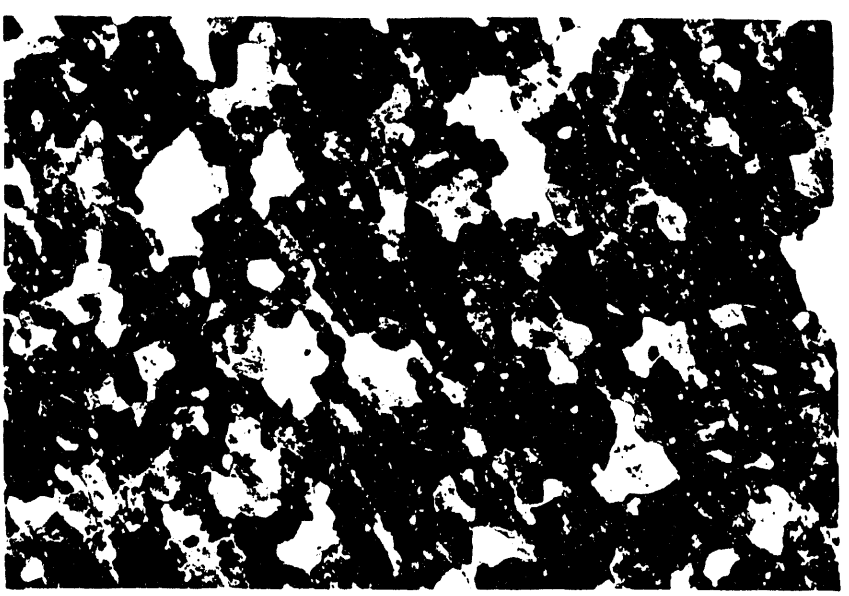

FIGURE 2.5

Recrystallized Structure of an Al + 1.5% Li Core

(Extruded at 200 C, heat treated 1 hr at 450 C. Here the grain size is considerably larger, indicating grain growth, and the extrusion texture more evident. Polarized Light (100X))

specimen which had a higher initial lithium content, 1.5% as opposed to 1.3%. Here the hardness increase is even greater and may, in part, account for the slower adjustment to equilibrium.

On the basis of these data, a recrystallization treatment of 1 hr at 450 C was chosen. This treatment resulted in a recrystallized structure with a minimum of grain growth.

N-Fuel Element Support Scratching Tests - J. W. Weber

Test charging of prototype N-reactor fuel elements in full-sized N-reactor Zircaloy-2 process tube have shown that scratching of the process tube occurs under some conditions.

A series of tests has been conducted to determine to what extent the reactor process tube is damaged by the repeated corrosion of the bare Zircaloy-2 that is exposed by scratching by the fuel element supports. The test cycle consisted of passing steel support shoes forty times over a single path on the process tube followed by autoclaving the tube in 400 C, 1500 psi steam for 14 days to give a corrosion product buildup on the bare Zircaloy-2 equivalent to that expected to form in-reactor between the charge and discharge of the fuel elements.

The sixth and last autoclave cycle has been completed and 40 passes made on the process tube in the same damaged region as the previous tests. After the third, fourth, and fifth autoclave cycles, 50 passes with steel shoes were made with no sign of scratching the process tube and it was necessary to intentionally initiate scratching in order to continue with the original purpose of the tests. However, in this last cycle the scratching started immediately. The maximum total depth of the damaged region after the last 40 passes is 0.0025 in. and the average over the length of the tube is 0.0016 inch. From the data on these tests, the increase in scratch depth per cycle is 0.00035 to 0.00045 inch. This rate of wear extrapolates to 0.018 to 0.023 in. in 2000 passes as compared to a maximum of 0.003 in. wear in a test in which 2000 passes were made on a tube without intermediate autoclaving.

There are two possible sources for the difference in wear rates. The removal of the autoclave film formed between each series of passes may result in deeper total scratch depth in the cyclic scratch autoclave test, or the autoclaving cycle at 400 C may cause recovery of the cold-work thought to be induced in the surface of the tube during the scratching test. In reactor, the cold-worked surface of the tube would not be annealed as in the autoclaving, but there would be a corrosion film formed.

To determine how much of the damage is caused by removal of the corrosion film and what the possible annealing effects are in the autoclave tests, two new series of tests have been started. In the first test a section of process tube, designated as Section B, is scratched with 50 passes of steel shoes and then is heated in a vacuum at 400 C for 14 days. This is the same heating cycle as used in the autoclave tests. Two series of 50 passes with a heating cycle between them have now been completed. The second series of passes increased the depth of the scratch a maximum of 0.0002 inch.

The second test being conducted on process tube Section A consists of 500 passes with steel shoes followed by a heating cycle of 400 C for 14 days in a vacuum. The first 500 passes resulted in a maximum scratch depth of 0.0012 inch. The second series of 500 passes after a heating cycle did not increase the the scratch depth.

From the results of the test on process tube Section B it appears that the tube is work hardening as a result of the scratching and that the autoclave heating cycle does not result in a recovery of the work hardening. The results from the test on process tube Section A are not inconsistent with this if it is assumed that at the end of the first 50 passes the work hardening is not complete and that, therefore, in the next series of 50 passes material continues to be removed. Further tests on tube Section A should then show a decrease in the amount of material removed as the work hardening increases.

Additional tests are being run on both tube sections.

Alternate Core Materials - R. S. Kemper

The particle size and distribution of intermetallic compounds in standard N-fuel (150 Fe - 100 Si) is being determined for material in the single beta heat treated, braze heat affected and single beta heat treated, and the straightened and re-beta heat treated conditions. These data will serve as a basis for structure comparison of alternate compositions being studied as dispersed phase systems. The major difference observed in optical microscopy is the development of a preferred distribution of compounds in the braze heat affected region of the fuel sections, resulting from the gamma phase treatment of this region.

N-outer tube stock with the core material containing 640 ppm aluminum, 400 ppm iron, and 85 ppm silicon was studied to determine the effects of heat treatment on the size and dispersion of UAl_2 and $U_6Fe(Si)$ compounds. Particle density determined from electron micrographs of cathodically etched specimens and utilizing a Zeiss particle size analyzer to obtain particle size distributions in a computer program similar to that employed for analysis of fission gas porosity has yielded values of 1.5×10^{11} and 8.2×10^{11} particles/cc in specimens beta treated and alpha aged and gamma treated and alpha aged respectively. The etching procedures used for preparation of specimens for electron microscopy is continuing in attempts to arrive at a standard procedure yielding true structure in these dispersed phase alloys.

Additional materials being studied include arc cast buttons of 1) U-wt% Zr-200 ppm Fe-350 ppm Al, 2) U-1 wt% Zr-350 ppm P and, 3) U-400 ppm Fe-700 ppm Al. Sections of these were treated 3 days at both 800 C and 1050 C, water quenched, and reheated 100 hr at 600 C. The resulting structures and distribution of intermetallic compounds are being studied by optical and electron microscopy.

Analysis of Fuel Element End Caps - K. R. Merckx

The difference in thermal expansion between fuel and end cap materials in metallic fuel elements is a potential cause of fuel element failures. A numerical method of stress analysis for shaped end closures with thickened or re-enforced cladding near the end cap has been developed, programmed, and numerically evaluated. General case studies have been run for transitions with linear and power laws of thickening. These studies indicate that major reductions in bending stresses can be obtained with the use of transitions. If the transition length is prescribed, the linearly thickened cladding, when properly designed, will give the lowest bending stresses throughout the cladding region, but if the thickening becomes too great then the strains will occur at the end of the thickened region and the transition zone will have little effect on reducing the maximum stress conditions. Properly designed transitions described by power relationships of thickening have nearly the same bending stresses as the optimum designed linearly thickened cladding. The transitions which are described by power laws have lower bending stresses near the end cap and are less critical in regard to the length-to-height ratio of the transition. In order to show how the method of analysis is applied to an actual fuel element, case studies were run for the "N"-inner and "N"-outer fuel elements. Figure 2.6 shows the increase in thickness versus length of transition for the inner and outer cladding for an "N"-inner fuel tube for an optimum shape of a linearly thickened transition. Assuming that the entire width of the fuel component is to be utilized for the closure, the closure designs for the "N"-inner fuel tube, Figure 2.7 and the "N"-outer fuel tube, Figure 2.10 have been found. A comparison of the stresses on inner and outer claddings for fuel elements with and without transitions are given in Figures 2.8, 2.9, 2.11, and 2.12. The general case studies and the designs for the end closures are described in Document HW-77816.

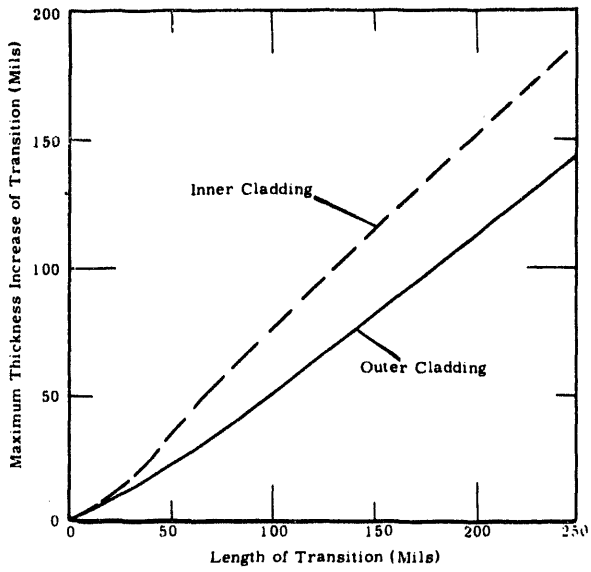

FIGURE 2.6

Ideal Transition Length to Thickness Ratios for Linearly Thickened Cladding
(Inner and outer cladding of N-Inner Fuel Tube with transition region under uniform bending stress)

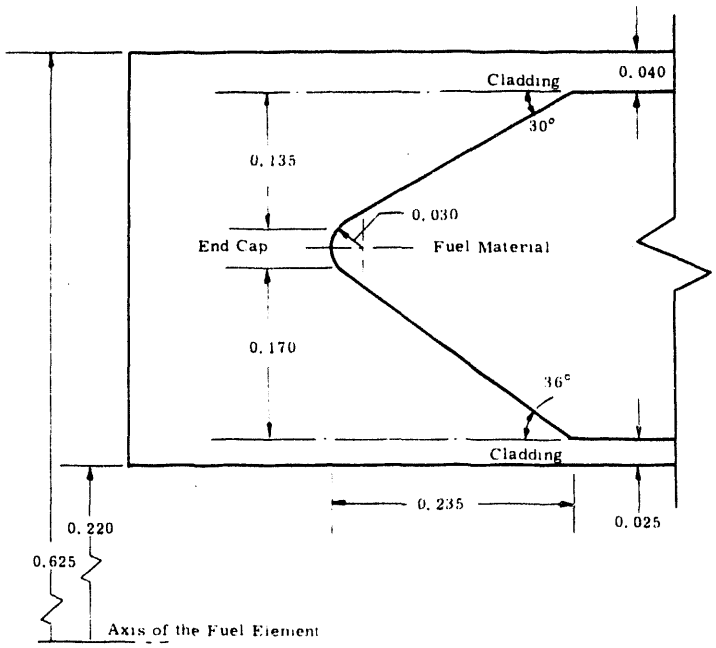

FIGURE 2.7

N-Inner Fuel Tube with V-Shaped End Cap
(Designed to have transition zones under uniform bending stress.)

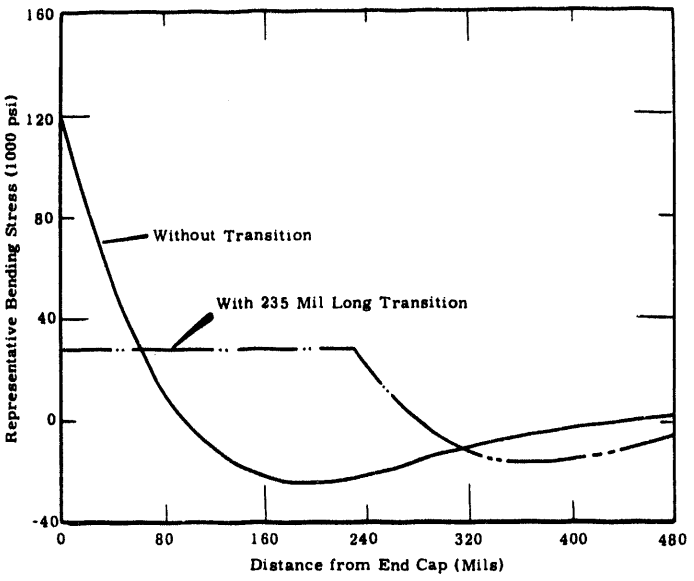

FIGURE 2.8

Bending Stress Distribution Versus Distance from End Cap
(Outer cladding of N-Inner Fuel Tube with 235 mil linear transition length and ideal transition length to thickness ratio.)

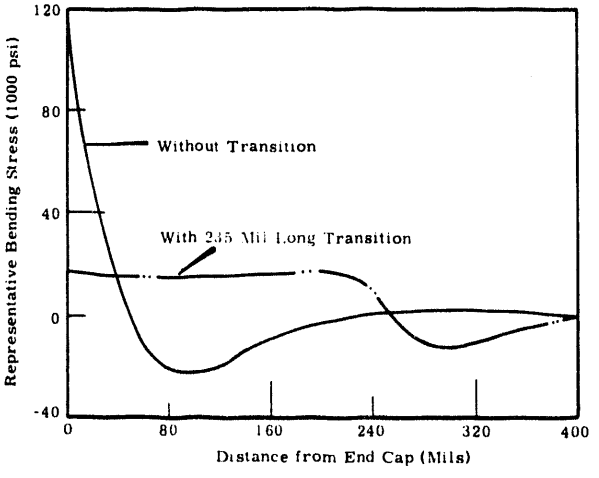

FIGURE 2.9

Bending Stress Distribution Versus Distance from End Cap
(Inner cladding of N-Inner Fuel Tube with 235 mil linear transition length and ideal transition length to thickness ratio.)

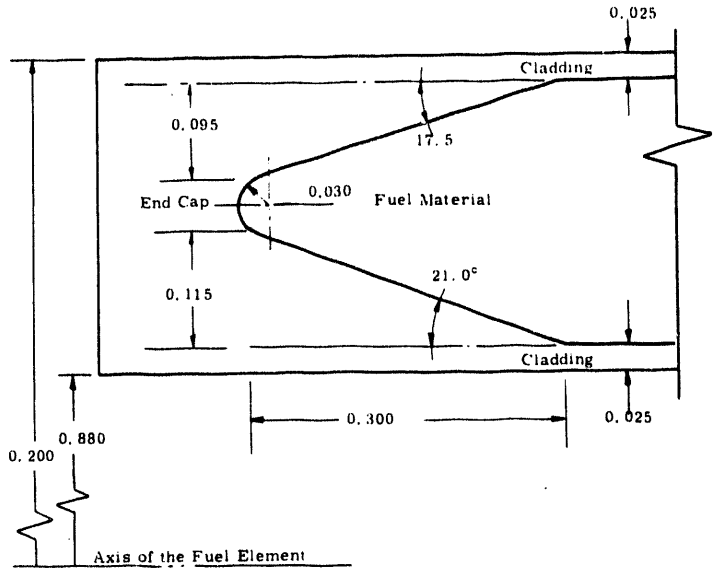

FIGURE 2.10

N-Outer Fuel Tube with V-Shaped End Cap
(Designed to have transition zones under uniform bending stress.)

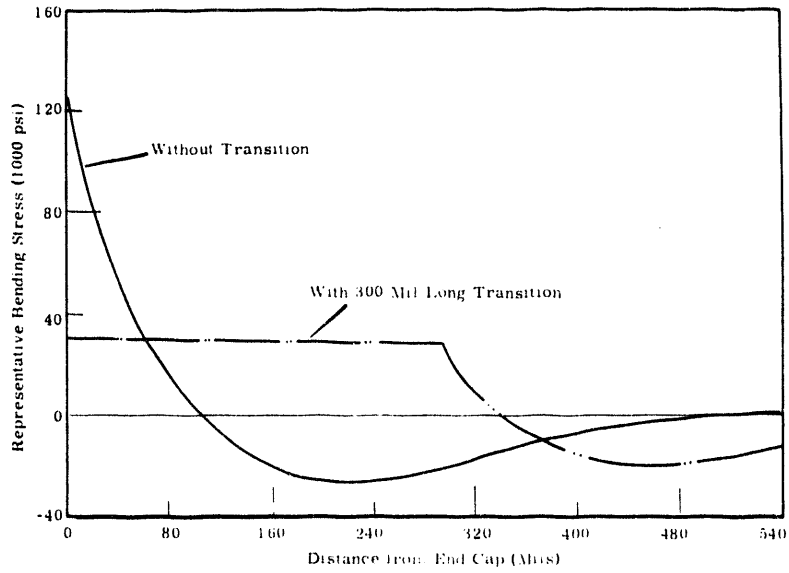

FIGURE 2.11

Bending Stress Distribution Versus Distance from End Cap
(Outer cladding of N-Outer Fuel Tube with 300 mil linear transition length and ideal transition length to thickness ratio.)

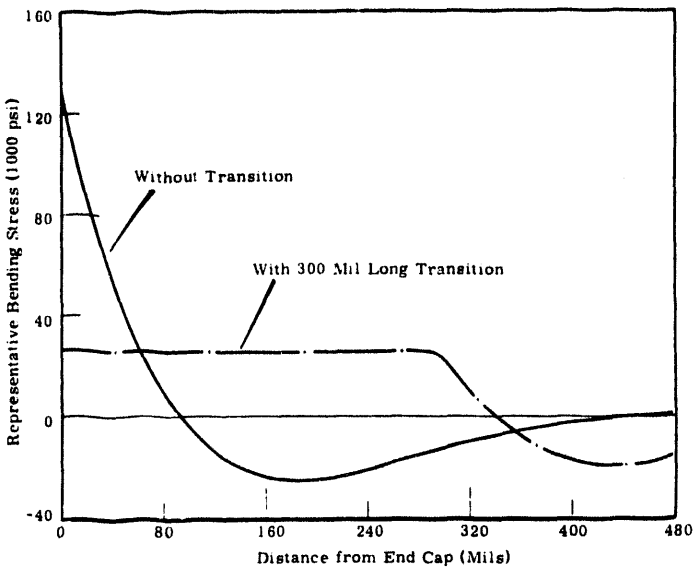

FIGURE 2.12

Bending Stress Distribution Versus Distance from End Cap (Inner cladding of N-Outer Fuel Tube with 300 mil linear transition length and ideal transition length to thickness ratio.)

Since an experimental fabrication program is in progress for developing hot-headed closures, a series of cases were run which represented the actual geometries obtained from fuel elements already fabricated. These fuel elements could not be represented by the power dependent thickening. A power dependent exponential, which resembled the probability function, was used to represent these closures. Case studies were run on these geometries. The studies covered the effect of maching off various amounts of the hot headed closure before projection welding, various lengths of the transition zone, and various rates of cladding thickening. Machining off part of the hot headed region did not significantly change the stresses in the maximum stress area. The actual shape of the transition near the cladding had the most important effect. For the closures presently being formed, the bending stresses were from two to three times less than for those encountered without transitions.

Besides the mechanical analyses, analyses of the temperature distribution, based on a nodal point solution, has been programmed and numerical results obtained on a representative case. The fluted fuel element closure studied is described in another section of this report. Figure 2.23 (p. 2.35) shows the isotherms obtained from this program. The numerical solution will apply to fuel elements with arbitrarily shaped end closures as long as the fuel element has a cylindrical geometry and the closure has axial symmetry.

Vibrational Studies - K. R. Merckx

A theoretical study has been completed on the effect of process tube vibrations and their relation to fuel element support design. Two programs were developed: One vibrates a fuel assembly using a two component model, and the second provides for the calculation of the spring constants of various shaped supports. The spring constant program only applies to nonsized supports. The vibrational program can be used with either calculated or measured values for the support spring constants. A document describing these programs (HW-77515) has been published.

FABRICATION DEVELOPMENT

Self Brazed Closure - E. A. Smith

The development program for NPR inner tubes was concluded with the completion of a high-temperature loop test on three specimens (6 closures), one of which had been faced off on the end to expose the annulus of braze material to the reactor coolant water. The objective was to learn whether the braze material would be sufficiently resistant to corrosion to permit full-term irradiation of the element even though it might have a leak in the primary closure (weld bead). After 96 hr in the steam autoclave, and 108 days on the TF7 high temperature loop (formerly known as ELMO 7) under standard test conditions (530 F, pH 10 water), the exposed brazed layer appeared unaffected. Thus it appears that the very thin layer of this Zr-Cu-Ni braze material used in the "Self-Brazed" closure will be

satisfactory for use in making closures on production elements. In addition, this closure process offers several advantages over the normal Zircaloy - 5 Be braze which make it favorable for production use. A test lot of elements with closures processed by this method has been prepared for charging in-reactor, and is awaiting the preparation of papers to cover such test.

Hot-Headed Closure Studies - W. F. Brown

Since the last reporting period, effort on the Hot-Headed Projection Welded and Bonded Closure was applied to studies of various elements of the welding procedure in an attempt to improve the closure. A brief summary of this effort and the results are described below.

The procedures currently used to produce sound projection welds on Hot-Headed NIE type fuel elements utilize ring projections which are machined 0.030 inch wide at the base of the projection. After projection welding, the weld widths are approximately 0.035 - 0.040 inch on the OD weld and 0.030 - 0.035 in. on the ID weld. When the width of the machined projections was increased 0.040 in., the weld widths increased to approximately 0.045 - 0.050 inch. This increase in weld size produces a weld which is larger than the thickness of the fuel element cladding. The quality of these welds was not as consistently sound as the narrower welds. This variation in quality may have occurred because the welds were made with the maximum current output of the laboratory machine. It is planned to make welds on equipment with greater current capacity.

Immediately after the projection welds are made, postheat current at reduced levels is applied to the joint while pressure is maintained to effect bonding at the joint interfaces between projection. Several series of samples were welded using different postheat current levels and time. It was demonstrated that a variety of postheat schedules can be used to obtain bonding of both the uranium-Zircaloy and the Zircaloy-Zircaloy joints. The uranium-Zircaloy joints are bonded before the Zircaloy-Zircaloy joints. Apparently the uranium in the vicinity of the joint reaches the melting point during a successful closure weld.

[redacted]

Copper which is used to assist in obtaining bonds at the joint interface between ring projections is placed on the end caps by immersion plating techniques. To study the effects of the quantity of copper on the joints, a series of samples were made using varying amounts of copper. The amount of copper was varied by controlling plating time. The following table indicates the relationship between plating time and the amount of copper deposited on Zircaloy. Although these studies are not complete, cursory metallographic examination of single cross sections of each joint showed no apparent differences in the uranium-Zircaloy joints but did show improvements in joint geometry and thickness of the Zircaloy-Zircaloy joints as the amount of copper was reduced.

TABLE 2.1

PLATING TIME VERSUS COPPER DEPOSITION

Time, sec.	Thickness, in.	Coverage, % Cu
15	0.00081	56.1
30	0.00085	71.2
45	0.00080	80.2
60	0.00081	81.2
75	0.00081	87.1

To prevent plastic deformation of the fuel element during welding, a cylindrical ceramic restraining ring with parallel walls was used. Measurements of sample fuel elements after closure welding revealed that the diameter of the element decreased in the joint region under the restraining ring. The extent of change varies with welding conditions. It was found that control over dimensional change can be obtained by grinding a suitable taper over a portion of the ID of the restraining ring. Figure 2.13 is a schematic diagram showing the fuel element configuration and the essential steps in producing a Hot-Headed Projection Welded and Bonded Closure.

[redacted]

[redacted]

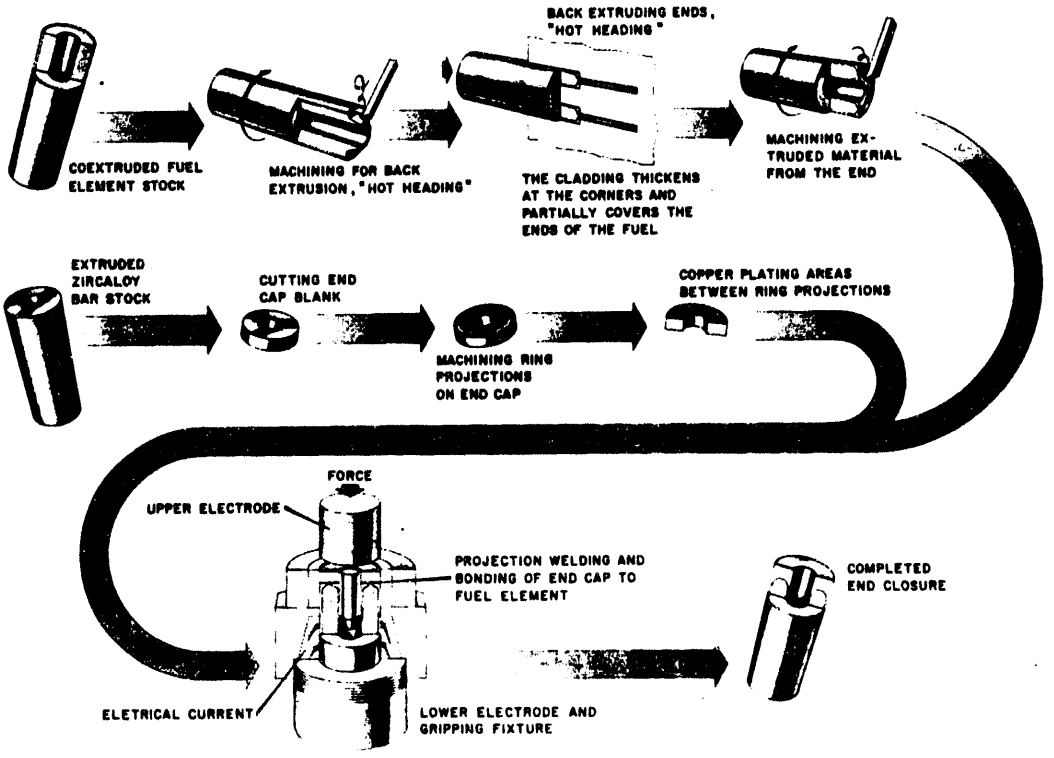

FIGURE 2.13

Schematic Diagram Showing the Fuel Element Configurations and the Essential Steps in Producing a Hot-Headed Projection Welded and Bonded Closure

N-Reactor Fuel Support Development - D. P. O'Keefe

In the assembly of the inner and outer tubes which make up the N-fuel it is necessary to "size up" the inner supports to center the inner fuel and produce a specified spring constant in the inner fuel support system. The sizing operation is done by mechanically deforming the support to decrease its length and increase its height after the inner fuel

is in place. This operation is done after the fuel components have been autoclaved in 400 C steam for 72 hours. Although the supports have more than adequate ductility to take the sizing deformation without damage in the "as fabricated" condition, it was found that sizing would produce cracks in autoclaved supports. The cracks originated on the inner surface of the loops in the supports where the sizing operation imparted a tensile strain of about 10%. This susceptibility to cracking was found to result from the presence of hydride platelets which form in the Zircaloy-2 during slow cooling (about 1 C/min) in the autoclave. Either the crystallographic orientation or mechanical texturing of the zirconium in the loops of the supports was such that the hydride platelets formed approximately normal to the inner surface of the bend where large compressive strains occurred during forming. Since the sizing operation places this region of the part in tension, the hydrides act as crack initiators (Figure 2.14). Elsewhere in the support the platelets form parallel to the rolling direction of the strip and do not influence the bend ductility.

After autoclaving, the supports contain a maximum of about 70 ppm hydrogen. Since this concentration of hydrogen may be put in solution in Zircaloy-2 at about 275 C, it was found that a solution anneal at 300 C followed by quenching eliminated the large platelets and restored the ductility of the part. This postautoclave annealing procedure was incorporated in the manufacturing process for N fuels and has eliminated the support cracking problem during sizing.

Annealing studies also indicated the possibility of altering the texturing in the Zircaloy-2 that orients the platelets. By annealing the support at between 600 and 750 C before autoclaving, the ductility of the part is retained after autoclaving. The apparent influence of alpha phase annealing on texturing in this part is being investigated.

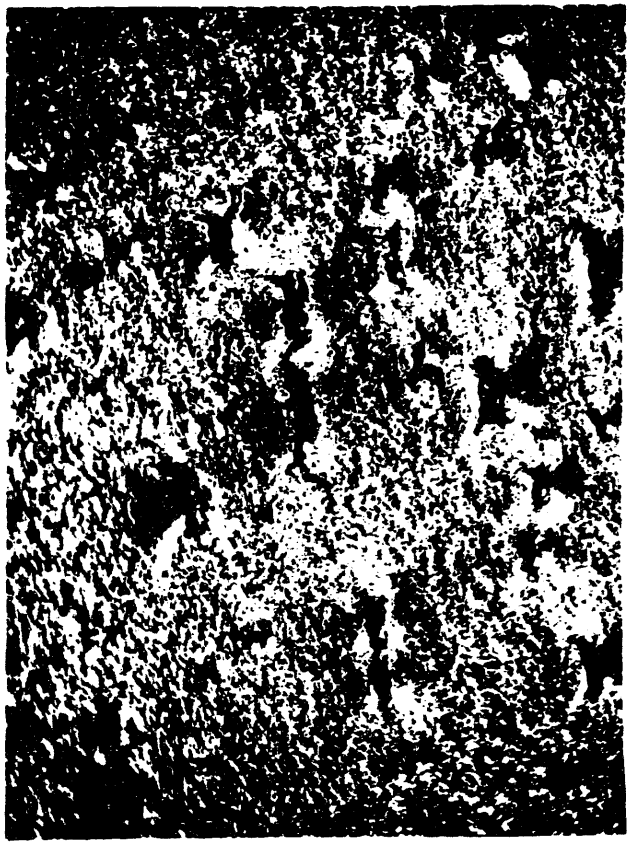

100X

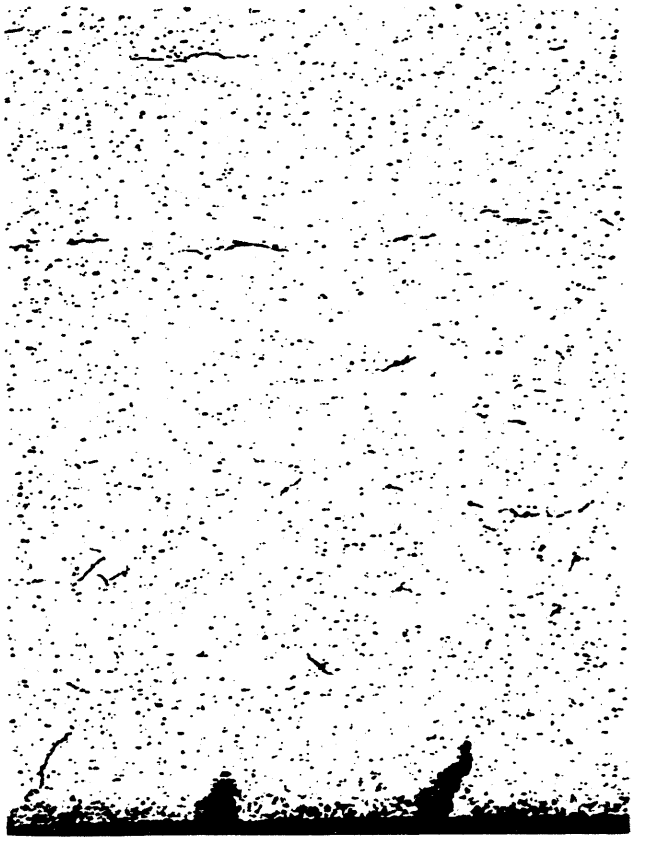

250X

FIGURE 2.14

Zircaloy-2 Support Furnace Cooled from 300 C

(Inner surface of loop with about 10% tensile strain shown at the left. At the right is a longitudinal section through this area.)

Fuel Element Support Fabrication - J. P. Pilger

In support of N Reactor Department, a considerable development effort on fuel support hardware continued throughout the quarter. A total of 58,153 inner supports were dimpled on the crankpress. Total throughput of inner supports for the crankpress was 102,307 parts.

Outer supports and steel shoes were fabricated during the same period. During the last quarter 26,885 steel shoes were formed on the crankpress. The total number of shoes formed was 52,903. Supplying 74,909 outer supports during the last quarter has permitted continual processing of the N-outer fuel elements. A total of 96,999 outer supports have been fabricated to date.

Phosphorus Impurity in Uranium - R. S. Kemper

Phosphorus, in quantities to 400 ppm at the ingot stage, was introduced into the metal for N-Reactor and the enriched I & E fuel due to a change in scrap recovery processes at the AEC Feed Materials Production Center. The effect of this additional contaminant on the uranium structure, fabricability, properties, and fuel element quality is being studied.

The formation of a eutectic between the compound, UP, and uranium at an estimated concentration of 1000-1500 ppm phosphorus was reported in the previous quarterly report. Microprobe analysis by NLO and MCW confirmed the identity of the compound as UP (11.52 wt% phosphorus). Sections of derby metal containing 430 ppm phosphorus were held 4 hr at 900, 950, 1000, and 1050 C and water quenched. Metallographic examination showed no indication of solubility of the phosphorus at any of these temperatures. Additional melting point determinations on ingot stock containing phosphorus continue to show a depression in melting point of approximately 10 C compared to nonphosphorus metal of similar base composition.

Two 11 in. diameter cast and beta heat treated ingots were examined in the ingot condition, after primary extrusion at HAPO, and following coextrusion in the finished fuel condition (braze closed and beta heat treated). One of these was NIE stock (135 ppm phosphorus) and the other NOE stock

(280 ppm phosphorus). Additional NIE coextruded elements containing 170 and 300 ppm phosphorus and NOE coextruded elements containing 80 ppm phosphorus were also examined. The eutectic structure is broken up during primary extrusion and coextrusion and the UP inclusions are dispersed in much the same manner as uranium carbides in the finished fuel sections. No detrimental effects on clad to core bonding, braze to core bonding, or core structure were observed at any of these phosphorus levels. Tensile property data to 200 C are shown in Table 2.2. The addition of phosphorus lowers the room temperature ductility resulting in brittle fracture and thus lowers the ultimate strength. At temperatures of 100 C and higher no differences due to phosphorus are noted.

TABLE 2.2

EFFECT OF PHOSPHORUS CONTENT ON TENSILE PROPERTIES OF URANIUM*

Coextrusion Number	Phosphorus Content, ppm	Test Temperature, °C	0.2 Yield Strength, 1000 psi	Ultimate Strength, 1000 psi	Elongation-Percent in 1 in. gage
1151	<50	Room Temp	56.1	132.2	17.5
		100	40.2	99.0	26.0
		200	43.4	72.3	27.0
1779	170	Room Temp	54.3	100.5	7.0
		100	44.0	97.8	23.0
		200	39.6	72.3	30.0
1861	296	Room Temp	47.0	110.1	13.0
		100	43.1	94.2	23.0
		200	40.8	75.9	26.0

* Samples prepared from NIE coextrusions in the beta heat treated condition. All standard iron and silicon addition.

Attempts to prepare higher phosphorus contents by arc melting buttons of uranium with UP have resulted in structures composed of uranium, uranium-UP eutectic, and an additional compound that is apparently a uranium oxygen-phosphorus phase. The complete eutectic structure has been observed in segregated sections of these melts but not in quantities satisfactory for analysis.

Sulfur Impurity in Uranium - R. S. Kemper

An alternate scrap recovery process at NLO will use uranyl ammonium sulfite (UAS) to replace the uranyl ammonium phosphate (UAP) feed to the Winlo process. The effects of sulfur additions to uranium are being studied. Arc melt buttons were prepared using uranium and US to yield approximately 500 and 2500 ppm sulfur. Compound formation was observed that was confirmed as uranium sulfide by J. W. Colby at NLO by microprobe examination. Variable sulfur content in the compound was observed, indicating either "coring" or possibly variable oxygen content in the US phase. Specimens were held 4 hr at 800 C and either water quenched or slowly cooled. Apparent eutectoid decomposition of the gamma structure was noted. The quenched sample appeared to retain the sulfur content of the eutectoid in solution. These features are shown in Figures 2.15 and 2.16.

2500 ppm Sulfur

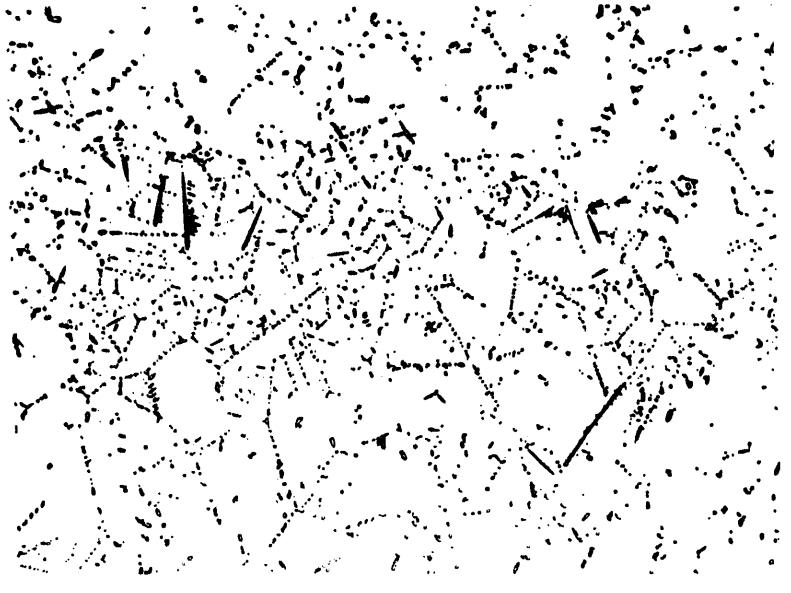

5000 ppm Sulfur

FIGURE 2.15

Uranium Sulfide (US) Inclusions in Arc Melted Dingot Uranium Buttons
As Polished 100 X

4 hr 800 C - Water Quenched

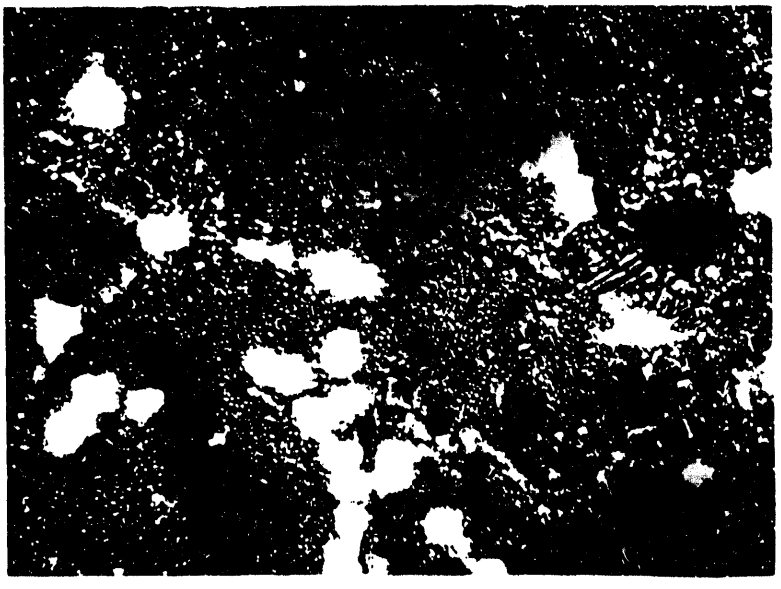

4 hr 800 C - Slow Cooled

FIGURE 2.16

5000 ppm Sulfur in Uranium

(Shows apparent gamma phase solution (upper) and eutectoid formation (lower), bright inclusions, arc-US compound. 500X polarized light. Phosphoric electrolytic etch 10 sec - 18 volts 2 min - 6 volts.

Fabrication of Lithium Aluminum Target Elements - W. I. Steinkamp

A lithium aluminum target element design intended for irradiation in pressurized, high temperature water has been fabricated. The element design required canning a hollow rod of Al-Li in aluminum, canning a second time in Zircaloy-2, and finally providing supports for the rod. The welding processes are described below.

Lithium aluminum cores are placed in aluminum tubes and the ends stopped with steel plugs. This assembly is pushed through a die. The aluminum is trimmed to length and the steel plugs removed. Aluminum end caps 0.002 in. undersize are welded in place by electron beam welding. One end cap has a 0.040 - 0.060 in. hole through the center. The element is clamped in a collet on the resistance welder. After evacuation and backfilling with helium a disc is spot welded to the end to close the hole. See Figure 2.17. The pieces are given a helium leak check and are X-rayed. Whatever surface treatment is required for the aluminum is done at this point. The aluminum pieces are then put in Zircaloy cans. After evacuation and helium backfilling, these are TIG welded in a helium filled glove box. All elements in the PT were welded in the 308 Building glove box. The pieces are again helium leak checked and the Zircaloy welds X-rayed. Supports are attached by resistance welding.

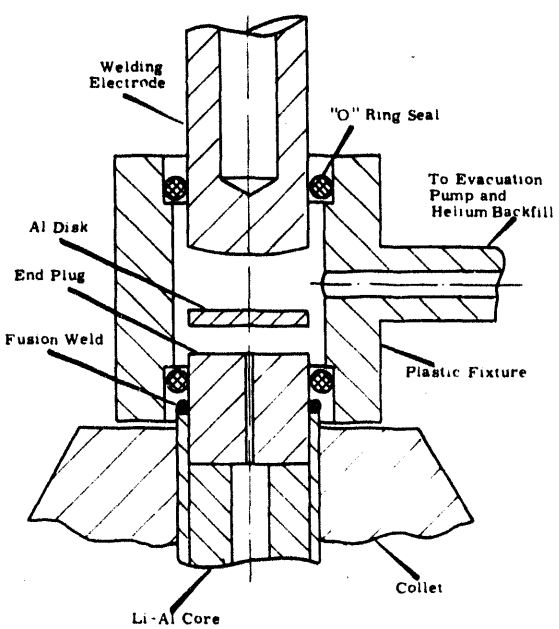

FIGURE 2.17
Section Showing Methods of Closing Target Elements

[redacted]

Initially it was planned to close the aluminum end caps by a threaded plug and a fusion weld. This was not at all successful because of gas voids in the welds. Replacing the threaded part with a tapered pin did not improve the yield enough to make it a practical method of fabricating elements. An attempt was made to close the elements without a weep hole using dc helium + TIG welding. Again the yield was too low to be acceptable because of a tunnel shaped void at the base of the weld. See Figure 2.18.

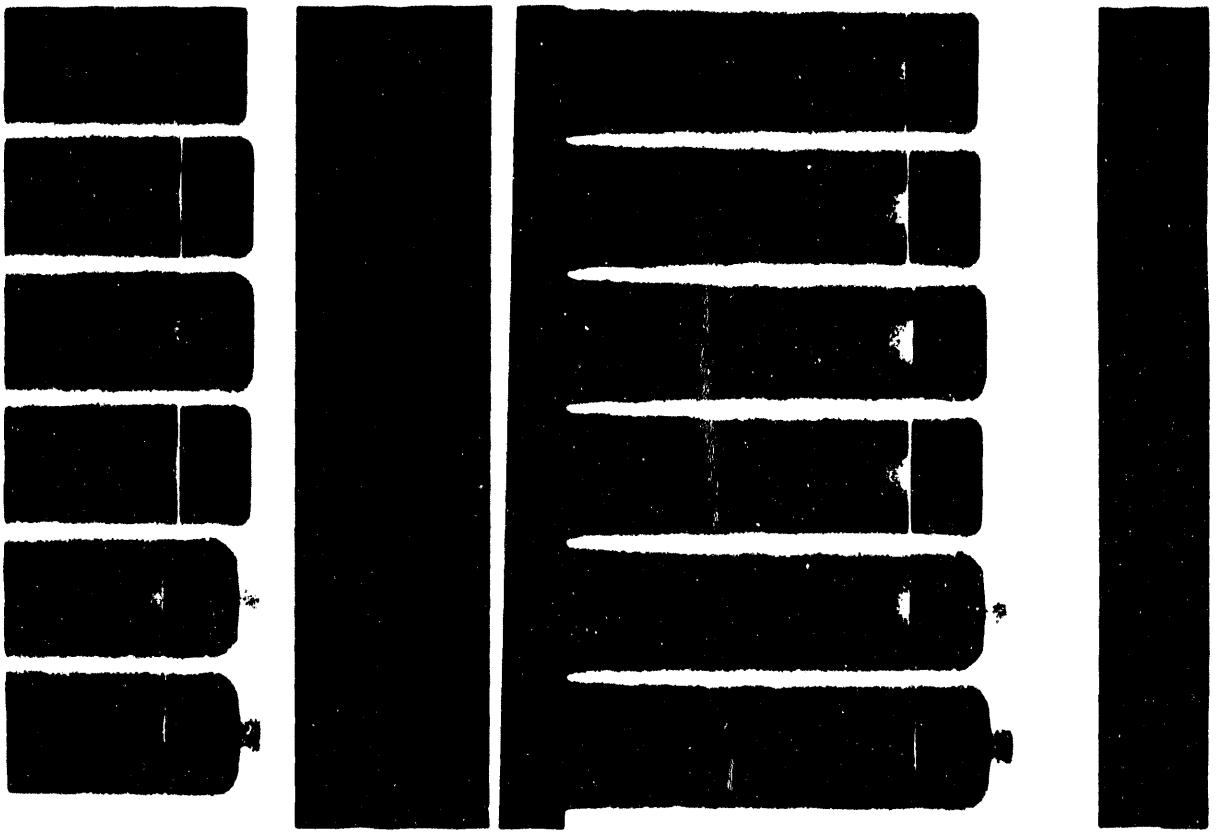

FIGURE 2.18

X-Ray of Aluminum Welds on Target Elements Showing Tunnel Type Void Encountered in TIG Welding Without Relief Hole

[redacted] [redacted]

Drawing Vanadium - F. B. Quinlan

It was requested that a 1/4 in. diameter vanadium rod be drawn down to 10 mil wire. The rod contained 0.1% of cobalt and was made by the Vanadium Corporation of America. They had been requested to supply the finished wire but were unable to get beyond the 1/4 in. diameter rod size.

The first step in reducing the rod to a wire was to remove numerous superficial mechanical defects (folds, laps, and notches) from the surface. The rod was then cold swaged to 1/8 in. diameter and vacuum stress relief annealed at 800 C. Cold worked vanadium recrystallizes in the temperature range of 800 to 1000 C irrespective of the purity of the metal.

From 1/8 in. diameter the rod was swaged to 90 mil wire. This wire, without further anneals, was drawn down to 45 mils in diameter. At this point, further reductions tended to break and/or roughen the wire which indicates excessive work hardening. Since these final reductions amounted to an 87% reduction in cross section area, another stress relief anneal was long overdue.

Another vacuum anneal at 800 C did not completely correct this wire breaking problem. It is therefore possible that a more complete recrystallization is required. Further vacuum anneals at higher temperatures are being investigated and will be reported in the next quarter.

METALLIC FUEL DEVELOPMENT

N-Reactor Prototype Fuel Irradiations - J. W. Goffard

A test charge of 14 NAE's was discharged from KER Loop 4 after attaining an average exposure of 1800 Mwd/ton. The first two-thirds of the irradiation was conducted at "N" conditions and the last one-third was conducted at reduced coolant temperatures. Fuel swelling data obtained by postirradiation weighing in the basin show a range of 0.0 to 1.0% ΔV in the fuel of the inner component (NIE) and a range of 0.3 to 2.5% ΔV in the fuel of the outer component (NOE). These swelling data are shown graphically in Figure 2.19 and compared with the calculated theoretical minimum

based upon 3 vol% increase per at. % burnup. The observed and the calculated minimum swelling of the NIE's are in good agreement, while the observed exceeds the calculated minimum swelling of the NOE's. Fuel exposures are plotted for each component with the maximum for the inners being 2450 Mwd/ton and the maximum for the outers being 3100 Mwd/ton. Fuel operating temperature data are not yet available so the swelling performance of these fuels has not been evaluated in terms of the fuel swelling models described in previous quarterlies. Selected components will be transferred to Radiometallurgy for detailed examination.

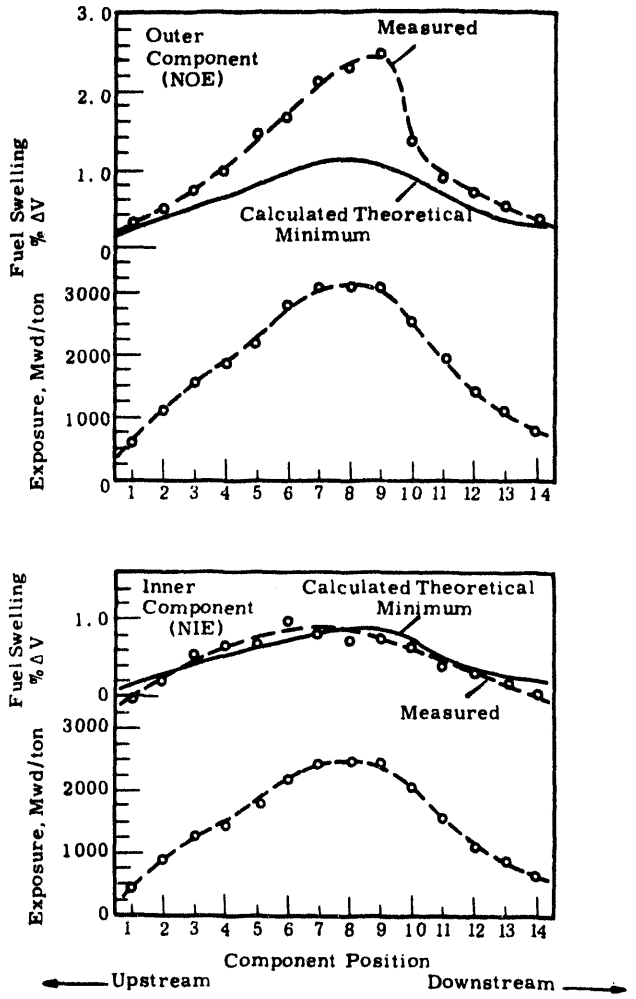

FIGURE 2.19

Top: Fuel Swelling and Exposure for Outer Component of an "N" Element Charge

Bottom: Fuel Swelling and Exposure for Inner Component of [redacted]" Element Charge

[redacted]

AEC-GE RICHLAND, WASH

The fuel swelling data of the components of 46 NAE's are plotted versus exposure on Figure 2.20. Fuel operating temperature has not been factored into this plot, thus there is a considerable spread in observed fuel swelling for any given exposure. The data in Figure 2.20, considered in terms of minimum observed swelling values, indicate a minimum swelling rate of perhaps 4.0 vol% increase per at. % burnup for N fuels. In the swelling models considered to date, a theoretical minimum swelling value of 3.0 has been used.

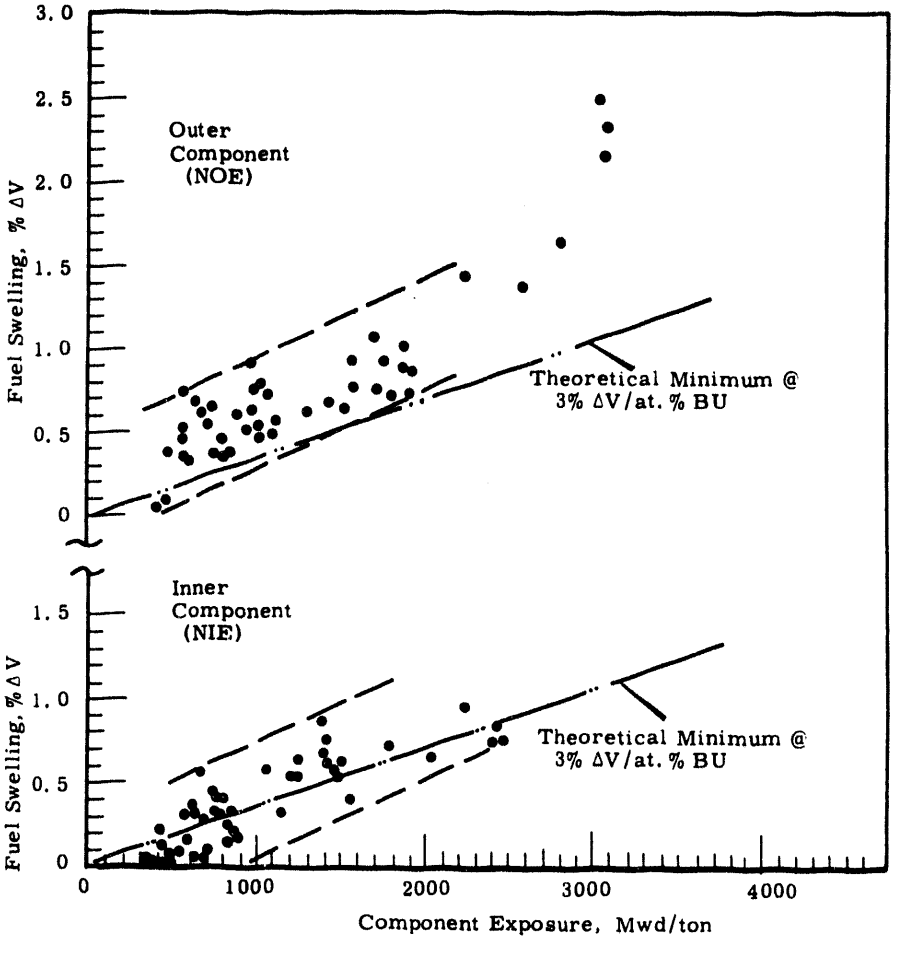

FIGURE 2.20

Swelling Behavior of Outer (NOE) and Inner (NIE) Components of 46KER Irradiated "N" Elements (NAE's)

Postirradiation Radiometallurgical examination has been completed on a charge of the 14 NAE's which attained an average exposure of 1200 Mwd/ton.[1] Three outer and two inner components were examined in detail. The components appeared to be free of any clad striations, bumps, or indications of clad thinning. The Be-Zr eutectic brazed closures for both components show no deficiencies in their irradiation performance. Crevices between the clad surfaces and the spot-welded support tabs have been examined and no indications of in-reactor corrosion or crud deposition have been observed. Zircaloy-2 clad samples have been analyzed for hydrogen with results in the range 60-110 ppm. No localized or large concentrations of hydrides have been seen metallographically. Contact areas between the inner surface of the outer tube and the inner tube supports have been examined with no evidence of fretting corrosion observed. Inner tube buggy spring supports have been studied in detail with no indication of inadequate performance. Metallographic examination indicates a tendency for hydride platelets in the supports to be oriented perpendicular to the surface at inside curves of bends and to be oriented parallel to the surface at outside curves of bends. Hydrogen content was analyzed to be 63 ppm which is approximately the preirradiation hydrogen content of the support.

High Temperature Irradiation of Tubular Fuel Elements - J. W. Goffard

A charge of KSE-5* single-tube fuel elements has been discharged from KER Loop 2 after attaining an average exposure of 1240 Mwd/ton at volume mean fuel temperatures ranging up to 535 C. The fuel swelling data (fuel density changes) obtained from the eight 12-inch long elements by postirradiation weighing extends our knowledge of the uranium swelling phenomena 70 C above that derived from earlier irradiation testing of KSE-3* elements. Operational data and the measured fuel volume changes are graphically summarized in Figure 2.21. The average exposures of the 1 ft long elements varied from 1070 to 1350 Mwd/ton (0.12 to 0.16 at.% BU). A span of 100 C in the volume mean fuel temperature prevailed in

---

(1) O. J. Wick. Quarterly Progress Report, Metallurgy Development Operation, October, November, December, 1962, HW-74379.

*KSE-3 and KSE-5 coextruded fuel elements have been described in previous quarterlies.

[redacted]

the column (433 to 535 C) and the experimentally determined swelling (% Δ V of fuel) ranged from 0.78 to 2.28%. The KSE-5 fuel swelling data is plotted versus the volume mean fuel temperature with the swelling data for KSE-3's also irradiated to a nominal 1200 Mwd/ton exposure. The observed fuel swelling of the two test element types (KSE-3 and 5) appear consistent with each other and indicate that swelling begins at a mean fuel temperature of 400 C and approaches a theoretical maximum, which is established by the loop coolant pressure and fuel temperature, at a mean fuel temperature of approximately 525 C.

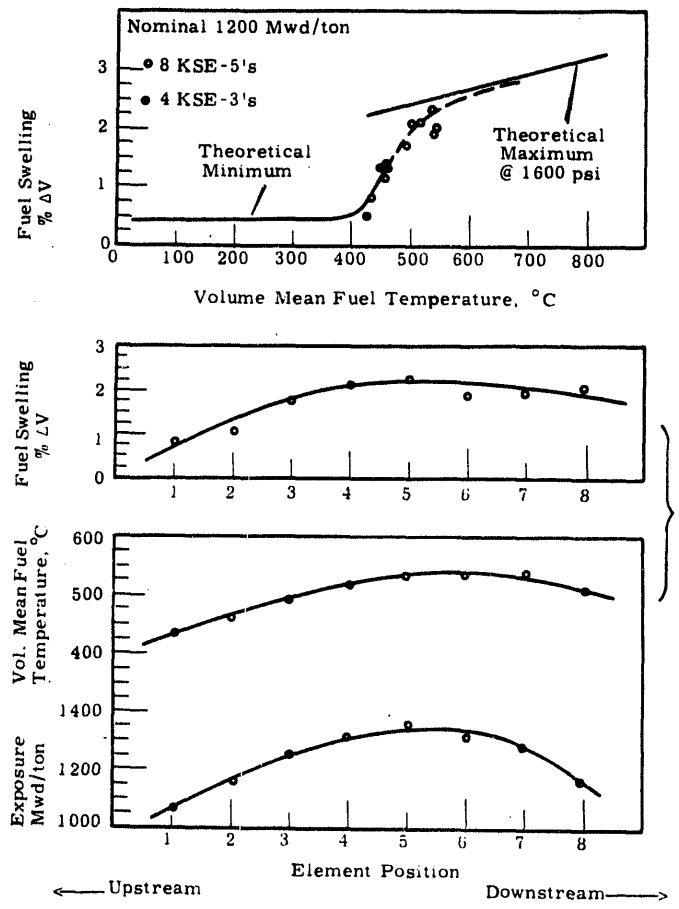

FIGURE 2.21

Top: Fuel Swelling Versus Volume Mean Fuel Temperature for KSE-3 and KSE-5 Elements
Bottom: Exposure, Volume Mean Fuel Temperature and Fuel Swelling for a Charge of KSE-5 Elements

The swelling data will be further evaluated using a previously described swelling model which describes fuel swelling for an incremental fuel volume in terms of burnup, temperature, and restraint.

Selected elements of the KSE-5 charge will be further evaluated at the Radiometallurgy facility.

Tapered End Cap Irradiation Test - G. S. Allison

Eight 17.5 inch long N-inner fuel components with tapered end caps (four bonded and four unbonded) have completed a 1900 Mwd/ton irradiation in high temperature water. The two types were alternately placed in the charge. The elements were centrally located in the process tube to produce calculated surface temperatures ranging from 168 to 226 C and specific powers above those anticipated for N-reactor. Density measurements taken in the basin indicate uranium swelling of 0.5 - 1.0% with no significant difference between the bonded and unbonded elements. Visual examination in both the basin and hot cell and dimensional measurements revealed no abnormalities or changes attributable to the irradiation. Preliminary examination of longitudinal sections of one end of each type element has revealed some brittle type cracking in the uranium between the tapered portion of the caps and the OD cladding of both elements. The cracks in the bonded element extend through the braze layer to the cap, but in neither element do the cracks extend into the cladding. No evidence of the clad shearing mechanism, as experienced with flat, flush, unbonded caps, has been observed on either of the tapered end cap designs.

Fluted Single Tube Fuel Elements - D. P. O'Keefe

two different fuel element geometries are being used in a study to evaluate the irradiation performance of fluted fuels. These fuel element shapes are shown in Figure 2.22 and have been described in previous reports of this series. The large fluted element represents a design that fulfills the operating requirements for single-tube N-reactor fuel. Geometrically, this design can accommodate a volume increase of 11% with only

bending strain in the cladding, thereby minimizing the possibility of cladding failure resulting from tensile strain generated in the cladding as when fuel swelling occurs.

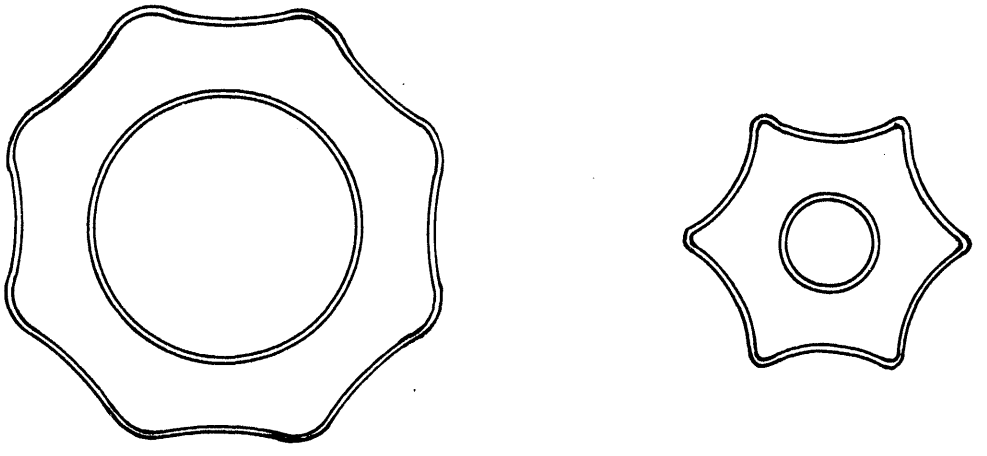

FIGURE 2.22

Cross Sections of Fuel Elements Used in Irradiation Test of Fluted Outer Surface Geometries

Since this fuel element shape is intended to undergo large volume expansions, it was necessary to provide a transition between the stable end closure and the fuel in order to avoid a highly localized strain discontinuity at the cap. To provide for this transition, the Zircaloy-2 caps were tapered to fit a V-notch in the end of the fuel. A computation of the heat distribution that would result from this type of joint was made using the analysis described elsewhere in this report ("Analysis of Fuel Element End Caps," by K. R. Merckx). A plot of the heat distribution in this portion of the element is shown in Figure 2.23.

[redacted]

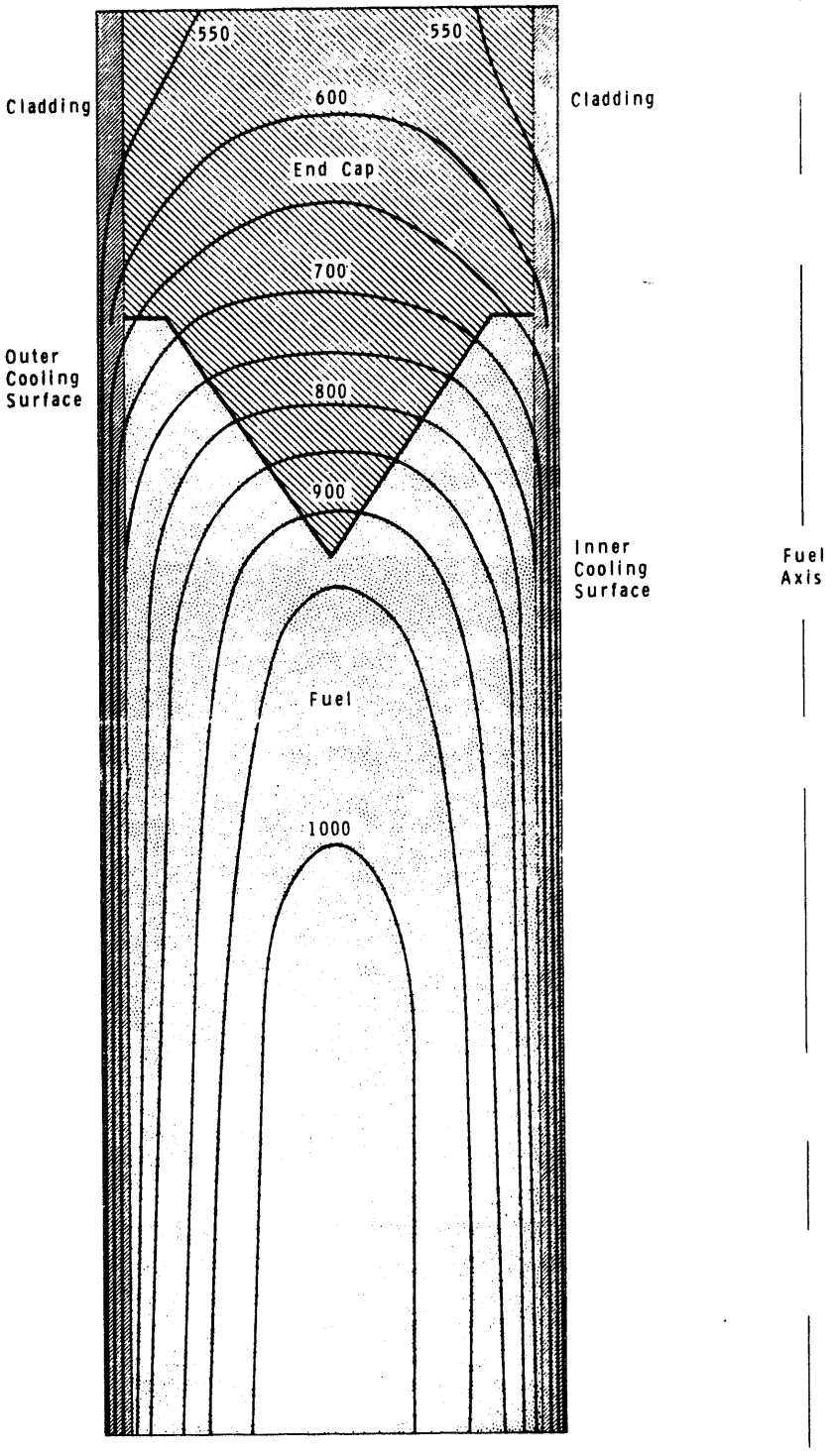

FIGURE 2.23

Longitudinal Sections Through One Wall of Fluted Single-Tube Element Showing Heat Distribution in End Closure and Vicinity (The indicated temperatures are in degrees Fahrenheit)

Two of the N-reactor single-tube size elements are being irradiated in the M-3 high pressure loop of the ETR. Operating at a power of about 130 kw/ft with a maximum metal temperature of 520 C, these elements have accumulated an exposure of about 800 Mwd/ton. Interim examinations of these elements have been made. There has been no visible change in the elements, and weight measurements indicate that about 0.3%, or the theoretical minimum, fuel volume increase has occurred.

The small fluted shape, shown in Figure 2.22, is approximately the size of the N-inner fuel tube. This six-fluted geometry is capable of a large volume expansion with bending deflections of the cladding. The computed shape changes that will occur with swelling are shown in Figure 2.24. An actual shape change that resulted from pressurizing the cladding is shown for comparison. One such element has been irradiated to an exposure of 1200 Mwd/ton in high temperature water in the P-7 loop of the ETR. With this exposure, the element has undergone a volume increase of about 3%. This test will continue with interim examinations until an exposure of about 3000 Mwd/ton is obtained.

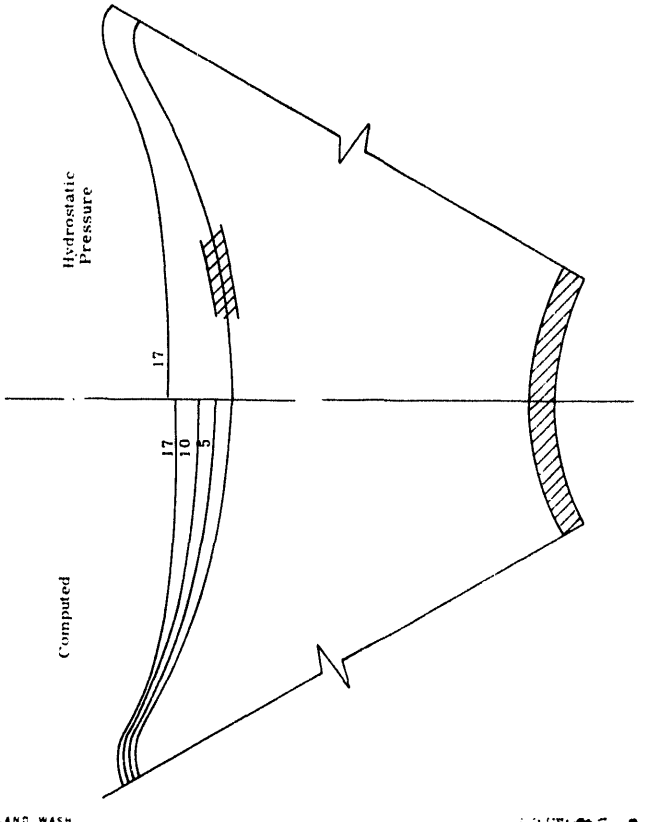

FIGURE 2.24

Partial Section Through a Small Fluted Element Showing Geometry Changes Accompanying Volume Increases (Figures represent percentage volume increases. An experimentally determined value obtained by pressurizing the cladding with water at room temperature is shown on the right.)

The cold-water irradiation of three small fluted elements was terminated at 2000 Mwd/ton exposure by the failure of one of the elements. These elements were to be given their final irradiation in the ETR-P7 high temperature water loop. The nature of the failure is not known at this time.

Cladding Deformation Studies - J. W. Weber

Localized thinning or "necking"* and ultimate failure of Zircaloy-2 cladding has occurred in test fuel elements irradiated in pressurized water, and on several rods irradiated under a variety of conditions in NaK-filled capsules. The characteristics of the failures are similar and have been described in previous quarterlies.

To study the effects of cladding thickness variations on the susceptibility to failure, a program of irradiating Zircaloy-2 clad uranium rods in NaK capsules with intentional striations in the cladding is being conducted. Nine of thirty-six capsules which were discharged from the reactor at an approximate fuel exposure of 1200 Mwd/ton have been opened and initial examination of fuel samples is completed. Eight of the capsules contained three fuel samples each and the ninth contained a single sample used to monitor temperatures during irradiation.

After removal from the capsules, each fuel sample was cleaned and examined visually for defects in the cladding such as necking or splits and then photographed. Diameter measurements were made with micrometers at 0°, 120°, 240° around the circumference at each of three longitudinal locations. Table 2.3 lists the irradiation conditions of each fuel sample from the eight capsules, the maximum total strain in the cladding and the condition of the cladding as observed from the visual examination.

---

* The term "necking" is used to describe the localized deformation of the cladding that occurs during irradiation as a result of instability. The term "striation" is used to describe the intentional or unintentional thinning of the cladding resulting from extrusion or machining.

TABLE 2.3

RESULTS OF ZIRCALOY-2 CLADDING STRAIN STUDY

Capsule	Sample	Maximum Total Cladding Strain %(a)	Condition of External Cladding Surface(b)	Striation Depth Inch(3)	Striation Width Inch(3)	Average Cladding Temperature C
4021	76	0.44	B	---	---	342
	85	0.32	B	0.004	0.040	334
	92	0.32	B	0.005	0.035	322
3021	6	1.01	B	---	---	355
	23	0.44	Sm	0.005	0.030	348
	46	0.95	N	0.008	0.044	342
3A21	122	2.82	B	0.003	0.050	348
	126	2.89	FN	0.003	0.035	344
	130	2.51	N	0.007	0.050	341
3U31	14	2.06	FN	0.003	0.040	430
	38	1.53	N	0.004	0.040	429
	56	1.94	N	0.009	0.055	427
3U28	13	1.70	FN	0.003	0.040	376
	37	1.84	B	0.004	0.035	376
	55	1.71	N	0.008	0.043	377
3U11	2	2.40	N, Sp	---	---	330
	19	1.14	N, Sp	0.005	0.040	327
	42	3.17	N, Sp	0.006	0.045	328
3U27	12	1.58	B	---	---	352
	36	1.46	B	0.005	0.035	356
	54	1.91	N, Sp	0.008	0.045	362
3A24	125	2.66	Sm	0.004	0.023	313
	129	2.78	FN	0.005	0.032	314
	133	2.52	N	0.007	0.047	318

(a) Calculated from micrometer measurements of fuel sample diameters.

(b) Sm - Smooth N - Necked FN - Faint trace of necking
B - Bumped Sp - Split in Cladding

(c) Measured from macropictures of unirradiated control samples.

Three of the samples in the "as-received" condition are shown in Figure 2.25. These samples show "necking" of the cladding surface typical of that observed on other fuel elements that have suffered localized plastic instability of the Zircaloy-2 cladding. As described in previous quarterlies, each of these capsules contained two fuel samples with intentional striations coextruded into the uranium-cladding interface. The third sample was coextruded with as smooth an interface as possible.

The three diameter measurements made around the circumference at each longitudinal location were averaged and the maximum average increase in diameter was used to calculate the maximum total cladding strain on the fuel element. In the cases where splitting or failure of the cladding occurred, comparison of these cladding strains with unfailed fuel samples is invalid unless the width of the split is considered. In Figure 2.26 the maximum total cladding strains are plotted as a function of the mean cladding temperature during irradiation. The curve on the graph was established from an analysis of previous data on the effect of temperature on the failure or necking strain limit of Zircaloy-2 cladding.[1] This previous data indicated that below an average cladding temperature of 325-350 C the total cladding strain limit before plastic instability or necking occurred was approximately 1.5%. At cladding temperatures above 350 C the strain limit increased rapidly as shown by the curve. This temperature effect is probably related to annealing of irradiation damage which has been shown to decrease drastically the uniform strain of Zircaloy-2. The results from the recent irradiations would not, at first, appear to agree with the curve as drawn or with the postulate that irradiation temperature has any effect on the strain limit. However, because the cladding interface conditions are difficult to control in the coextrusion process, there results cladding thickness variations somewhat different than those nominally desired. Each fuel sample must, therefore, be carefully examined as to the interface variations before and after irradiation and these results considered in arriving at conclusions.

(1) J. J. Cadwell. Quarterly Report, Fuels Development Operation, April, May, June, 1962, HW-74377. July, 1962.

[redacted]

[redacted]

B6677 B6681

Sample No.						
Average Cladding Irradiation Temp. C	427	429	430	318	314	313
Maximum Total Cladding Strain - %	1.94	1.53	2.06	2.52	2.78	2.66

FIGURE 2.25

Zircaloy-2 Coextrusion Clad Irradiated Fuel Samples (The necking observed on the external cladding surface of all but 14 and 125 are related to intentional cladding striations on the fuel-cladding interface.) 1X

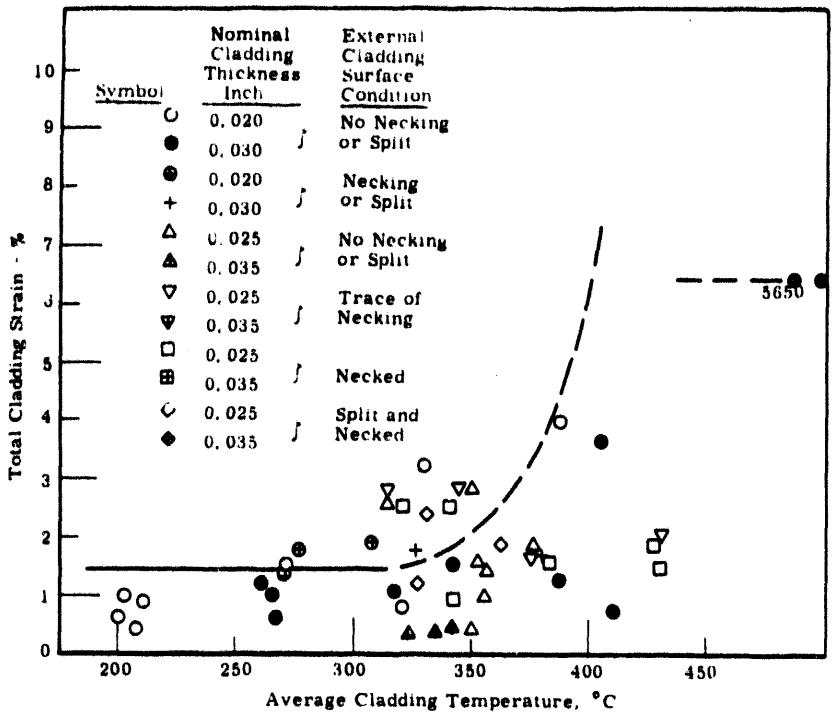

FIGURE 2.26

Total Cladding Strain as a Function of Average Cladding Temperature

A temperature effect is not readily apparent in the unstriated, unalloyed fuel samples as there were no strains significantly higher than 1.5% at cladding temperatures above the range 325-350 C. Samples 13 and 14 which experienced necking although they were supposed to be unstriated are being examined more closely to see if conditions exist under which they might be expected to exhibit plastic instability. These two fuel samples were from the same coextruded rod and separated only by a three-fourths inch unirradiated control sample. Metallographic examination of the control samples adjacent to 13 and 14 showed localized thinning of the cladding which is in the region of the necking on the irradiated samples. Thus, these two samples, 13 and 14 cannot be considered as unstriated. Preirradiation autoradiographs are being re-examined to establish the actual cladding thickness variations that existed on Samples 13 and 14 before irradiation.

Striations of the forms coextruded into these fuel samples are a major cause of plastic instability and can lower the strain limit significantly when the depth reaches approximately 0.004 in. and greater. This is demonstrated in Samples 19, and 46, and from examination of the autoradiographs, this is probably the cause of the necking and failure of Samples 14, 38, and 56. The effect of striations on the plastic instability is also shown in the results from the six alloy samples.

The cross-sections of control samples shown in Figure 2.27 illustrate the shape and size of striations in some of the samples recently irradiated. Metallography has been completed on the cladding from a transverse cross-section of irradiated Sample 133. Figure 2.28a shows the cladding striation on the adjacent control sample and Figure 2.28b shows the necking of the cladding on irradiated Sample 133. From Table 2.3 the depth and the width of the striation of the control sample in Figure 2.28a is shown to be 0.007 and 0.047 in. respectively. Measurement made on Sample 133 after irradiation indicates that the depth of the striation has not increased, but the width of the striation has increased from approximately 0.047 to 0.055 inch. The depth of the ingress on the external cladding surface and the thickness of the cladding at the thinnest locations of the striation is 0.004 and 0.012 in. respectively. The sum of the striation, the external ingress, and the cladding thickness agrees with the cladding thickness measured adjacent to the striation. The necking then occurred primarily inward from the external surface of the cladding.

A comparison of the increase in width of the striation and the increase in cladding circumference shows that about 15% of the total strain occurred in the 0.047 in. wide striation. The striation did not, therefore, concentrate the entire cladding strain at one location. Figure 2.29 is a photomicrograph of the cladding at the necked area showing the extent of strain concentration in the striation. The deformed grains extend over a gage length of approximately 0.024 inch. Although the grain deformations do not show beyond this distance, the geometry of the ingress on the external

Irradiation Fuel Sample - 6, Maximum Striation Depth - ~0.001 in.

Irradiation Fuel Sample - 19, Maximum Striation Depth - 0.005 in.

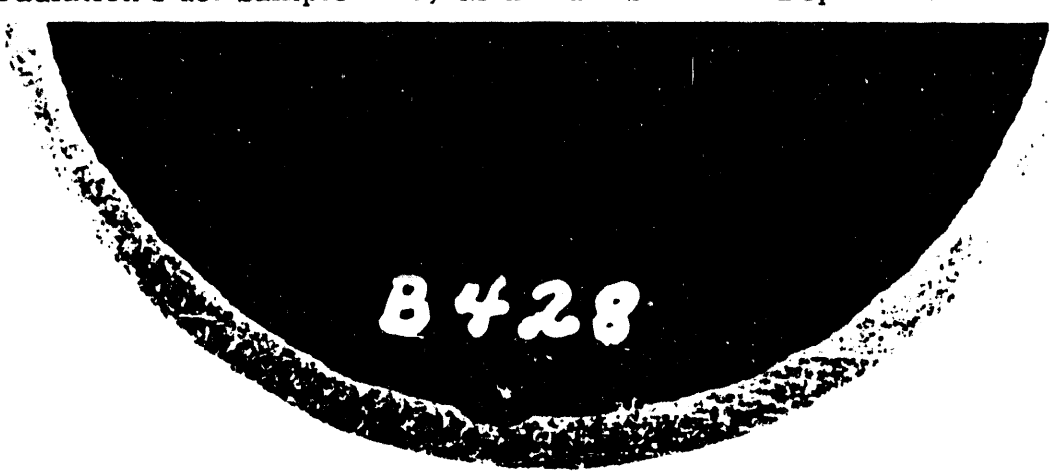

Irradiation Fuel Sample - 55, Maximum Striation Depth - 0.008 in.

FIGURE 2.27 Fuel Cladding Interface 10X
(These macro pictures are from cross sections of unirradiated control samples. The maximum measured striation depth and adjacent irradiated fuel sample number are given below each.)

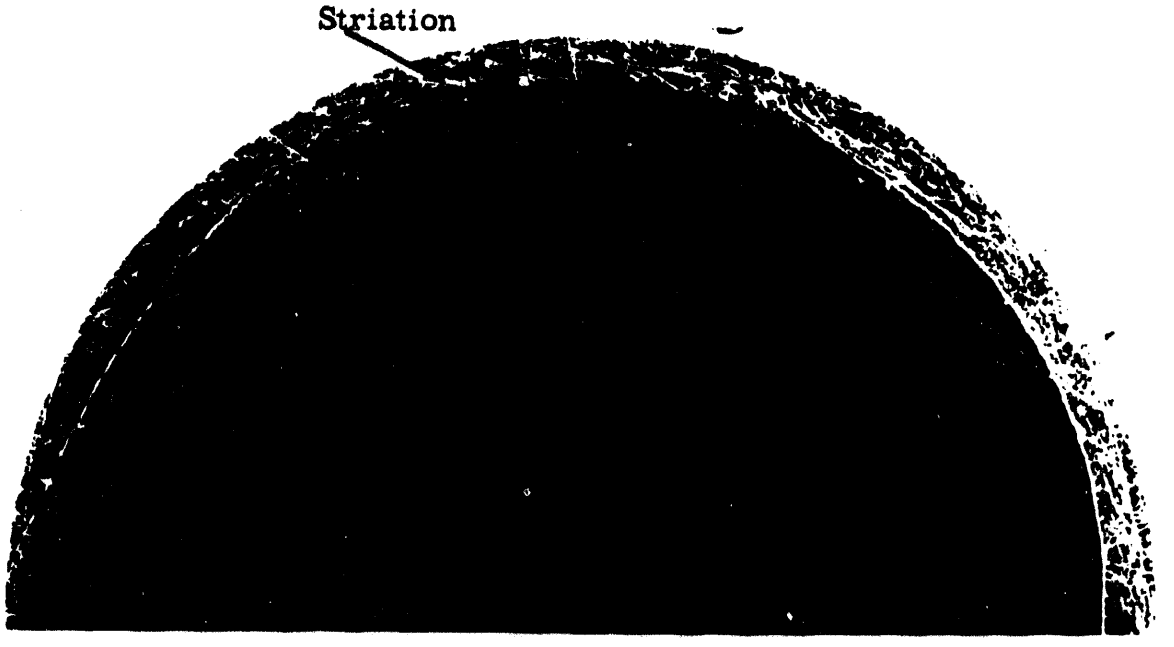

a. Unirradiated Control Sample

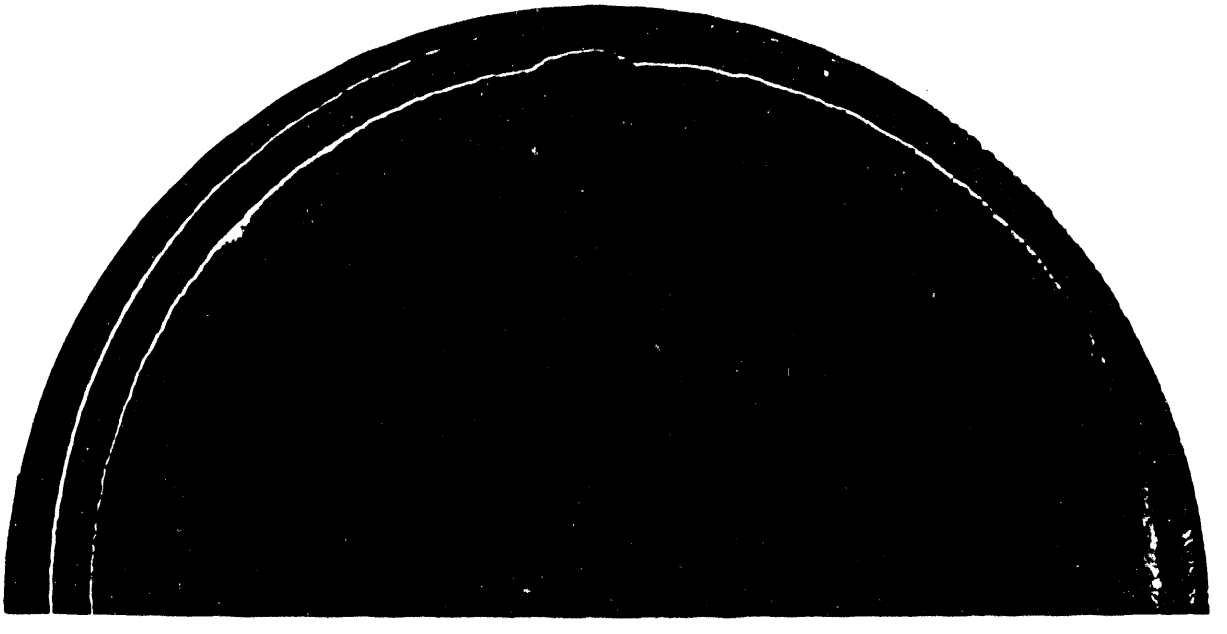

b. Irradiated Fuel Sample 133

FIGURE 2.28

Comparison of the Shape and Size of Striation on Fuel Sample 133 Before and After Irradiation

cladding surface makes it obvious that some straining is occurring throughout the width of the striation. The strain in the deformed region may be as high as 30%.

The unstriated alloy fuel samples exhibited the ability to withstand a greater total cladding strain without necking than the unstriated unalloyed samples and the samples from the previous irradiations. This may be related to differences in properties of the alloyed and unalloyed uranium. That is, the fuel itself may affect the strain distributions in the cladding.

Examination of these fuel samples will continue. The remaining 24 capsules have been discharged at an estimated fuel exposure of 1800 Mwd/ton and are being returned to Radiometallurgy for examination.

MTR Irradiation of I&E Fuel Elements - J. W. Weber

Irradiation of uranium at temperatures near 400 C have resulted in volume increases considerably in excess of those that would be predicted solely from fission gas swelling. Examinations have shown that extensive grain boundary tearing has occurred in the uranium resulting in large numbers of irregularly shaped voids.

Four Hanford tubular I&E fuel elements have been irradiated in the GEH-4 loop facility in the MTR to investigate the susceptibility of these elements to the grain boundary tearing phenomenon. A rather severe longitudinal flux gradient along these samples resulted in a range of exposures from a maximum of 3130 Mwd/ton to a minimum of 350 Mwd/ton. The temperature variations were also large. The maximum fuel temperature ranged from 700 C to 50 C and the uranium volume average temperature from 525 to 50 C. These conditions give an extensive range of temperatures and exposures over which to study the susceptibility of the elements to grain boundary tearing. These elements will be returned to Hanford in July or August for examination.

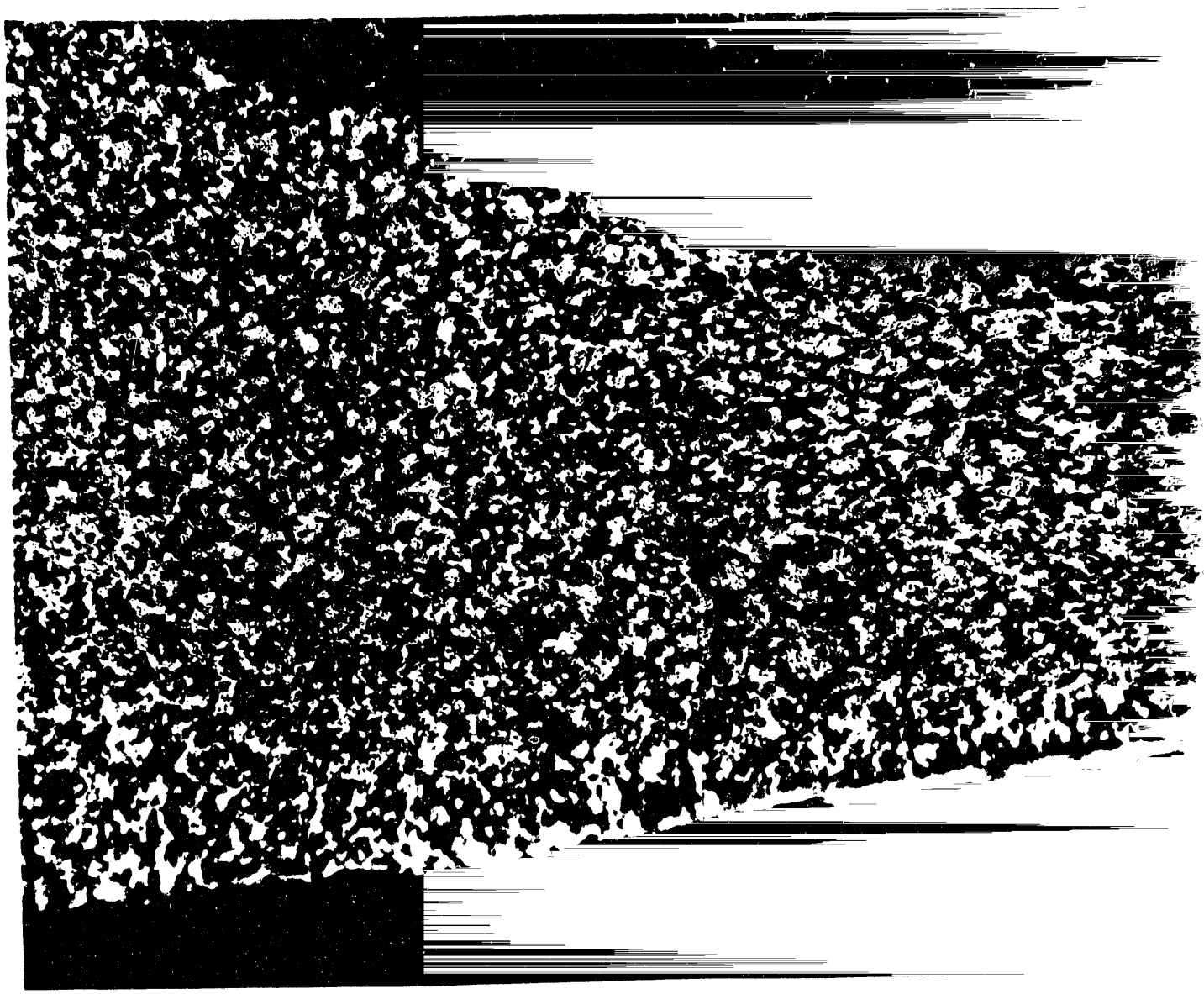

FIGURE 2.29

Micropicture of Zr-2 Cladding on Fu
deformation grains can be seen conc
half of the necked area.)

Fuel Element Data System - L. E. Kuhlken

Approximately 300 N-fuels have been measured on the Sheffield air-transducer measuring equipment to date. The large supply of data received from these measurements can only be sorted and analyzed using computerized statistical analysis. In addition to pre-irradiation dimensional data available now, there will be a large amount of postirradiation dimensional and operational data (temperatures, burnups, volume changes, etc.) that also need to be compiled and analyzed. To provide a convenient storage for this information, a magnetic tape file has been created with 174 separate sections for each individual fuel.

Input to the file is provided by results from the P3 temperature distribution program for irradiated fuels, output from the TUM measurement program (HW-71521 REV), and data sheets made up by the engineer responsible for the irradiation of the fuel. This information is transferred to cards (30 for each element), and the cards become input to FEDSY (Fuel Element Data System) which writes and maintains the magnetic tape file.

The first 30 sections are non-numeric remarks about the fuel performance and history including dates, document numbers, and fabrication materials. The rest are numbers which describe the alloy contents, dimensions, and operation history of the fuel. The file currently contains data for approximately 400 test elements including prototype N-fuel components.

The most immediate use of this data will be in an analysis program which will order the data, plot the variables as a function of each other, and statistically screen the data using simple bivariate analysis.

III. METALLIC FUELS DEVELOPMENT

Irradiation Testing of Thorium-Uranium Fuel Elements - J. W. Goffard

Three Zircaloy-2 clad Th-2.35 wt% U^{235}-1 wt% Zr alloy fuel elements, 4.45 cm (1.75 in.) OD x 2.67 cm (1.05 in.) ID, fabricated by the coextrusion process, are being irradiated under power reactor conditions in the high-temperature, high-pressure, water-cooled ETR P-7 facility. The facility is being operated with a 204 C (400 F) coolant inlet temperature and an inlet pressure of 110 atmospheres (1600 psig). The three 20 cm (8 in.) long test elements are undergoing their third cycle of irradiation and will have accumulated a maximum of 8.33×10^{19} fissions/cc (2400 Mwd/ton) at the conclusion of this cycle (August 4, 1963). The initial fuel element operating conditions of 70.6 w/g (214 kw/ft length of element), maximum fuel temperature of 603 C (1117 F), and maximum-surface heat flux of 8.5 cal/cm^2/sec (1,080,000 Btu/(sq ft)(hr)) have not changed significantly in the course of irradiation.

The fuel elements were examined and weighed at the end of each of the first two cycles with no significant changes being noted in either appearance or density. Irradiation is scheduled to continue to approximately 10^{21} fissions/cm^3, or 3 at. % BU.

Zircaloy-2 Clad Thorium-Uranium Rods for Visual Autoclave - R. G. Nelson

Rod stock for autoclave defect testing was coextruded to 0.525 in. diameter with 0.025 in. thick Zircaloy-2 cladding. Specimens will be prepared from this material for autoclave defect studies using motion pictures. Fuel composition was Th-2.5 wt% U (normal) -1.0 wt% Zr. All of the processing of these rods was kept as nearly identical as possible to that used on the enriched thorium fuel elements now under irradiation in the ETR.

Two 6 ft long rods were coextruded at 760 C with a reduction ratio of 17.4 to 1. Maximum extrusion constant was 19 tsi.

Rod Stock for Thermocoupled Elements - R. G. Nelson

Melting and coextrusion of stock for the fabrication of a long life constant power heat source has been completed. This material will be used for studying the variation in heat transfer with film buildup on a Zircaloy-2 surface during irradiation.

The extruded stock consists of a 1.030 in. OD solid rod with a 0.028 in. thick Zircaloy-2 cladding and a 0.470 in. diameter central core of Zircaloy-2. The fuel annulus between cladding and core is Th-1.5 wt% U-1.0 wt% Zr.

The fuel material was prepared by double vacuum arc melting two 60 lb x 3.82 in. diameter ingots. One of the ingots was alloyed with natural uranium and is being used as pilot stock for developing suitable fuel element fabrication procedures. The other ingot is alloyed with fully enriched uranium. Final fuel element assemblies for irradiation will be made from the enriched material.

Coextrusion was performed on the 700 ton press at 760 C and the 15.5 to 1 reduction ratio gave an extrusion constant of 17.2 tsi for the normal ingot and 18.7 tsi for the enriched ingot. Final length of the extrusions was 135 inches.

Samples were cut from the front, middle and rear of each extrusion and measured with an optical micrometer microscope. Traverses were made on three equally spaced diameters of each of the specimens, the results of which are summarized in Table 3.1.

The uniformity of dimensions of these coextruded rods are better than similar rods made in the past using uranium as fuel material. The tendency toward more uniform clad thickness on recent thorium tubular fuel elements has also been noted.

Metallographic examination of the thorium rod sections showed uniform and complete bonding of Zircaloy core to thorium and Zircaloy clad to thorium. The outer surface of the Zircaloy-2 cladding shows a much

TABLE 3.1

CRUD PROBE MEASUREMENTS

		Enriched Stock Heat No. 138				Pilot Stock Heat No. 137			
		Clad Thickness	Zircaloy OD	Core Diameter	Thorium Wall	Clad Thickness	Zircaloy OD	Core Diameter	Thorium Wall
FRONT	Min	0.0293	0.9981	0.4512	0.2394	0.0282	1.0272	0.4687	0.2317
	Max	0.0316	1.0016	0.4573	0.2461	0.0289	1.0291	0.4707	0.2415
	Spread	0.0023	0.0035	0.0061	0.0067	0.0037	0.0019	0.0020	0.0098
MIDDLE	Min	0.0382	1.0049	0.4658	0.2358	0.0277	1.0258	0.4669	0.2380
	Max	0.0294	1.0099	0.4700	0.2452	0.0305	1.0293	0.4688	0.2434
	Spread	0.0012	0.0050	0.0042	0.0094	0.0028	0.0035	0.0019	0.0054
REAR	Min	0.0252	0.9980	0.4711	0.2310	0.0274	1.0296	0.4608	0.2398
	Max	0.0293	1.0084	0.4810	0.2404	0.0293	1.0312	0.4632	0.2475
	Spread	0.0041	0.0104	0.0099	0.0094	0.0019	0.0016	0.0024	0.0077

rougher surface than the Zircaloy-thorium interfaces, and appears to be somewhat rougher than similar extrusions made with uranium fuel. There also appears to be a slight reaction between the Zircaloy cladding and the copper can. This indicates that the 760 C extrusion temperature is a maximum. Higher extrusion temperatures will require can material other than copper.

Effect of Thorium on Corrosion Resistance of Brazing Alloy -R. N. Johnson

Autoclaving tests have been performed on brazed end caps which have been removed from thorium fuel elements. The cap was sectioned to expose the full length of Zircaloy-5 Be braze to the high temperature water. Autoclaving conditions were 10 hr and 50 hr in 360 C water at 3000 psi. As shown in Figure 3.1, the braze nearest the thorium fuel showed white oxide corrosion gradually changing to a uniform black oxide coating on the braze the furthest from the thorium. This shows that thorium contamination of the braze has a definite detrimental effect on the corrosion resistance of the braze. A series of braze alloys containing thorium contamination ranging from 0.012% thorium to 3.1% thorium have been made by arc melting. The arc-melted buttons have been analyzed and are being machined into coupons for corrosion studies to establish what levels of contamination are allowable in the brazing alloy.

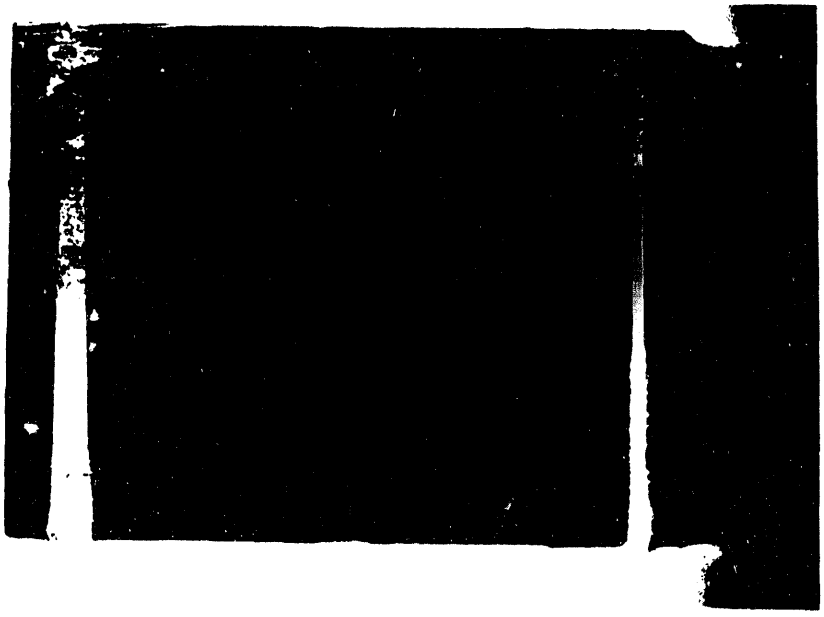

FIGURE 3.1
Autoclaved Brazed Section Showing Effect of Variable Thorium Contamination on Corrosion Resistance. Autoclaved 50 hr in 360 C Water
10 X

IV. PLUTONIUM PHYSICAL METALLURGY

Phase Transformation Kinetics and Mechanisms T-T-T Curves of the $\gamma \rightleftharpoons \beta \rightleftharpoons \alpha$ Transformations - R. D. Nelson

T-T-T curves of the $\gamma \rightleftharpoons \beta \rightleftharpoons \alpha$ transformations of moderately high quality plutonium, less than 250 ppm total impurities by weight, were obtained by the fluid displacement technique and are presented in Figure 4.1. The analysis of the metal used in these T-T-T studies is given in Table 4.1. No analysis was made for hydrogen, oxygen, nitrogen, and many of the rare earths. The as-cast density of this metal was 19.65 g/cc and the density after hydrostatic pressing at 90,000 psi and cooling under pressure from 180 C (356 F) was 19.75 g/cc. These densities and the chemical analysis indicate that this metal is of fairly high purity. It is typical of metal used for plutonium physical metallurgy research at Hanford.

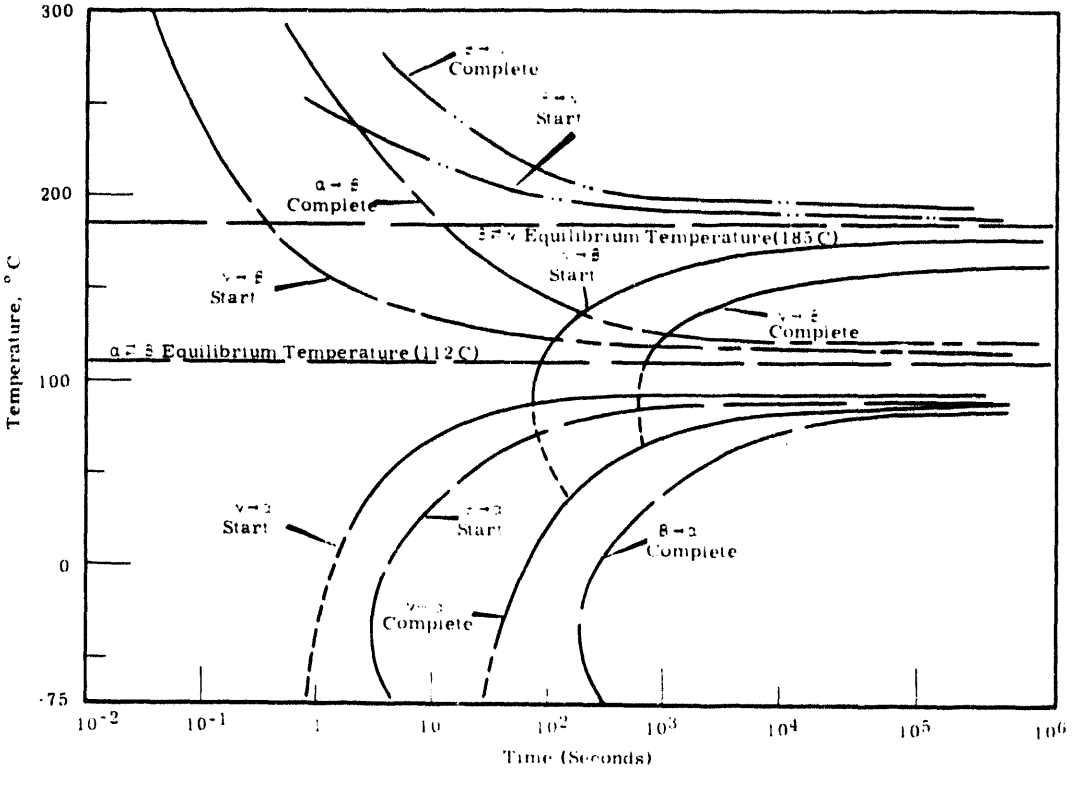

FIGURE 4.1

T-T-T Curves of the $\alpha \rightleftharpoons \beta \rightleftharpoons \gamma$ Transformations of Plutonium

TABLE 4.1

ANALYSIS OF PLUTONIUM USED FOR OBTAINING T-T-T CURVES CURVES OF THE $\gamma \rightleftharpoons \beta \rightleftharpoons \alpha$ TRANSFORMATIONS

Carbon	70
Copper	10
Iron	74
Manganese	20
Nickel	50
Others	<50

There are some pronounced differences between this set of curves and the set published earlier for plutonium containing 1000 ppm impurities. The most significant difference is that all of the T-T-T curves of the higher quality metal are shifted to the left of the corresponding curves derived from the lower quality metal. The incubation time for the formation of alpha directly from the gamma phase is less than the incubation time for the formation of alpha from the beta phase at the same temperature. The difference between the two incubation times is less for the high quality than for the poorer quality plutonium.

The T-T-T curve of the $\gamma \rightarrow \beta$ transformation does not show a nose prior to its intersection with the $\gamma \rightarrow \alpha$ T-T-T curve. Previously the nose of the $\gamma \rightarrow \beta$ T-T-T curve was observed to be at 100 C (212 F). However, in the higher quality metal the incubation time of this transformation was very nearly the same at 88 C (190 F) as at 100 C (212 F), implying that this is the temperature range in which the maximum $\gamma \rightarrow \beta$ transformation rate occurs; no well defined nose in the T-T-T curve exists. The $\gamma \rightarrow \beta$ T-T-T curve would very likely contain a nose in this temperature range but for the competing $\gamma \rightarrow \alpha$ transformation which is the primary reaction below 80 C (176 F).

The position of each T-T-T curve depends upon many variables. For example, the incubation time of the $\beta \rightarrow \gamma$ transformation at 195 C (382 F) was 15 min when the beta phase was formed from the alpha phase at this temperature, whereas, the incubation time was 10 - 20 hr at 195 C (382 F) when the beta phase was first allowed to transform from the alpha phase at 120 - 130 C (248 - 266 F). In addition, the incubation time for the $\beta \rightarrow \alpha$ transformation at 80 C (176 F) was 2 min after beta heat treating 45 min at 160 C (320 F), whereas, the incubation time was 2 hr after beta heat treating 47 hr at 180 C (356 F). There are many additional variables such as deformation, stresses, specimen size, etc., which influence the transformation rates. The significance of these variables becomes less the higher the transformation rate. This appears to be the case for the $\gamma \rightleftharpoons \beta \rightleftharpoons \alpha$ transformations. The study of the effect of the variables influencing the transformation rates constitutes a large portion of the research effort.

Mechanisms of the $\beta \rightarrow \alpha$ Transformation - A program is underway to determine the mechanisms of the $\beta \rightarrow \alpha$ transformation by metallography. Previous work showed that the alpha phase which forms at 60 C (140 F) or higher has a microstructure consisting of bands of columnar grains. In unrestained specimens these bands are distributed randomly throughout the specimens, whereas in restrained specimens the bands have a preferred orientation.

A series of speciemns, 0.50 in. in diameter and 0.10 in. in thickness, were beta heat treated 20 hr at 185 C (364 F) and then allowed to transform to yield 5, 10, 15, 25, 50, and 90% of the alpha phase at 78.0 C (172.4 F). The incubation time for this particular metal under these conditions was 3500 - 4500 seconds. The $\beta \rightarrow \alpha$ transformation was interrupted after these percentages of alpha phase had formed by quenching in an inert fluorochemical and dry ice bath at -75 C (-102 F). The specimens were examined metallographically to study the banding which occurs when alpha forms at temperatures high in the alpha phase. During the quenching to -75 C (-102 F) the $\beta \rightarrow \alpha$ transformation produces very small grains.

The microstructures were examined to determine the maximum grain size and maximum band width as a function of transformation time, the origin of microcracking, and a possible nucleation parameter. These parameters are being determined as a function of the isothermal transformation temperature. At the present time they have not been investigated in sufficient detail to permit conclusions to be derived.

Pronounced surface distortion, referred to as surface veining, has always been observed in plutonium when isothermally transformed at high temperatures. This phenomenon is common in as-cast plutonium, but it has been most frequently observed and is most pronounced in metal which has either been deformed in one of the high temperature phases or transformed to the alpha phase in the range 60 - 80 C (140 -176 F). This surface distortion has the appearance of veins. The surface veins are removed during mechanical polishing but reappear after electrolytic polishing 30 sec at 60 - 70 volts in an electrolyte of 25% tetraphosphoric acid, 17% water, and 58% 2-ethoxy ethanol. This etchant is merely a slight modification of the 20-30-50 etchant commonly used for etching plutonium. The amount of water was reduced to decrease the degree of pitting. This electropolishing procedure reveals the veining and microstructure quite clearly.

The microstructure of the specimens partially transformed at 78. 0 C (172. 4 F) consisted of bands of columnar grains which were randomly distributed throughout the specimens, as shown in Figure 4. 2. The veins observed visually were identified in the microstructure as these bands. The bands are the first beta to transform to the alpha phase and due to the large volume decrease they produce surface distortions which appear as veins on the specimen.

FIGURE 4.2

Microstructure of a Beta Heat Treated Plutonium Specimen

Polarized Light Illumination 100 X
Electrolytically Polished

(Plutonium specimen which had been beta heat treated 20 hr at 185 C, isothermally transformed to yield 10% of the alpha phase at 78.0 C, and then completely transformed by quenching at -75 C. The bands are the alpha phase which were formed at 78.0 C and the smaller grains are the alpha which formed during the quench to -75 C. These bands observed in metallographic sections are the veins observed visually on the free surface of specimens undergoing transformation.)

Mechanisms of the $\delta \rightarrow \gamma$ Transformation - One of the most interesting phenomena in the study of the phase transformations of plutonium is the presence of stair-steps on the dilatometric cooling curves of the $\delta \rightarrow \gamma$ transformation. These steps are most pronounced in metal of low purity. They have not been observed during $\delta \rightarrow \gamma$ isothermal transformation of high purity plutonium but have been observed during isothermal transformation of impure plutonium

Neg. No. 8816
AEC-GE RICHLAND WASH

Sharp discontinuities were observed near the start of the $\delta \rightarrow \gamma$ transformation of metal known to contain impurities, Figure 4.3. However, most of the transformation proceeds in a continuous manner. The magnitude of these discontinuities at the start of the transformation is greater the lower the temperature of transformation. The chemical analysis of this metal has not as yet been determined.

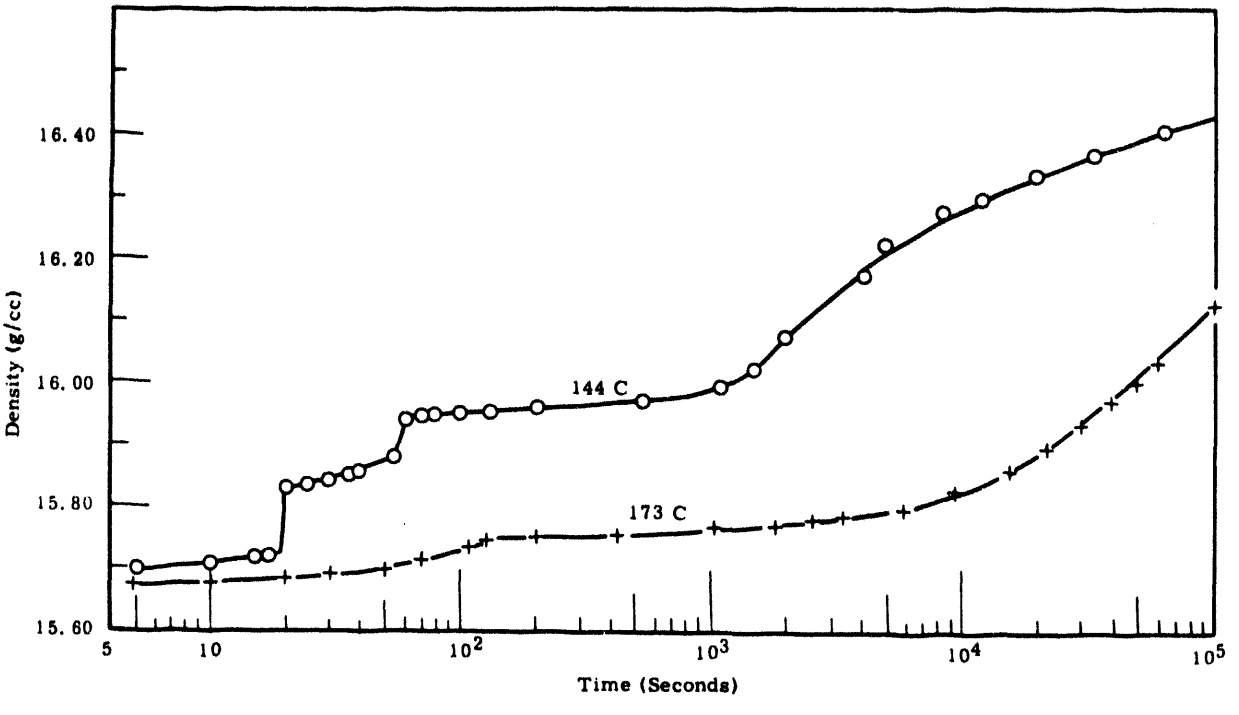

FIGURE 4.3

Isothermal Reaction Curves of the $\delta \rightarrow \gamma$ Transformation of Impure Plutonium Showing Discontinuities at the Start of the Transformation

The volume decrease associated with each of these discontinuities was very rapid, almost instantaneous. There were two such discontinuities at 130 and 144 C (266 and 291.2 F). At 173 C (345 F) there was only one discontinuity and this was less than either of the two at the lower temperatures. The major portion of the transformation proceeded continuously at 173 C (345 F). If the specimen were allowed to completely

transform they would have a density of approximately 16.9 g/cc. However, the completion of the transformation is extremely sluggish, even at room temperature.

The $\gamma \rightarrow \beta$ transformation was significantly more sluggish in this material than in high purity plutonium. The incubation times for the start of the $\gamma \rightarrow \beta$ transformation at 100 C (212 F) were 80 and 13,000 sec for the pure and the impure materials, respectively. This implies that with proper alloying additives and heat treatment, the gamma phase may exist in a metastable state for long periods of time. This possibility is merely speculative and will require detailed research.

It has been found that phase transformations can contribute to the weakening of a material when under stress. Common descriptive terms for this phenomenon are: amorphous plasticity, super plasticity, and phase transformation strain. The latter term is the one used in this report.

An exploratory program has been initiated to study the phase transformation strain of plutonium. This metal has low temperature transitions between phases which have differences in crystal structure and ductility. Plutonium is therefore a good candidate for study of phase transformation strain.

Compression tests were performed isothermally in a nitrogen atmosphere under constant load conditions at 80 - 85 C (176 - 185 F) for the $\beta \rightarrow \alpha$ transformation and 124 - 129 C (255 - 265 F) for the $\alpha \rightarrow \beta$ transformation. Apparatus employed in these experiments is shown in Figure 4.4. Cylindrical samples with a radius of 1/8 in. and length of 3/8 in. are placed between the platens which are inserted into a vertical tube furnace. Dial gages sensitive to 0.0001 in. were used to measure changes in length of the sample. Dial indicators are now being replaced by change in length recording devices which have greater versatility. The observed strain is composed of:

1. Phase transformation strain
2. Creep strain of the individual phases
3. Length change due to phase transformation

The creep strain of the individual phases was measured at 100 C (212 F) and the length change due to phase transformation was calculated. Therefore the observed strain is an indirect measure of transformation strain.

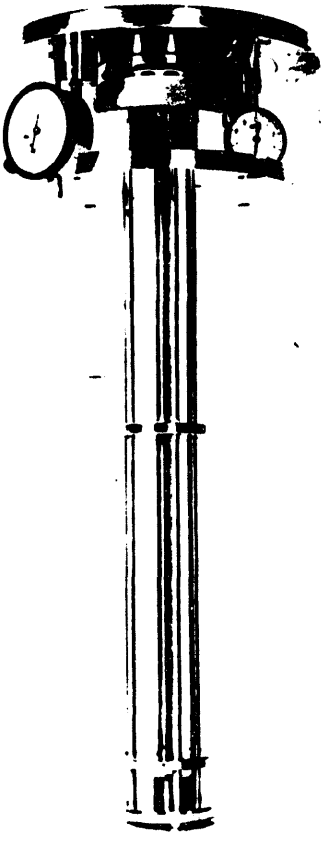

FIGURE 4.4

Fixture for Measuring Phase Transformation Compressive Strain of Plutonium

The observed strain appears to be slightly dependent upon the temperature used. Since the transformation rate is very sensitive to temperature it follows that the transformation strain can be expected to be transformation rate dependent.

The strain rates of plutonium during the $\alpha \rightarrow \beta$ and the $\beta \rightarrow \alpha$ transformations under compressive loads of 100, 1000, and 2000 psi are one

to three orders of magnitude larger than the creep strain of either of the phases individually. Therefore the creep strain rates of alpha and beta-plutonium may be neglected. The change in length due to phase transformation was calculated for a sample with a radius and length of approximately 1/8 in. and 3/8 in., respectively, assuming the expansion and contraction to be isotropic. Table 4.2 lists the pertinent length change data and Figure 4.5 gives the experimentally observed strain versus time information for one of these tests. These data are essentially qualitative and will be used as a guide in directing further research activities. Several conclusions which can be derived from the experimental data are:

1. Transformation strain is a significant portion of the total strain
2. Transformation strain is a function of applied stress
3. Transformation strain is greater for the $\alpha \rightarrow \beta$ transformation than for the $\beta \rightarrow \alpha$ transformation.
4. Transformation strain increases as the initial grain size decreases.
5. Transformation strain is transformation rate dependent.

TABLE 4.2

LENGTH CHANGES IN PLUTONIUM SPECIMENS UNDER COMPRESSIVE LOADING DURING $\alpha \rightarrow \beta$ AND $\beta \rightarrow \alpha$ TRANSFORMATIONS

Observed Length Change, Inch	Length Change Due to Phase Transformation, Inch	Length Change Due to Phase Transformation Strain, Inch	Transformation	Stress, psi	Original Alpha Grain Size, mm
-0.020	-0.012	-0.008	$\beta \rightarrow \alpha$	2000	0.001
-0.012	+0.012	-0.024	$\alpha \rightarrow \beta$	2000	0.001
-0.020	-0.012	-0.008	$\beta \rightarrow \alpha$	1000	0.001
+0.002	+0.012	-0.010	$\alpha \rightarrow \beta$	1000	0.001
-0.012	-0.012	0	$\beta \rightarrow \alpha$	100	0.001
+0.008	+0.012	-0.004	$\alpha \rightarrow \beta$	100	0.001
+0.003	+0.012	-0.009	$\alpha \rightarrow \beta$	2000	0.05
+0.006	+0.012	-0.006	$\alpha \rightarrow \beta$	1000	0.05

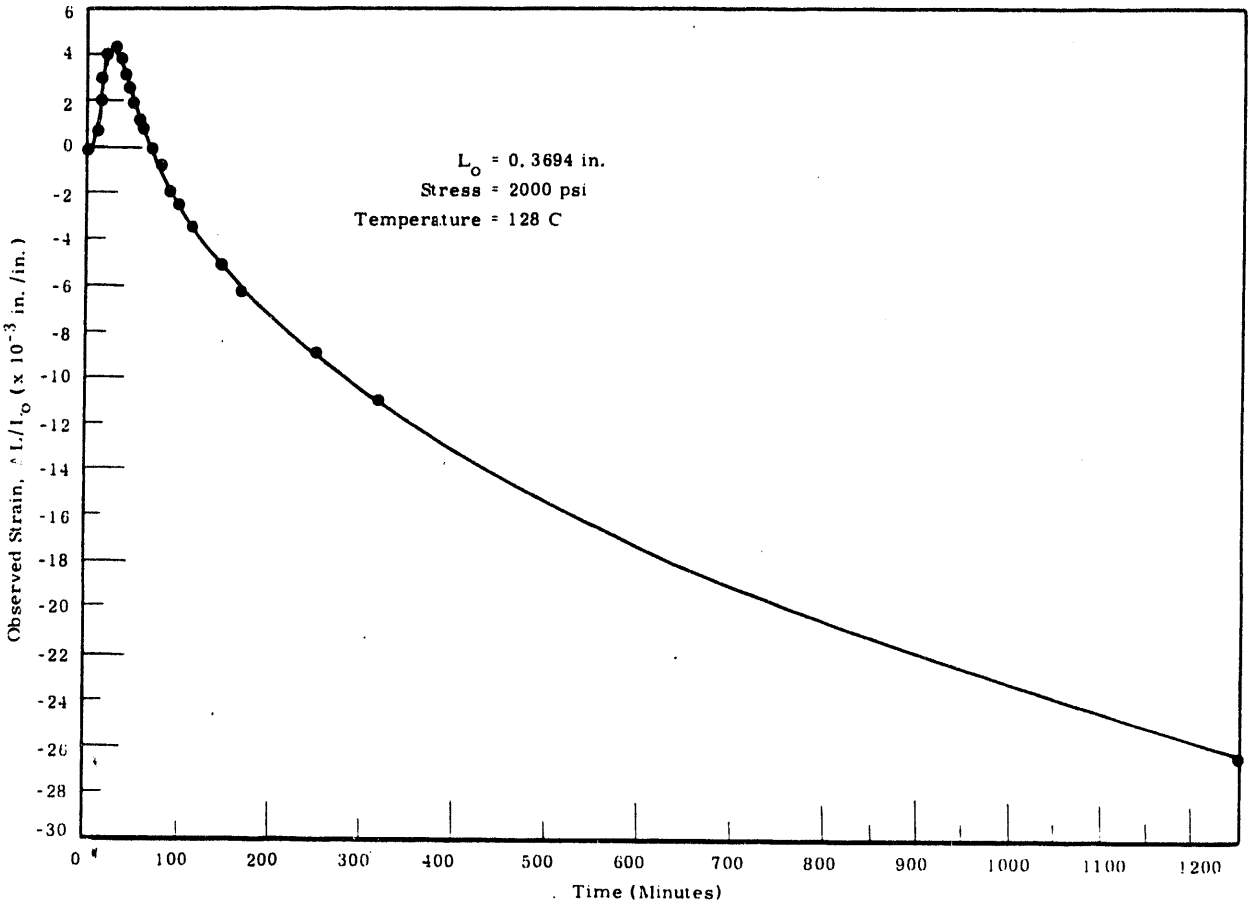

FIGURE 4.5

Observed Creep Strain Versus Time During
$\alpha \rightarrow \beta$ Transformation of Plutonium

Deformation and Fracture Mechanisms; Recovery, Recrystallization, and Grain Growth - V. C. Asmund and F. C. Bowman

Establishing the mechanics involved in the plastic deformation and ultimate fracture of the complex monoclinic structures, represented by alpha and beta plutonium, constitutes a portion of the research activities in progress. In addition, attention is also being given to the recovery, recrystallization and grain growth processes which are active in these materials, as well as the resulting effects upon various physical and mechanical properties.

Alpha Deformation - Despite the fact that alpha plutonium exhibits only about 1% elongation when subjected to tensile loading, it has been shown at the Argonne National Laboratory that significant reductions in area can be achieved by rolling. In their work the deformation was accomplished by reductions of the order of 0.001 in. per pass.

With this background a study was initiated to determine in greater detail the rolling characteristics of alpha plutonium. The deformed material resulting from this program is being employed in the investigation of the recovery, recrystallization and grain growth phenomena, preferred orientation, the anisotropy of various physical and mechanical properties and a detailed study of the atomic arrangement as it is affected by severe cold deformation.

Rolling has been done on a hooded Stanat mill equipped with provisions for heating both the rolls and tables. Initially a four-high setup was employed but was found unsatisfactory due to slippage, since the work rolls were not driven. The present arrangement employs a two-high setup with 6 x 8 in. rolls driven at approximately 16 sfm.

The stock prepared for the initial rolling investigation was from two heats. Series I was cast into ingots 1 x 6 x 0.125 inches. Series II was cast in two sizes 1.5 x 7 x 0.100 in. and 1.5 x 7 x 0.200 inches. The analysis of these two heats are presented in Table 4.3. It can be seen that the major difference lies in the iron content. The higher iron resulted in an almost continuous grain boundary film of the plutonium-iron eutectic.

TABLE 4.3

SPECTROCHEMICAL ANALYSES OF PLUTONIUM ROLLING STOCK IN PARTS PER MILLION

Element	Series I	Series II	Series III
Silver	5	5	5
Aluminum	32	20	-
Calcium	50	5	2
Chromium	25	25	25
Copper	100	5	10
Iron	860	250	375
Magnesium	5	100	25
Molybdenum	-	10	10
Manganese	25	10	25
Sodium	100	25	5
Nickel	100	100	50
Lead	25	5	5
Silicon	5	10	25
Tin	5	5	5
Zirconium	-	-	250

The initial rolling with the Series I plates was done with six passes per 0.001 in. reduction in roll setting. The roll and table temperatures were between 70 and 80 C. After a reduction of about 20% the sample fractured so severely that further working was impossible. A second attempt was made with the roll and table temperatures at 70 C using a 0.005 in. reduction with two passes per change in roll setting. A 10 min interpass holding period on the table was also employed. In this case a 90% total reduction was obtained with only relatively minor edge cracking. This latter roll pass schedule was repeated with the 0.100 in. thick material from Series II. Hardness and density determinations were made at each 10% reduction. The results are given in Table 4.4. It appears that the work hardening which has taken place is inconsequential and that the changes in density are inconclusive.

TABLE 4.4

UNALLOYED PLUTONIUM HARDNESS AND DENSITY AS A FUNCTION OF REDUCTION BY ROLLING AT 70 C (158 F)

Thickness (As-Cast), Inch	Hardness R_A	Density, g/cm^3
0.104	59	19.55
0.094	61.3	19.65
0.082	62	19.66
0.072	61.8	19.65
0.060	61.5	19.65
0.050	61.6	19.57
0.040	60.7	19.56
0.030	61.2	19.65
0.020	60.7	19.60
0.012	60.8	19.54

An attempt to roll the 0.200 in. thick plate with a similar schedule was unsuccessful. Severe cracking was encountered after about 25% reduction.

Despite the apparently extreme brittleness of alpha plutonium it can nevertheless be plastically deformed to an extensive degree by rolling. Accordingly, the influence exerted by various variables in the deformation process is being studied.

In order to minimize, as far as possible, the variable in the starting material, a third series of specimens was cast. A 3 kg heat of high quality (low impurity) plutonium was cast into a coated graphite mold designed to provide eight ingots 1.5 x 7 x 0.100 inches. The nominal pouring temperatures was 1000 C and the mold was heated to about 500 C. The long mold dimension was horizontal with the result that not all cavities were filled to the end. The ingots were scored and broken into four pieces

so that a total of 32 pieces were available for rolling. The density of the as-cast pieces varied from 19.53 g/cm^3 to 19.63 g/cm^3. The hardness values measured on the surface of the as-cast piece ranged from 59 to 61 Rockwell A. The spectrochemical analysis of this material is included in Table 4.3.

Initially the 70 C roll pass schedule calling for 0.005 in. reduction per pass with a 10 min interpass holding period was employed to verify the similarity between the Series III material and that from Series II. Figures 4.6 through 4.14 show a comparison between the as-cast stock and the rolled material at each 10% reduction. It will be noted that the extent and progression of edge cracking was not significantly changed as the reductions increased. Following this run the holding period was eliminated; no apparent change in the behavior of the metal resulted. More recently, however, larger reductions were made at 70 C. Reductions of 40 and 45% per pass have been made with no ingot treatment prior to rolling and no additional severity of cracking apparent. Parts were rolled to a total of 90% reduction.

FIGURE 4.6

Plutonium, As-Cast (0.102 in.), Versus 10% R_A (0.092 in.)

Neg. No. E4586

AEC-GE RICHLAND, WASH

UNCLASSIFIED

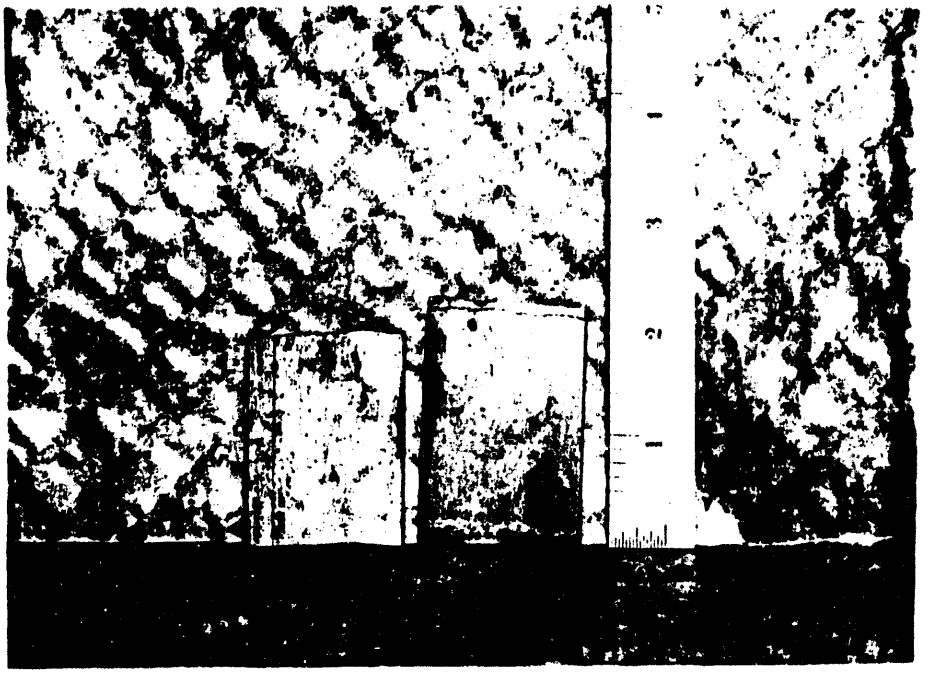

FIGURE 4.7

Plutonium, As-Cast, (0.102 in.) Versus 20% R_A (0.081 in.)

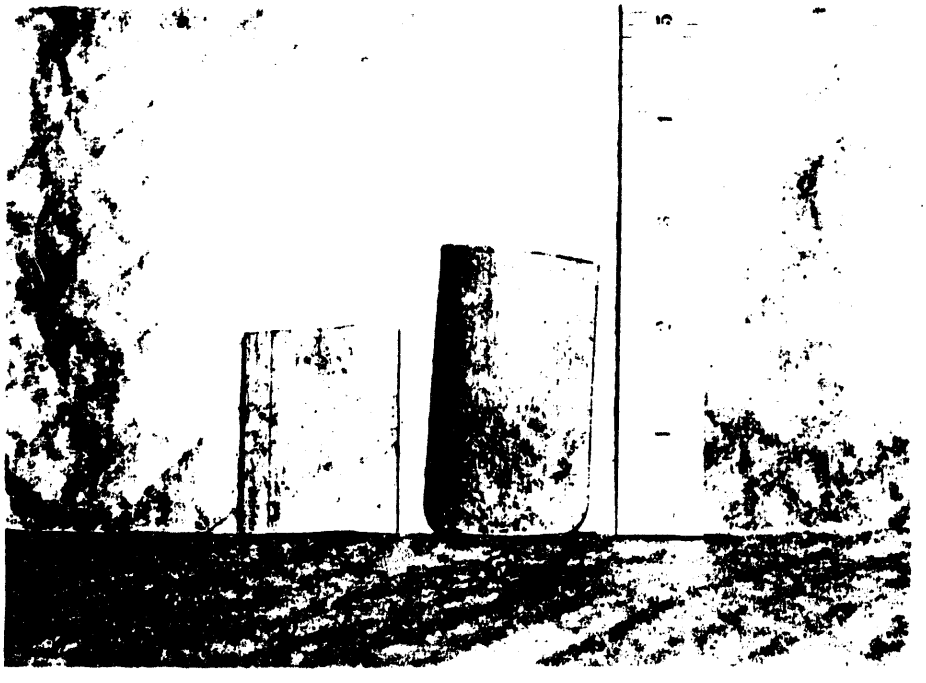

FIGURE 4.8

Plutonium, As-Cast (0.102 in.) Versus 31% R_A (0.070 in.)

Neg. No. E4588, E4589

AEC-GE RICHLAND, WASH

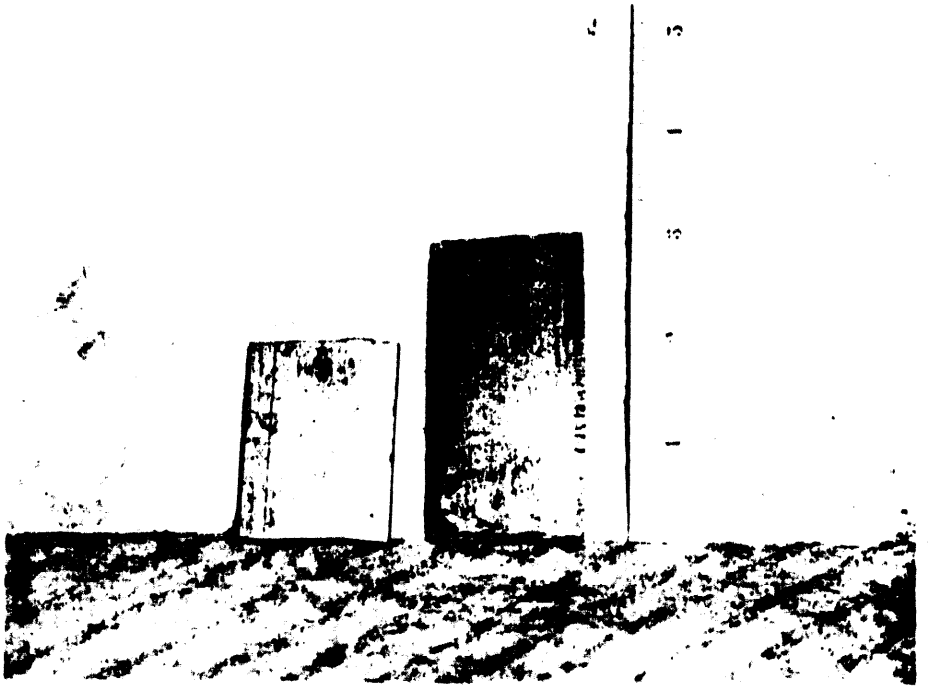

FIGURE 4.9

Plutonium As-Cast, (0.102 in.) Versus 40% R_A (0.059 in.)

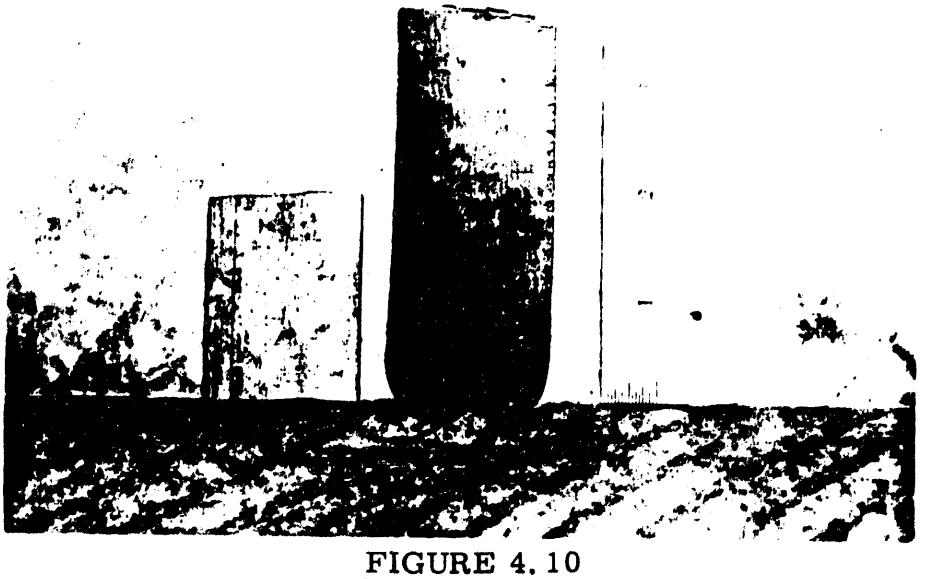

FIGURE 4.10

Plutonium, As-Cast (0.102 in.) Versus 51% R_A (0.050 in.)

Neg. No. E4591, E4593

AEC-GE RICHLAND, WASH

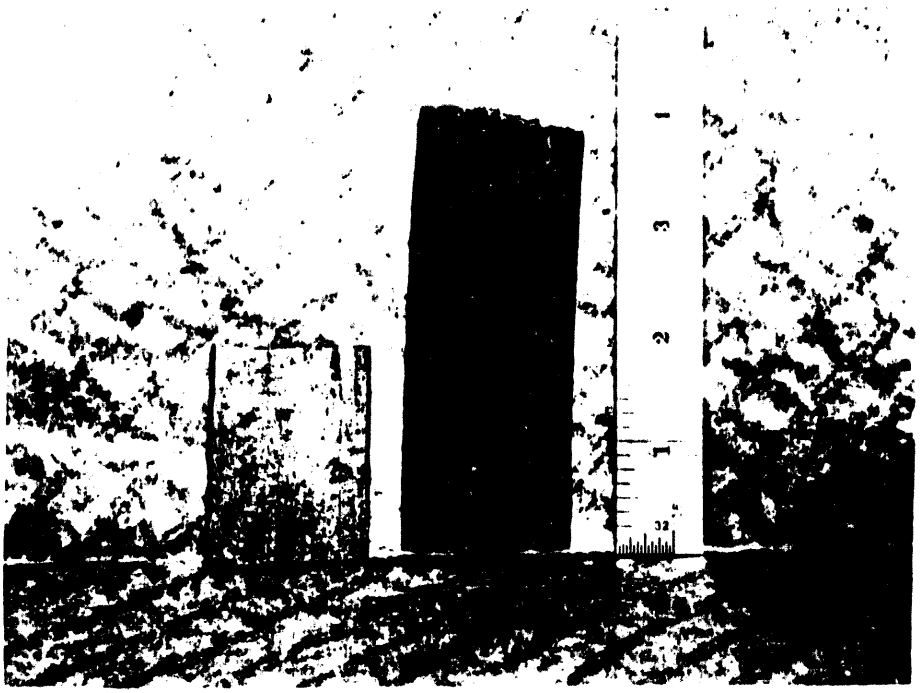

FIGURE 4.11

Plutonium As-Cast (0.102 in.) Versus 60% R_A (0.041 in.)

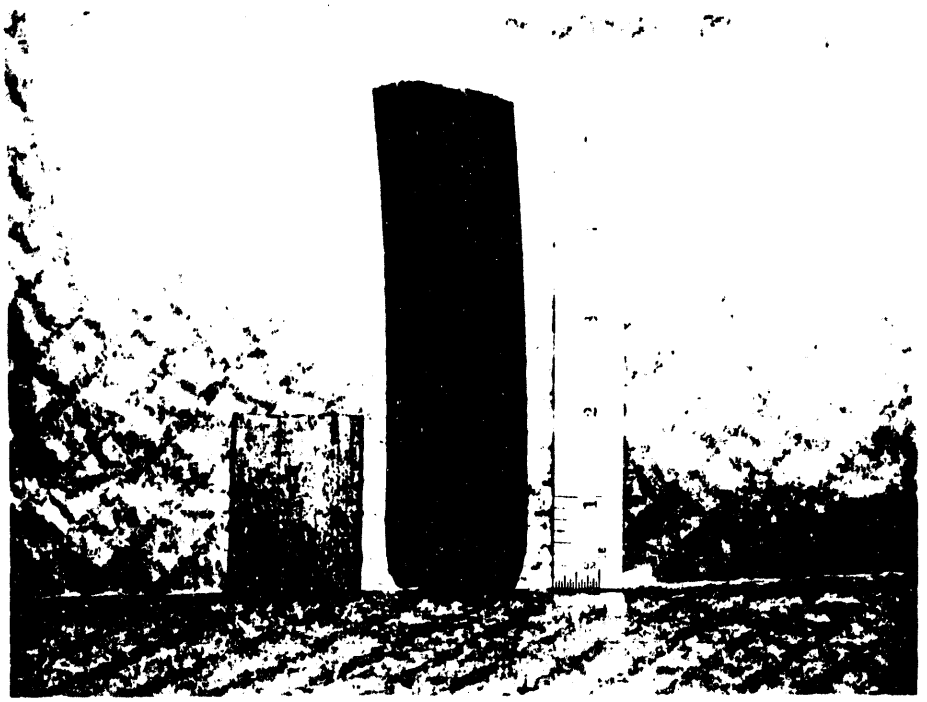

FIGURE 4.12

Plutonium, As-Cast (0.102 in.) Versus 69% R_A (0.032 in.)

Neg. No. E4601, E4600

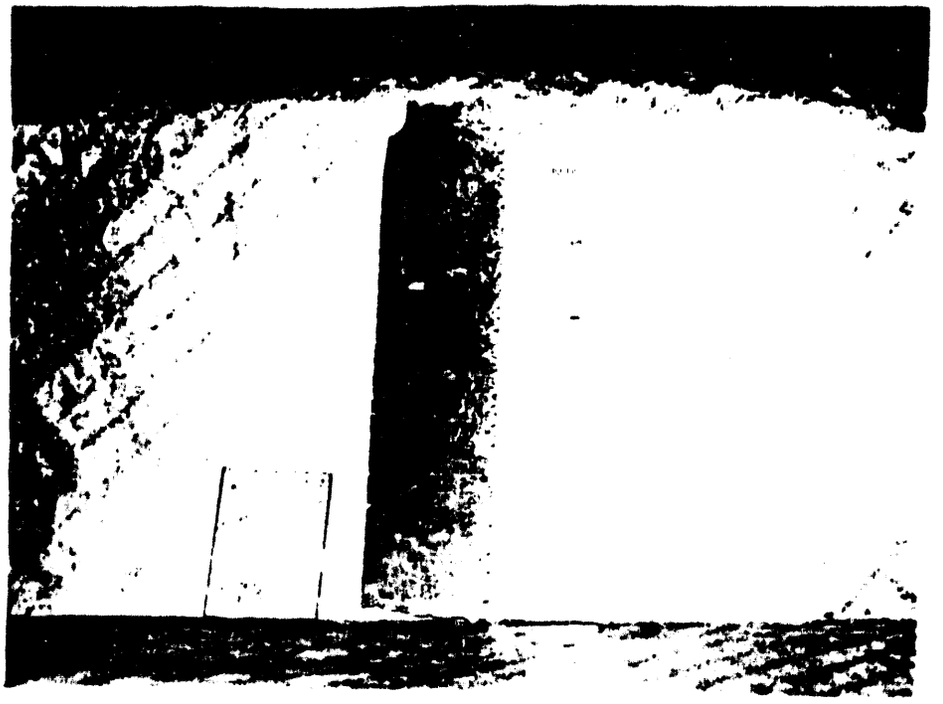

FIGURE 4.13

Plutonium, As-Cast (0.102 in.) Versus 79% R_A (0.021 in.)

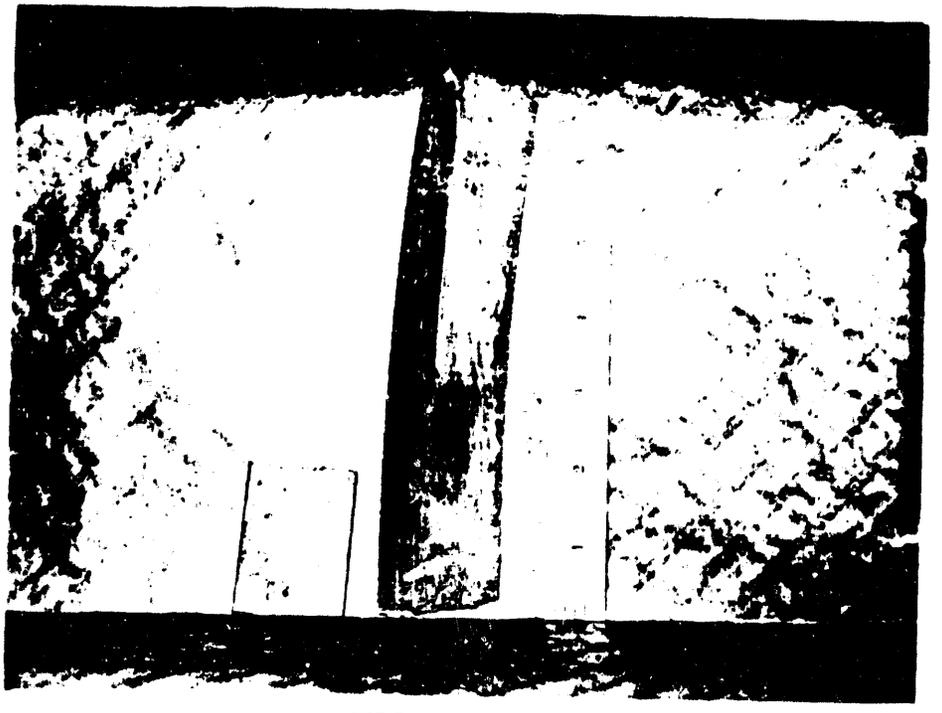

FIGURE 4.14

Plutonium, As-Cast (0.102 in.) Versus 86% R_A (0.014 in.)
Neg. No. E4595, E4597

AEC-GE RICHLAND, WASH

Further attempts were made to reduce thicker starting alpha plutonium than the thickest previously rolled material of 1/8 inch. The material was in the shape of a round bar of 0.625 in. diameter cut to 2.0 in. length and rolled flat.

The first bar was rolled at 70 C and cracked over the entire part after a single pass of 7% reduction. The second bar was also rolled at 70 C but with 0.005 in. reduction in setting each pass. Cracking started at 10% reduction and rolling was stopped at 22% reduction due to failure of the rolling stock.

To possibly induce some degree of orientation a third part was rolled at 170 C in the beta phase to a thickness of 0.400 in., then further reduced in 0.005 in. increments at 70 C. Cracks were introduced during beta rolling, however, and only 17% reduction in the alpha phase caused failure.

To eliminate the cracking before alpha rolling the fourth part was rolled at 230 C in the gamma phase down to 0.350 in. and cooled to 70 C. With 0.005 in. reductions at 70 C, 20% reduction produced failure of the rolling stock.

The first variable considered was the rolling temperature. With a constant 0.005 in. reduction in roll setting per pass, the roll and table temperatures were held at 50 C, 40 C, 30 C, and ambient box temperatures for four series of rolling experiments. Reductions of about 85% were obtained at both 50 and 40 C although the cracking encountered was somewhat more severe than at 70 C. At 30 C the material had cracked sufficiently at about 80% reduction to force the termination of the schedule At the ambient box temperature, both longitudinal and transverse cracking made reductions beyond about 67% impossible. Hardness readings taken on this latter material after both 47 and 67% reductions yielded results of 61.2 R_A and 61.4 R_A, respectively. It would appear from these results that the recovery and possibly the recrystallization temperature of alpha plutonium are below about 25 C.

Since excessive cracking was encountered during early stages of the rolling done at the ambient box temperature, it was decided to attempt to break up the as-cast structure at a higher temperature prior to further low temperature rolling. Castings were reduced 15 and 30% respectively at 70 C prior to further reductions at ambient temperature. Both pieces were successfully reduced a total of 85% at room temperature after this initial elevated temperature breakdown. In these cases the amount of edge cracking appeared to be even less than in those cases where the entire schedule was completed at the higher temperatures.

Since 70 C appeared to be at or near the optimum working temperature, this condition was selected for the investigation of the effects of increasing the reduction per pass. The rolling schedules were established on the basis of a constant percentage change rather than a constant change in roll setting. Schedules calling for 10, 20, 25, 30, 35, 40, and 45% reductions per pass have been completed on cast material 0.100 in. thick. In all cases the initial pass was made on the as-cast material with no attempt being made to alter either the internal structure or surface. In all cases total reductions of 90% or greater were obtained with no serious cracking encountered. The ultimate reductions appear to be slightly greater than those which could be achieved with the original 0.005 in. reduction per pass. If any comparison can be made at this time, it is that the heavier reductions appear to yield more favorable results than the lighter ones.

In order to obtain samples of greater thickness after 90% reduction, attempts have been made to roll heavier cast stock, both plates and round bars. No pass schedule has as yet been found which will permit reductions of more than 25% prior to destructive cracking on material greater than about 0.125 in. in starting thickness. Initial breakdown in the beta region has not effectively improved the lower temperature rolling characteristics of these heavier castings.

The cross rolling characteristics have also been investigated to the extent that one piece has been reduced 88% in thickness using the 20%

reduction per pass schedule and alternating the rolling direction 90 degrees with each pass. Edge cracking was encountered but was only slightly more severe than that resulting from straight rolling.

Crystallographic Investigations - H. E. Kissinger

The results which have been obtained to date demonstrate clearly that alpha plutonium, an apparently inherently brittle material, can be drastically deformed by flat rolling. A detailed study of the mechanisms by which this deformation takes place, as well as the effects produced, has been undertaken.

Only the initial qualitative steps toward these objectives have, as yet, been taken. The apparently textured structure exhibited by the microstructure of the severely worked material, as shown in Figure 4.15,

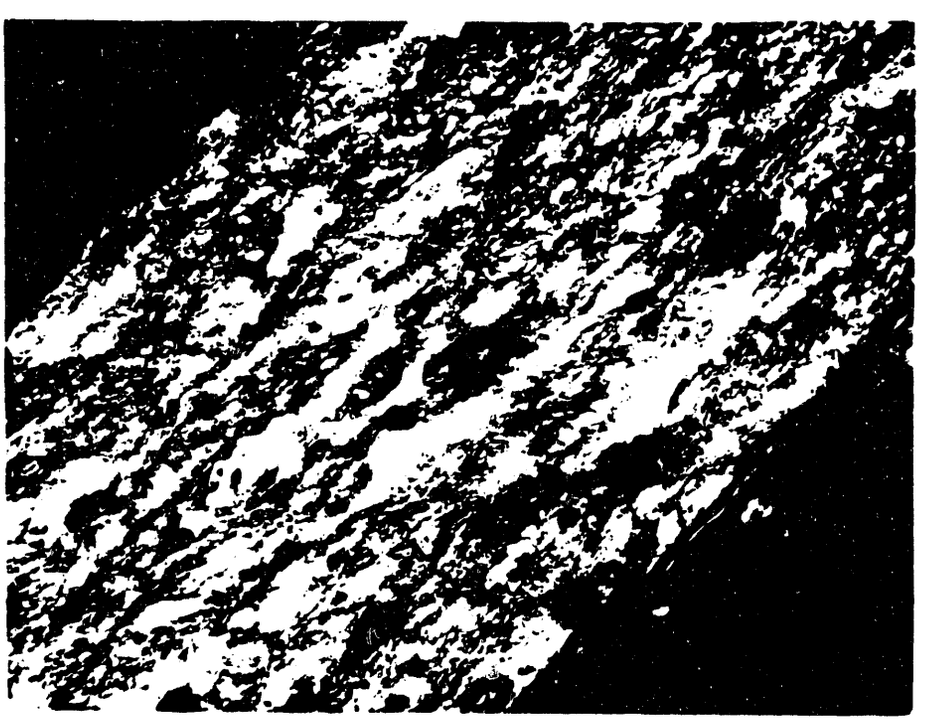

FIGURE 4.15

Typical Structure of Alpha Plutonium After 90% Reduction (0.104 to 0.012 in. in thickness) by Rolling at 70 C 250X

Neg. No. 8684 UNCLASSIFIED

suggests the existence of some degree of preferred orientation. To establish with a greater degree of certainty the actual existence of this condition, X-ray diffraction patterns have been obtained of both the as-cast material and that having been reduced a total of 90%, 30% at 70 C and the remainder at ambient box temperature. These patterns were obtained on the standard Norelco diffractometer using filtered copper radiation. The etched surface of both the casting and the rolled stock were exposed to the X-ray beam.

Of particular significance is the absence of evidence of line broadening in the diffraction pattern of the worked material. This coupled with the hardness data indicates rather conclusively that both the recovery and recrystallization temperatures of alpha plutonium are below the temperature of working, in this case about 25 C. This tends to confirm similar conclusions which had been drawn from the deformation work done at the Argonne National Laboratories.

Table 4.5 presents a comparison of the data derived by Zachariasen and Ellinger[1] and soon to be published with those obtained in the present work. It is apparent that the working has resulted in a significant alteration in the diffraction pattern particularly with respect to relative line intensities. There are also indications of changes in the lattice parameters although the work done to date is not of sufficient precision to warrant a definite statement in this regard. Equipment is currently being installed which will permit a more quantitative investigation of this phase of the work.

An initial attempt has been made to determine the effects of annealing above the normal stability maximum. A sample was isostatically pressed at 180,000 psi and then heated to 180 C for 7 hours. It was cooled under pressure to below 100 C. The microstructure indicated equiaxed grains with no significant grain growth. It is not certain at this time that the material had not transformed at the annealing temperature and further work along this line is planned.

---

(1) W. H. Zachariasen and F. H. Ellinger, "Crystal Structure of Alpha Plutonium Metal," Acta Cryst., (in press).

TABLE 4.5

COMPARATIVE X-RAY DIFFRACTION DATA FROM ALPHA PLUTONIUM IN THREE DIFFERENT CONDITIONS

	Zachariasen and Ellinger				As-Cast		Rolled	
hkl	2θ	I_{calc}	I_{abs}	I/I_o	2θ	I/I_o	2θ	I/I_o
013	31.08	56.3	56	20	31.02	8	31.08	12
$11\bar{3}$	32.20	128.7	122	43	32.18	16		
201	32.28	64.9	64	22.5			32.30	100
004	33.36	98.4	105	37	33.30	9	33.35	30
$20\bar{3}$	34.66	142.1	152	54	34.60	8	34.65	25
020	37.28	270.6	246	87	37.25	100		
211	37.42	301.4	284	100			37.38	56
014	38.36	105.6	121	43	38.37	13	38.40	20
$11\bar{4}$	38.60	72.6	86	30				
024	50.85	60.2	70	25	50.85	11	50.88	8
$22\bar{3}$	51.80	91.2	95	33	51.78	12	51.80	5

V. PLUTONIUM MECHANICAL PROPERTIES

Creep Test Facility - D. D. Hays

Nominally pure aluminum creep specimens have been tested in the creep testing facility using cemented SR-4, 10% post yield strain gages connected to a 4 channel Brush amplifier-recorder. This system will be used to obtain very accurate creep data for small strains. These data will be used in calculating the stress relaxation behavior of delta stabilized plutonium. An optical system will be used to measure larger strains for conventional creep data.

Installation of calibrated "heli-pots" in the bridge circuits of the Brush amplifiers is being done to enable re-balancing of the bridge circuit while testing. This will extend the range of the recorder while maintaining the same recording accuracy.

VI. PLUTONIUM MECHANICAL METALLURGY

Machinability of Unalloyed Alpha and Delta Stabilized Plutonium -

D. A. Armstrong, R. W. E. Peterson, J. H. Rector

The primary purpose of this program was to investigate the cutting properties of both unalloyed alpha and the delta stabilized phases of plutonium. The objective being the optimum conditions under which they can be cut. The term machinability has a very vague meaning, depending on the purpose of the machining operation. Measurements of "Machinability" (on a relative scale only) were obtained through the use of a three axis tool post dynamometer. Measurements were made of the actual tangential, transverse, and radial cutting forces for each cutting condition studied. On the preliminary tests, optimum machinability was believed to exist for the set of conditions that reduced the resultant of the cutting forces to a minimum. From a power input standpoint, this statement is probably true. However, it has been found that if the objective is to achieve the best possible surface finish, this scale is not always reliable. Currently, work is being conducted to investigate machinability from a surface finish standpoint. Some definitions of machinability are based on tool wear. For the type of machining done at this facility, the tolerances required do not allow use of this definition. It is not currently known what maximum amount of tool wear would be permissible, although it is known that this quantity is very small.

Several factors were studied in an attempt to determine the optimum cutting conditions. These tests were based on a cutting force standpoint. The controlled variables were:

1. Cutting speed
2. Cutting feed
3. Use of Lard Oil mist for a lubricant/coolant
4. Depth of cut
5. End clearance angle
6. Side rake angle

7. Back rake angle
8. Tool nose radius
9. Cutting edge quality
10. Tool surface finish

There are numerous variables that enter into an investigation such as this. During the course of this program, an attempt was made to hold as many of the variables constant as was possible. The controlled factors were inspected rigorously to maintain reliability in the data. There were however, several factors which could not be maintained to such rigid standards. The uncontrollable variables that have been recognized were:

1. Workpiece density and homogeniety
2. Variations in tool material
3. Directions of grinding and lapping marks on the faces of the tools.
4. Volume of lubricant/coolant applied

The plutonium used for this program was cast into cylinders as shown in Figure 6.1. Each of these cylinders had the following approximate

FIGURE 6.1

Typical Plutonium "Pipe"

dimensions: length, 3-1/2 in.; OD, 3 in.: ID, 2-1/2 inches. Densities varied from 19.35 g/cc to 19.63 g/cc for the alpha plutonium and 15.74 to 15.76 for the delta stabilized plutonium. Because of the many variables present, it was hard to assess the change in machinability with changing density, but it was observed that the higher density materials would require slightly higher cutting forces.

It must be emphasized that the tests involved in this investigation were of short duration. No attempt was made to conduct tool life tests. In spite of the short term aspects of the tests, there are many indications which show that the low force tools may have a longer life. Figure 6.2

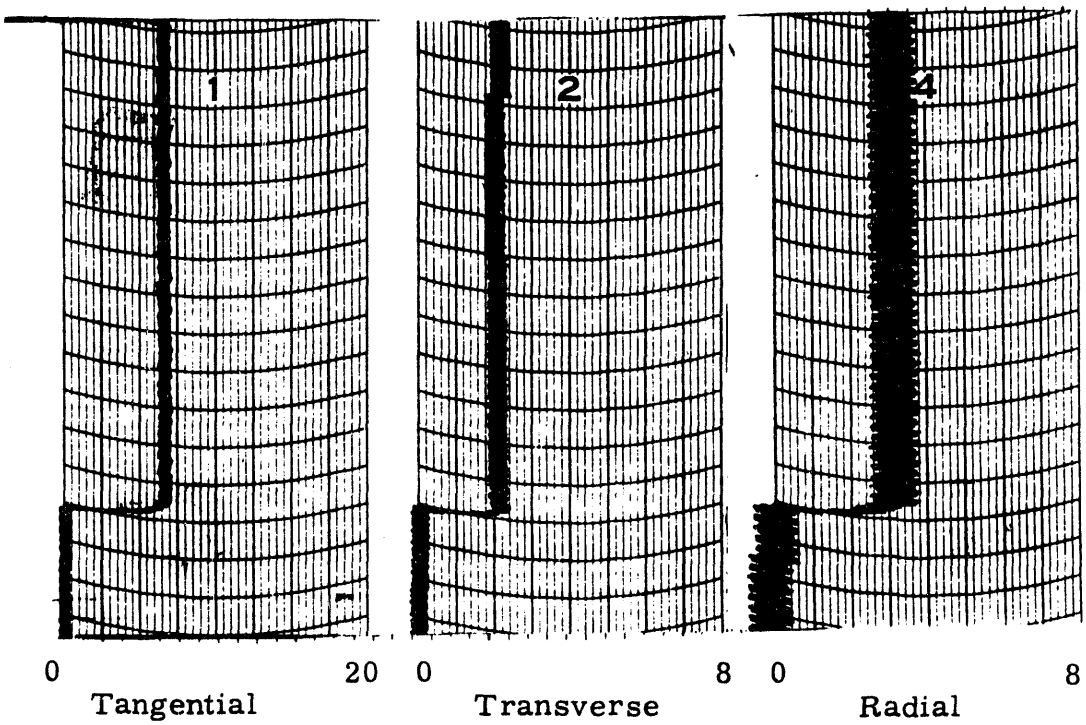

FIGURE 6.2

Forces in Pounds on Tool at 200 sfm

shows the cutting forces for a tool with 15° clearance angle, 5° side rake, 5° back rake, and 0.015 in. nose radius when operated at 200 sfm with 0.005 cm/revolution feed and 0.010 depth of cut on alpha plutonium material. This same tool will have a force-time chart as shown in Figure 6.3 when operated at 800 sfm, all other conditions remaining constant. The instability of

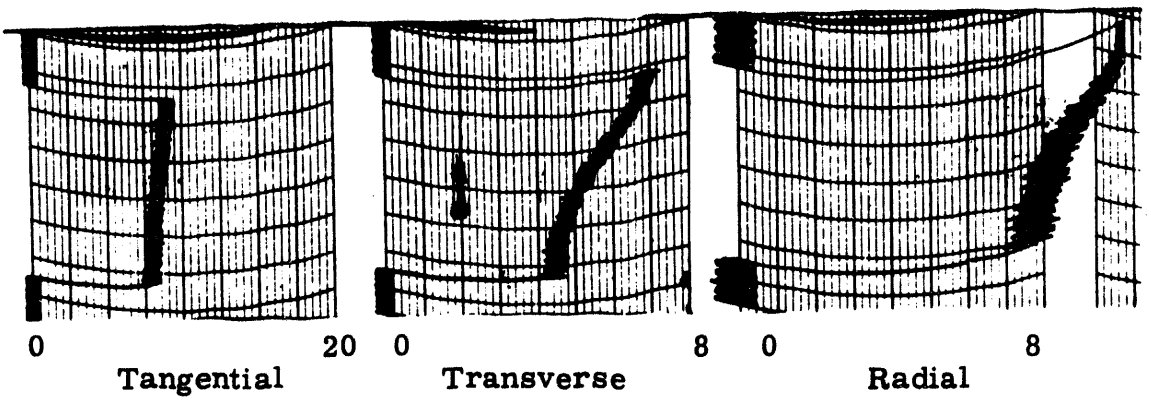

FIGURE 6.3

Forces in Pounds on Tool at 200 sfm

the transverse and radial cutting forces is thought to be due to breakage or wearing of the front face. This worn condition is shown in Figure 6.4. The affect of this wear is essentially to decrease the front clearance angle to zero. This condition is known to produce higher cutting forces due to buildup that will occur on the top of the tool. The cutting tools that were used throughout these tests were "Carboloy" grade 999 carbide, or "Carboloy" grade 999-S carbide.

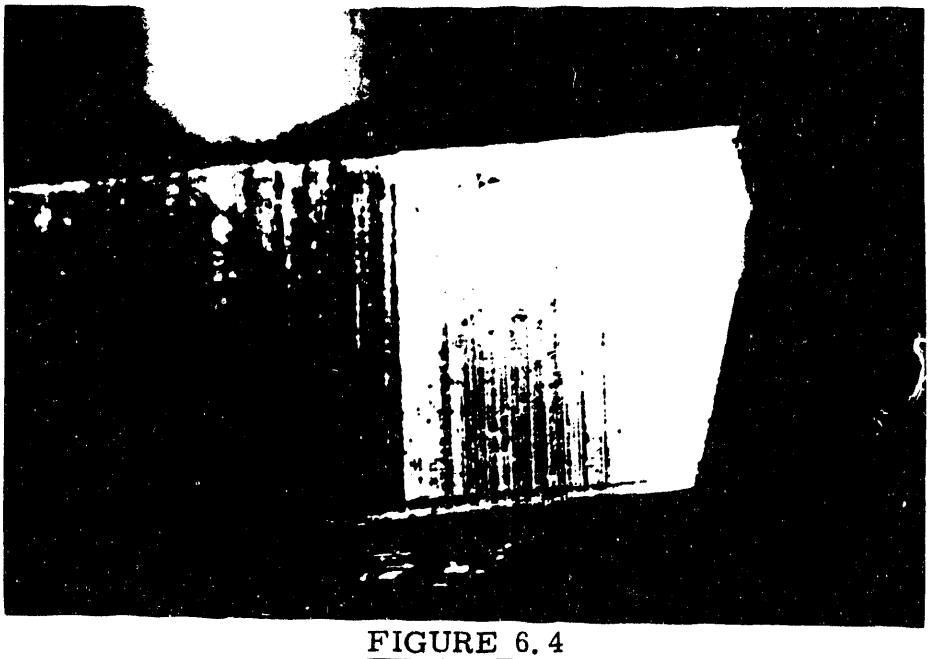

FIGURE 6.4

Front Land Wear

The range of cutting speeds which bring the forces on the tool to a minimum for unalloyed alpha plutonium has been found to be 200-250 sfm. Below this speed, rapid buildup is likely to occur. Above this range, rapid breakage or wear of the tool will occur, causing the forces to become unstable. A plot of the cutting forces versus cutting speed, Figure 6.5, shows this minimum region. Figure 6.6 gives the rms surface finish that may be expected from this cutting condition. It has been seen that the quality of the tools cutting edge will affect the workpiece surface finish more than the cutting forces. The values of the cutting forces for a slightly chipped tool and a perfect tool may not be changed, yet the surface finishes may be changed considerably. Chip buildup on the tool seems to be the primary cause of unstable cutting forces at low speeds.

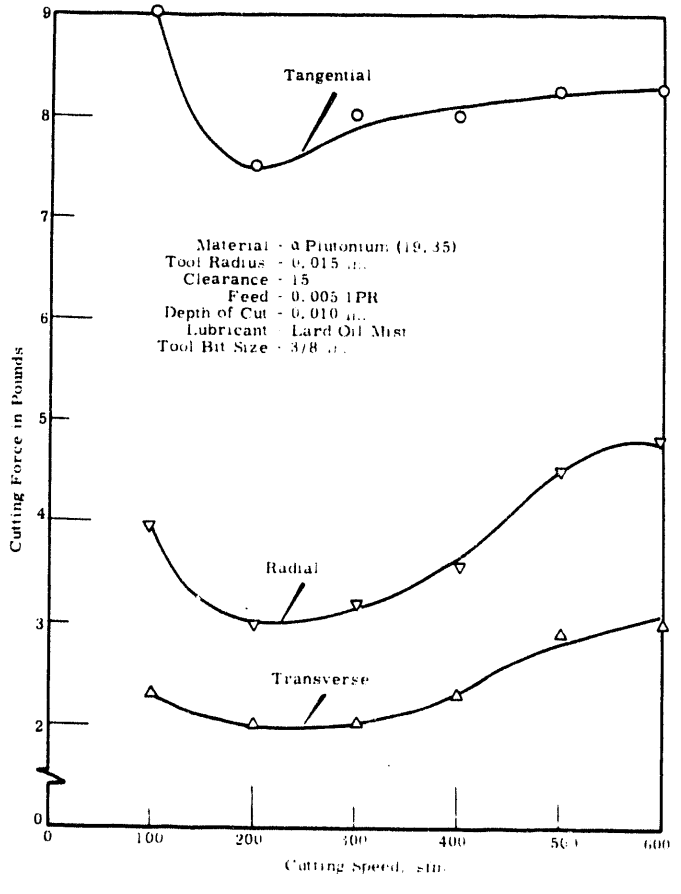

FIGURE 6.5

Tool Forces at Various Cutting Speeds on Alpha Plutonium

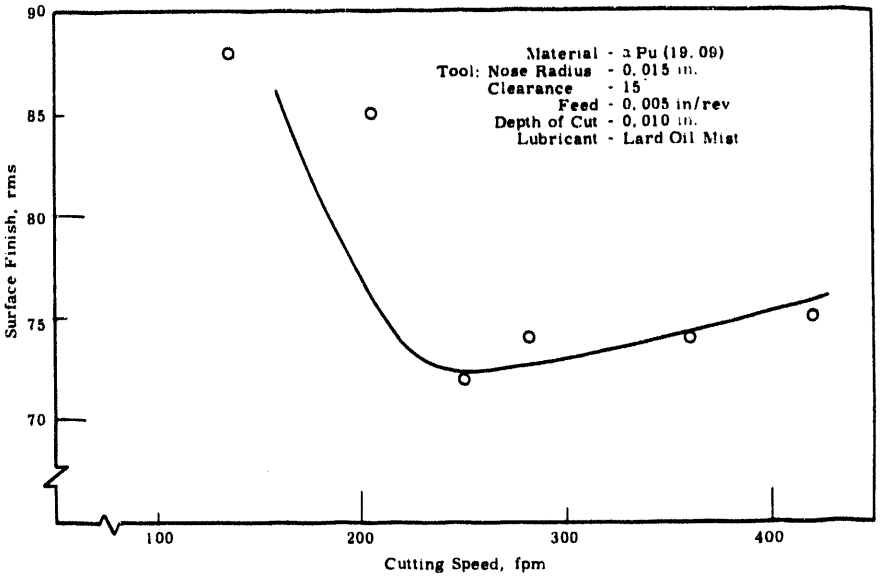

FIGURE 6.6

Surface Finish for Various Cutting Speeds

As the depth of cut was increased from 0.005 in. to 0.050 in., all three of the tool force components increased linearly. This proportionality may be seen in Figure 6.7. Note that for this case the tangential force increases the most rapidly. This general trend appears to be the same regardless of tool geometry. The slopes of the lines will change however.

Tool forces have been found to increase with an increase in nose radius. It has also been found that roughness of the workpiece surface finish will increase with the nose radius. These findings show that force values cannot be used to predict optimum machining conditions from a surface finish standpoint for tools of different geometry. For any one style of tool, the minimum force condition will also generally be the operating point where the most desirable surface finish will be produced. This has been seen in the comparison of Figures 6.5 and 6.6.

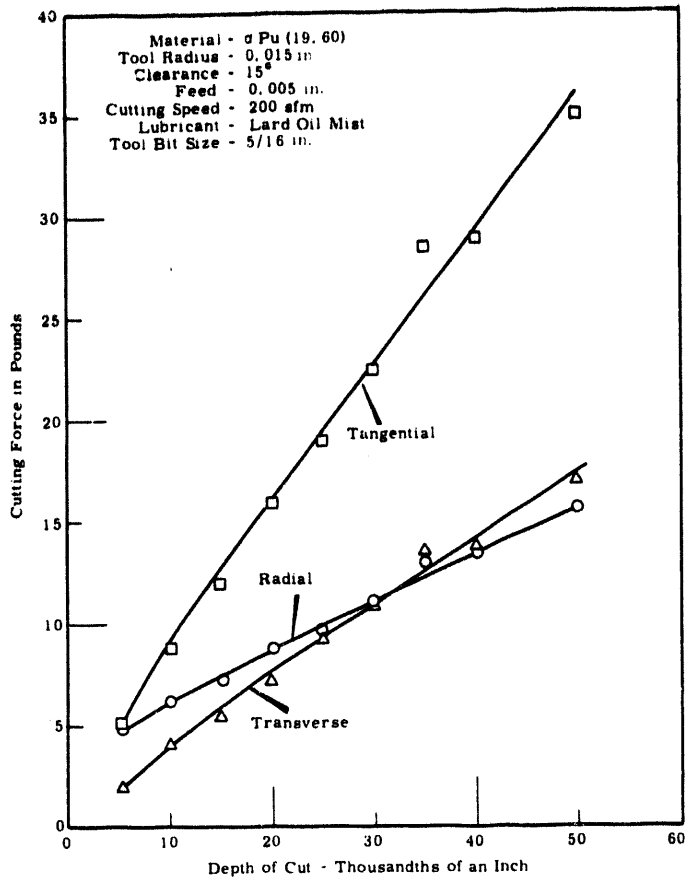

FIGURE 6.7

Tool Forces at Various Depths of Cuts

Although it has been found that increases in side and back rake will decrease the tool forces, it has also been seen that the surface finish will be impaired. The effect is not thoroughly known since most of the attention has been placed on tools that are suitable for X-Y tracer use.

The delta stabilized phase of plutonium machines quite differently from the unalloyed material. At present, indications are that this material may be machined at speeds up to 2500 sfm. The optimum range being 1500 to 2500 sfm. This data is from a force standpoint only, no work has been done to determine the effect that these speeds have on surface finish. The variation in cutting force versus cutting speed is shown in Figure 6.8.

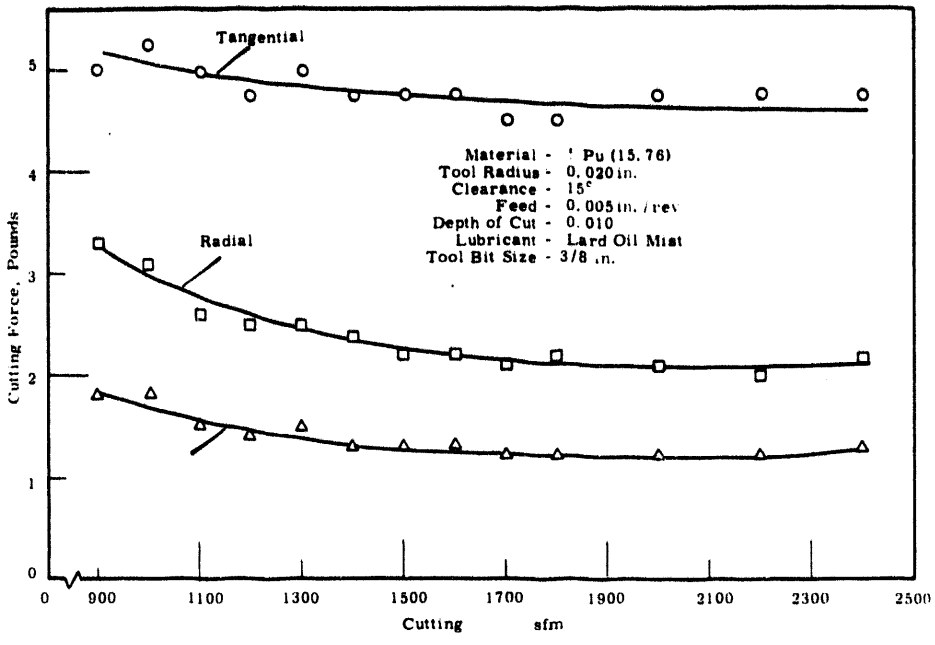

FIGURE 6.8

Tool Forces at Various Cutting Speeds on Delta Plutonium

Several tests were run with and without the use of Lard Oil Mist. The use of the Lard Oil will improve machinability in all cutting ranges for both the unalloyed and stabilized material. The actual amount of tool life extension is not known, but it is expected that the use of Lard Oil is a definite aid.

The forces involved in machining delta plutonium are less than for the unalloyed material. The cutting forces will increase linearly with increased depth of cut, similar to Figure 6.7.

Again, it has been seen that rake angles will decrease the cutting forces. It is not known what affect the addition of either back or side rake angles have on surface finish for the delta material. Lowest forces were obtained with clearance angles up to 20°, but it is expected that tools with this high of a clearance angle have a shorter life than the 10-15° tools. Very low clearance angles will cause rapid buildup on both the front and top of the tool.

Fabrications of Criticality Experiment Cubes - R. E. Falkoski

An additional 43 pieces of 15 to 1 H:Pu ratio, plutonium oxide polystyrene cubes was requested by the Critical Mass Physics Group. Six different sizes were needed varying from 1/2 x 1/2 x 1/2 in. to 1 x 1 x 2 inch. Since the plastic is limited to a 2 x 2 in. dimension, the pieces were all machined from 2 x 2 in. slabs of varying thickness.

About 30 of the cubes which were completed several months ago, developed blisters between the spray coat of paint and the rubber latex used as a contamination barrier. The rubber was peeled off and the cubes recoated.

Fabrications of Thorium-Plutonium Alloy - R. E. Falkoski

The Physical Metallurgy Operation has requested Plutonium Metallurgy Development Operation to fabricate a small number of half-cylinders of thorium-plutonium alloys containing three, 1-1/2 and 3/4 in. wt % plutonium. The half-cylinders are to have an outside diameter of 1/2 in., a 0.030 in. wall thickness, and a length of 3/4 inch.

The method of fabrication will be to arc-melt the alloy, roll to desired thickness, cut out rectangular plates and curve to the desired shape.

Four thorium-plutonium alloys were rolled at room temperature from the arc-melted button (about 1/4 in. thick) to a final thickness of 0.030 inch. A thorium button and a thorium alloy containing 3 wt% plutonium with an unknown small quantity of copper rolled with no difficulty and no edge cracking. One button of thorium with 3 wt% plutonium which was arc-melted in an atmosphere containing some oxygen was quite brittle and broked into several pieces during the first rolling pass.

A good quality thorium 3 wt% plutonium button was rolled to the 0.030 in. finished thickness, with some tearing and edge cracking. (Metallography of the as-rolled material is reported elsewhere in this document.)

Film Processing (Micrography) - D. D. Hays

The function of photomicrography is to accurately record or reproduce a microstructure. This is particularly difficult when the microstructure shows a high degree of contrast with structural detail in areas of high and low reflectivity. In an attempt to more accurately reproduce the microstructure of "cored" delta stabilized plutonium containing impurity inclusions (carbides, nitrides, iron-plutonium eutectic) in the light matrix and inclusions and possible shading differences in the dark cored areas, a study of the effects of photographic and processing variables has been started.

A series of photomicrographs have been taken of such a sample of CPO film. The film was exposed at the recommended time, 15% over and under the recommended time and 25% over and under the recommended time. The film was then developed in various developers for the recommended times for CPO film. The negatives were placed in numbered Kodapak clean plastic sleeves, shuffled and evaluated against a white background against the following standards: 1)overall general appearance (i.e., neither too much nor too little contrast), 2) structural detail visible in areas of high contrast.

The negatives were classified as unacceptable, poor, fair, and good. The best negative from the good grouping was then picked. The results of three different classifications is shown in Table 6.1.

Using CPO film, the best negative for this type of microstructure was judged to be one that was exposed 15 to 25% over the recommended exposure time and developed 4-1/2 min (at 23 C) in D-41 developer. A similar study will be made on SP film. Printing variables will also be investigated to more accurately reproduce this type of microstructure.

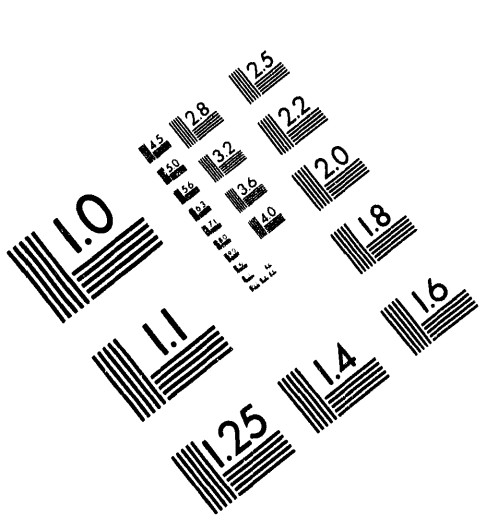

Association for Information and Image Management
1100 Wayne Avenue, Suite 1100
Silver Spring, Maryland 20910
301/587-8202

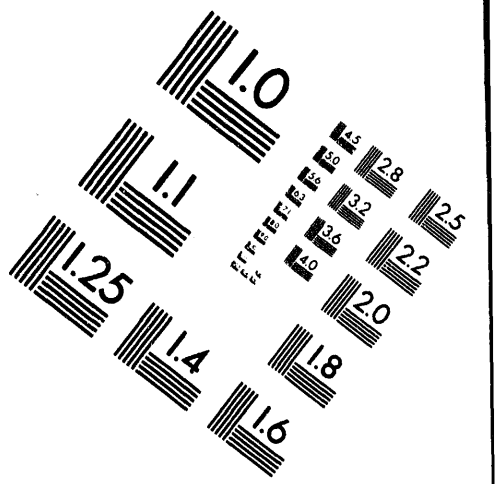

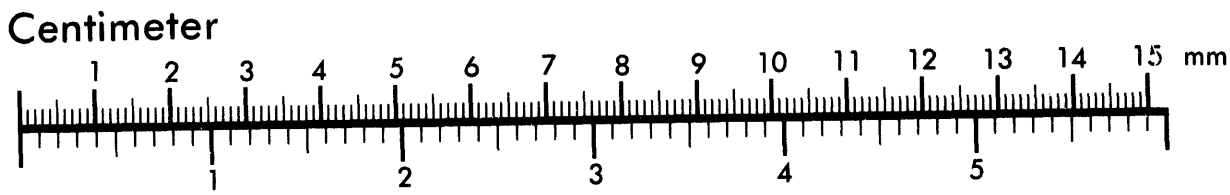

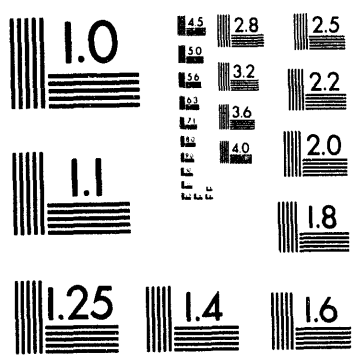

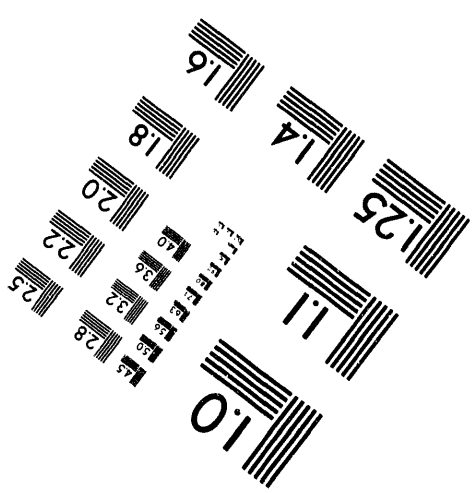

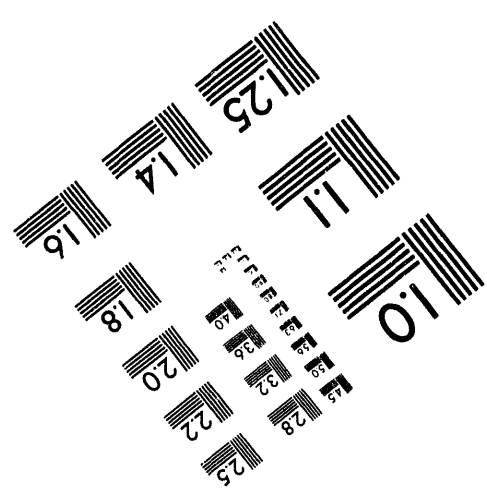

2 of 2

TABLE 6.1

CLASSIFICATION OF NEGATIVES

Developer	Exposure -25%	-15%	Normal	+15%	+25%	Comments
D-19 - 6 min at 23 C	UUU	PPP	PPP	UUU	UUU	All negatives were too contrasty
DK-50 - 6 min at 23 C	FFP	GGG	PPF	UUU	UUU	All negatives except the -15% were too contrasty
D-76 - 14 min at 23 C	UUU	UUU	UUU	UUU	UUU	All negatives were over-developed, contrast did not appear high.
D-41 - 4-1/2 min at 23 C	FFF	GGG	GGG	GGG	GGG	The +15% negative was picked as best in one determination and the +25% negative was picked as best in the other two determinations
D-42 - 4-1/2 min at 23 C	FFF	FFF	GGG	GGG	FGG	---

U = Unsatisfactory
P = Poor
F = Fair
G = Good

INTERNAL DISTRIBUTION

Copy Number	
1	F. W. Albaugh - H. M. Parker
2	T. W. Ambrose
3	J. A. Ayres
4	T. K. Bierlein
5	J. H. Brown
6	S. H. Bush
7	J. J. Cadwell
8	J. R. Carrell
9	D. R. deHalas
10	R. L. Dickeman
11	R. L. Dillon
12	E. A. Eschbach
13	E. A. Evans
14	T. W. Evans
15	J. E. Faulkner - J. L. Carter
16	S. M. Gill
17	J. W. Goffard
18	O. H. Greager
19	L. A. Hartcorn
20	H. Harty
21	W. M. Harty
22	R. S. Kemper
23	G. A. Last
24	L. M. Loeb
25	W. N. Mobley
26	W. P. McCue
27	J. E. Minor
28	T. C. Nelson
29	J. W. Nickolaus
30	K. W. Norwood
31	R. E. Olson
32	R. S. Paul
33	H. J. Pessl
34	W. H. Reas
35	J. W. Riches
36	R. K. Sharp
37	E. A. Smith
38	R. W. Stewart
39	J. T. Stringer
40 - 41	J. C. Tobin
42	M. T. Walling
43	R. G. Wheeler
44	O. J. Wick
45	D. C. Worlton
46	300 File
47	Record Center

EXTERNAL DISTRIBUTION (SPECIAL)

Copy Number	
48 - 50	Dow Chemical Company, Rocky Flats Attn: L. A. Matheson R. A. Vandegrift Luther Evans
51 - 57	University of California, Livermore Attn: W. F. Arnold E. H. Fleming M. D. Martin M. M. May W. M. Miller W. J. Ramsey D. C. Sewell
58	U. S. Atomic Energy Commission Rocky Flats Area Office
59	U. S. Atomic Energy Commission, RLOO Attn: A. T. Gifford
60	U. S. Atomic Energy Commission, SAN Attn: R. W. Hughey

EXTERNAL DISTRIBUTION

Number of Copies	
1	ACF-South Albuquerque Works
1	Aerojet-General Corporation
1	Aerojet-General Corporation (NASA)
2	Aerojet-General Nucleonics
7	Aeronautical Systems Division
1	Air Force Electronic Systems Division
1	Air Force Flight Test Center
2	Air Force Weapons Laboratory
2	AiResearch Manufacturing Company, Phoenix
1	Albuquerque Operations Office
2	Allis-Chalmers Manufacturing Company
2	Allis-Chalmers Manufacturing Company, Washington
2	Allison Division — GMC
2	Argonne National Laboratory
1	Army Ballistic Research Laboratories

EXTERNAL DISTRIBUTION

Number of Copies	
1	Army Combat Developments Command
1	Army Weapons Command
1	Astropower, Inc.
4	Atomic Energy Commission, Washington
1	Atomic Power Development Associates, Inc.
2	Atomics International
1	Avco Corporation
2	Babcock and Wilcox Company
1	Battelle Memorial Institute
1	Bendix Aviation Corporation (ALOO-705)
1	Bendix Corporation (AF)
1	Bridgeport Brass Company
1	Brookhaven National Laboratory
1	Brush Beryllium Company
1	Bureau of Medicine and Surgery
1	Bureau of Mines, Albany
1	Bureau of Mines, Salt Lake City
2	Bureau of Naval Weapons
1	Bureau of Ships
1	Carolinas-Virginia Nuclear Power Associates, Inc.
2	Central Intelligence Agency (NED)
1	Chicago Patent Group
1	Combustion Engineering, Inc.
2	Combustion Engineering, Inc. (NRD)
1	Denver Research Institute
1	Division of International Affairs, Brussels
1	Division of International Affairs, Tokyo
1	Dow Chemical Company, Rocky Flats
3	duPont Company, Aiken
1	duPont Company, Wilmington
1	Edgerton, Germeshausen and Grier, Inc., Goleta
1	Edgerton, Germeshausen and Grier, Inc., Las Vegas
1	Electric Boat Division
1	Foreign Technology Division (AFSC)
1	Frankford Arsenal
1	General Atomic Division
1	General Dynamics/Astronautics (AF)
1	General Dynamics/Astronautics (NASA)
2	General Dynamics/Fort Worth
1	General Electric Company (MSVD)
3	General Electric Company, Cincinnati
2	General Electric Company, San Jose
1	General Electric Company, San Jose (AF)

EXTERNAL DISTRIBUTION (contd.)

Number of Copies	
1	General Nuclear Engineering Corporation
1	General Technologies Corporation
1	General Telephone and Electronic Laboratories, Inc.
1	Gibbs and Cox, Inc.
1	Goodyear Atomic Corporation
1	IIT Research Institute
1	Ion Physics Corporation
1	Iowa State University
1	Jet Propulsion Laboratory
1	Johns Hopkins University (APL)
3	Knolls Atomic Power Laboratory
1	Ling Temco Vought, Inc.
1	Lockheed-Georgia Company
1	Lockheed Missiles and Space Company
1	Lockheed Missiles and Space Company (NASA)
3	Los Alamos Scientific Laboratory
1	M & C Nuclear, Inc.
1	Mallinckrodt Chemical Works
1	Marquardt Corporation
2	Martin-Marietta Corporation
1	Martin-Marietta Corporation, Denver
1	Massachusetts Institute of Technology (Evans)
1	Materials Advisory Board
1	Mound Laboratory
1	MSA Research Corporation (COO-765)
1	NASA Ames Research Center
1	NASA Langley Research Center
1	NASA Lewis Research Center
1	NASA Manned Spacecraft Center
2	NASA Marshall Space Flight Center
3	NASA Scientific and Technical Information Facility
1	National Bureau of Standards
2	National Lead Company of Ohio
1	Naval Air Engineering Center
1	Naval Engineering Experiment Station
1	Naval Ordnance Laboratory
1	Naval Postgraduate School
1	Naval Radiological Defense Laboratory
1	Naval Research Laboratory
1	Naval Weapons Laboratory
1	New Brunswick Area Office
1	New York Operations Office
1	New York Operations Office, Canel Project Office
1	North American Aviation, Inc. (AF)

EXTERNAL DISTRIBUTION (contd.)

Number of Copies	
1	North American Aviation, Inc., Downey
1	Nuclear Materials and Equipment Corporation
1	Nuclear Metals, Inc.
1	Nuclear Weapons Training Center Atlantic
1	Nuclear Weapons Training Center Pacific
1	Oak Ridge Operations Office
1	Office of Naval Research
1	Office of the Assistant General Council for Patents (AEC)
1	Office of the Chief of Naval Operations
1	Office of the Chief of Transportation
4	Phillips Petroleum Company (NRTS)
1	Pratt and Whitney Aircraft Division
1	Pratt and Whitney Aircraft Division (NASA)
1	Public Health Service
1	Richland Operations Office
2	Rocketdyne (NASA)
1	Sandia Corporation
1	Sandia Corporation, Livermore
1	San Francisco Operations Office
1	Savannah River Operations Office
1	Space Technology Laboratories, Inc.
1	Surgeon General
1	Sylvania Electric Products, Inc.
1	Tennessee Valley Authority
1	Tracerlab, Inc., Richmond
2	Union Carbide Nuclear Company (ORGDP)
5	Union Carbide Nuclear Company (ORNL)
1	Union Carbide Nuclear Company (Paducah Plant)
1	Union Carbide Nuclear Company (Y-12 Plant)
2	United Nuclear Corporation (NDA)
1	USAF Headquarters
2	University of California, Berkeley
2	University of California, Livermore
1	Walter Reed Army Medical Center
4	Westinghouse Bettis Atomic Power Laboratory
1	Westinghouse Electric Corporation
1	Westinghouse Electric Corporation, Lima
1	Westinghouse Electric Corporation, Lima (AF)
1	Westinghouse Electric Corporation (NASA)
1	White Sands Missile Range
1	Yankee Atomic Electric Company (NYOO-222)
40	Division of Technical Information Extension

DATE
FILMED
8/3/94
END